12-2000

A study of interactions between saccharomyces cerevisiae α-factor and its G protein-coupled receptor, Ste2p

Byung-Kwon Lee

To the Graduate Council:

I am submitting herewith a dissertation written by Byung-Kwon Lee entitled "A study of interactions between saccharomyces cerevisiae α-factor and its G protein-coupled receptor, Ste2p." I have examined the final electronic copy of this dissertation for form and content and recommend that it be accepted in partial fulfillment of the requirements for the degree of Doctor of Philosophy, with a major in Microbiology.

Jeffrey Becker, Major Professor

We have read this dissertation and recommend its acceptance:

Robert N. Moore, David Brian, John W. Koontz, Elizabeth E. Howell

Accepted for the Council:

Carolyn R. Hodges

Vice Provost and Dean of the Graduate School

(Original signatures are on file with official student records.)

To the Graduate Council:

I am submitting a dissertation written by Buyng-Kwon Lee entitled "A study of interactions between *Saccharomyces cerevisiae* α-factor and its G protein-coupled receptor, Ste2p." I have examined the final copy of this dissertation for form and content and recommend that it be accepted in partial fulfillment of the requirements for the degree of Doctor of Philosophy, with a major in Microbiology.

Dr. Jeffrey Becker, Major Professor

We have read this dissertation
And recommend its acceptance:

Robert V Moore

John W. Foster

David Brian

Elizabeth E Howell

Accepted for the Council:

Interim Vice Provost and
Dean of The Graduate School

A study of interactions between *Saccharomyces cerevisiae* α-factor and its G protein-coupled receptor, Ste2p

A Dissertation
Presented for the
Doctor of Philosophy
Degree

The University of Tennessee, Knoxville

Byung-Kwon Lee

December 2000

Dedication

To my mother, *Mrs. Jeong-Yun Kim* (김 정연) (1934-1998)

Acknowledgments

Many people have been exceedingly generous with me with their time, knowledge, or ideas, some of whom put in appearances here and some who do not. I can not begin to thank them all enough, but will try.

I would like to thank the members of my dissertation committee, Dr. Robert Moore, Dr. David Brian, Dr. John Koontz, and Dr. Liz Howell, for their suggestions and critical reviews on my work and a special thank you to Dr. Fred Naider of the College of Staten Island for his support and interest in my research.

I also wish to thank those individuals in the Becker lab, both past and present, who have given me encouragement and have shared their time with me. They include: Dr. Melinda Hauser, Dr. Keith Henry, Dr. Greg Abel, Dr. David Barnes, Dr. Mark Lubkowits, Jeff Wiles, Ayca Akal-Astrader, Vanny Narita, Amy Donhardt, Cagdas Son, Josh Sharp, Keith Goldstein, Sarah Kauffman, Christal Secrest, Kim Snyder, Shannon Matulis and all the undergraduate students in Becker's Lab. I want to acknowledge Dr. Greg Abel for his earlier work on α-factor receptor mutants which had become the basis of this dissertation. I am grateful to Dr. Melinda Hauser and Dr. Keith Henry for their companionship, intellectual stimulus and for providing just the right combination of criticism. It is pleasure to thank Dr. David Barnes, Dr. Mark Lubkowits, and Jeff Wiles for sharing their warm hearts with me.

I wish to offer my greatest thanks and appreciation to Dr. Jeff Becker who has had an intuitive grasp of my ideas for the research from the beginning. His patience, his critical intelligence, his sense of what this research should (and should not) try to be, his enthusiasm and encouragement, have helped my entire graduate years. For me he has become the ideal of how an advisor can guide a student. My debt to him is beyond words.

I would like to thank my family in Korea. Thank you my sisters, Sookhee and Sookyung for your love and support. A special thanks goes to my parents-in-law for praying for me all those years.

I owe thanks above all to my wife, Sung-Kyung, and to my little sons, Hansol and Hankyul, without whom I would have nothing. I LOVE YOU ALL!

Abstract

During the life cycle of the yeast *Saccharomyces cerevisiae*, haploid cells of opposite mating type can fuse during sexual conjugation to form a diploid cell. In preparation for conjugation, haploid cells secrete small diffusible peptide molecules [α-factor, a tridecapeptide pheromone and **a**-factor, a modified dodecapeptide pheromone] that specifically bind to cell surface receptors found on the opposite mating type cell.

The basic structure of the receptors (Ste2p for α-factor and Ste3p for a-factor) is evolutionarily conserved and places them among the 7-transmembrane, G protein-coupled receptors (GPCRs). Part 1 of this dissertation is an overview of the structure and the molecular mechanisms involved in ligand recognition and activation these receptor families with specific emphasis on peptide hormones and α-factor receptors.

Part 2 of this dissertation is a study of α-factor analogs in which Tyr^{13} was replaced with a number of side chains for the design of an iodinatable ligand for affinity labeling studies as a direct iodination at Tyr^{13} abolished function of α-factor. The result of binding and biological activity assays of these analogs showed the lack of strict requirement for Tyr^{13} and allowed the design of several multiple replacement analogs in which Phe or *p-F*-Phe were substituted at position 13 and Tyr was placed in other positions of peptide. One potential

receptor ligand [Tyr(^{125}I)^{1}, Nle^{12}, Phe^{13}]α-factor exhibited saturable binding with a *Kd*of 81 nM and was competed by α-factor for binding.

In Part 3, an analysis of the α-factor receptor was carried out using random and site-directed mutagenesis to try to understand pheromone binding and receptor activation mechanisms. Three receptors containing mutations F55V, S219P, and S259P were screened for their altered ligand specificity and analyzed for their biological responses to various α-factor analogs and for their ligand binding profiles. The S259P mutation demonstrated ligand dependent biological response to all peptides tested (α-factor, antagonists and a synergist). The S219P mutation responded to α-factor, some antagonist peptides and the synergist, but not to other antagonists. The F55V mutant receptor responded only to α-factor and the synergist peptide and not to any antagonist analogs. These results confirmed previous findings that the fifth and sixth transmembrane domain of the receptor are important for receptor activation. In addition, changes in binding affinity of α-factor and its analogs indicate that residue 55 of α-factor receptor is involved with ligand binding.

Part 4 of this dissertation is a study of identification of the α-factor binding region of Ste2p using site-directed mutagenesis and ligand modification. Affinities and activities of mutant receptors at serine 47 and threonine 48 residues were determined with analogs in which Gln^{10} of α-factor was replaced with various functional groups. All mutant receptors showed a similar number of binding sites and efficacy but different *Kd* and EC_{50} values for α-factor compared to those of

wild type receptor. A mutant receptor (S47K, T48K) had dramatically reduced affinity and activity for K^{10} and Orn^{10}-α-factors while the affinity of *S. kluyveri* α-factor(E^{10} with additional four variant reisdues) was increased over 40-fold compared to that of wild type receptor. In contrast to KK substitution, the affinity of K^{10}- and Orn^{10}- α-factor was greatly increased in a S47E, T48E mutant receptor while the binding of *S. kluyveri* α-factor was decreased over 100-fold. E^{10}-α-factor showed about two fold higher affinity in this mutant receptor than KK mutant receptor. The affinity of K^{10}- and Orn^{10}- α-factors for the EE mutant, however, dropped 4-6 fold in the presence of 1M NaCl while affinity of α-factor was not affected by this treatment. The results indicate that 10^{th} Gln residue of *S. cerevisiae* α-factor when bound to the receptor is adjacent to Ser47 and Thr48 residues in the receptor.

TABLE OF CONTENTS

LIST OF TABLES

LIST OF FIGURES

PART 1

General Introduction

CHAPTER 1

G protein-coupled receptors: An overview

G protein-coupled, seven-transmembrane receptors (GPCRs) comprise the single largest gene family, with > 800 present in *Caenorhabditis elegans* (1) and estimates of > 2000 in the human genome (2). The chemical diversity among the endogenous ligands is exceptional. They include biogenic amines, peptides, glycoproteins, lipids, nucleotides, ions, and proteases. Moreover, the sensation of exogenous stimuli, such as light, ordors, and taste, is mediated via this class of receptors (2, 3). GPCRs have been named based on their ability to recruit and regulate the activity of intracellular heterotrimeric G proteins. Activation of GPCRs by agonists induces a conformational change in the associated G protein α-subunit leading to release of GDP followed by binding of GTP (4). Subsequently, the GTP-bound form of the α-subunit dissociates from the receptor as well as from the stable $\beta\gamma$-dimer. Both the GTP-bound α-subunit and the released $\beta\gamma$-dimer can modulate several cellular signaling pathways. These include, among others, stimulation or inhibition of adenylate cyclases and activation of phospholipases, as well as regulation of mitogen-activated protein kinase (MAPK) cascades and calcium channel activity (5).

Because of the breadth and importance of the physiological roles undertaken by the GPCR family, many of its members have become important

pharmacological targets. Indeed, it is estimated that over 50 % of all modern drugs are targeted at GPCRs (6), and represent around a quarter of the top 100 top-selling drugs worldwide with total combined sales during 1997 of nearly 16 000 million US$ (7). Another indication of the importance of GPCRs as targets is their link to a number of hereditary diseases, such as, color blindness, retinitis pigmentosa, hyperfunctioning thyroid adenomas, and familial precocious puberty (8). Other recent discoveries, such as the role of chemokine receptors in HIV infection (9) and the possible role of olfactory receptors in developmental pattern formation (10), also attest to the biological importance of GPCRs.

Structural classification – Sequence comparison between the different GPCRs revealed the existence of different receptor families sharing little or no sequence similarity. However all GPCRs have an extracellular N-terminal domain, seven TMs, which form TM core, three exoloops, three cytoloops, and a C-terminal domain (Figure 1). Each of the seven TMs is generally composed of 20-27 amino acids. On the other hand, N-terminal domain (7-595 amino acids), loops (5-230 amino acids), and C-terminal domain (12-359 amino acids) vary in size, an indication of their diverse structures and functions (6). GPCRs have usually been classified into six families (7). Most of these in turn contain a few or many subfamilies, whereas a few families are small and not further subdivided. Family A is the huge family of receptors related to rhodopsin receptors; family B consists of calcitonin-, PTH-, glucagon-receptors, etc,; family C contains metabotropic glutamate receptors and related subfamilies, among which are

Figure 1: Schematic structure of a GPCR. Transmembrane helices are shown as cylinders linked by loops drawn as lines. The upper diagram shows a receptor unfolded to indicate the transmembrane topology of GPCR. The intracellular loops are marked endo 1 to endo 3 and the extracellular loops are marked exo 1 to exo 3. The lower part of the diagram illustrates, in a highly simplified manner, how the seven helices pack together in three dimensions. Adapted from (6).

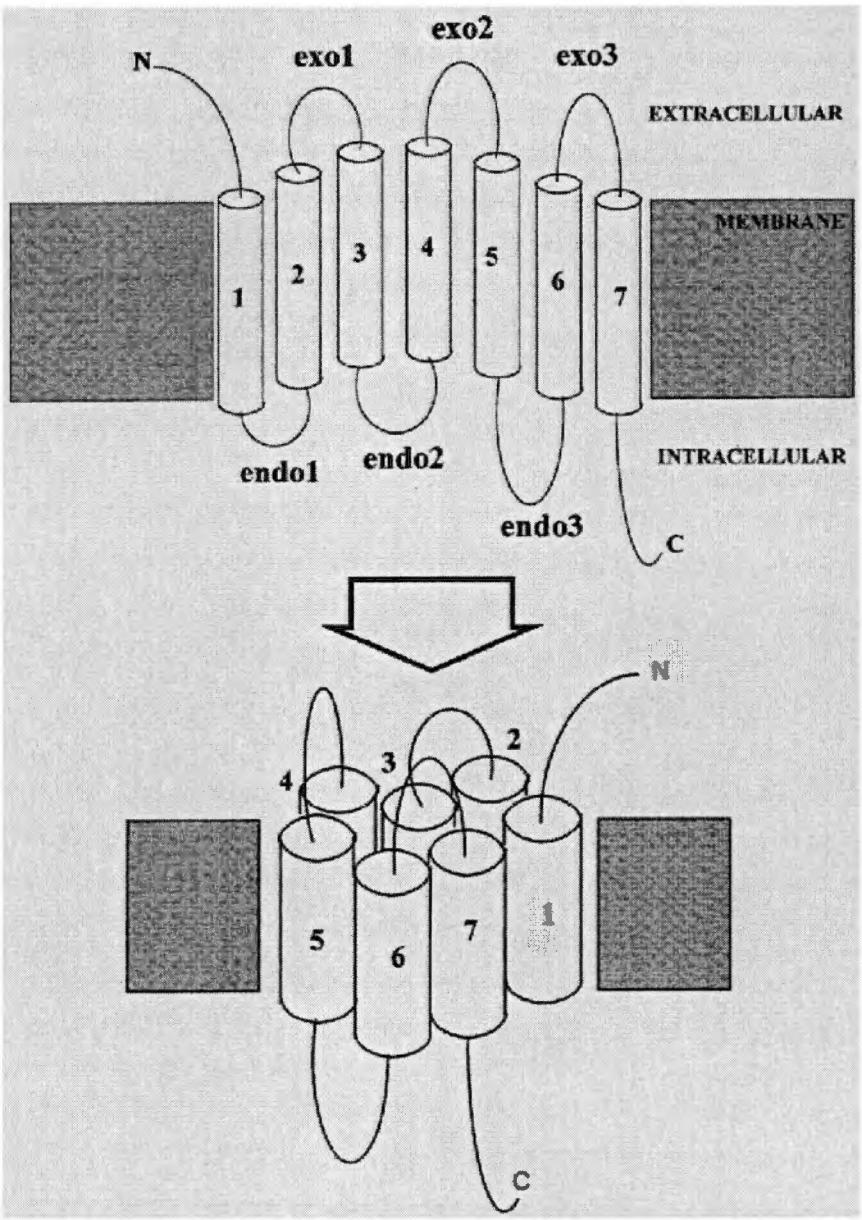
N
exo1
exo2
exo3
EXTRACELLULAR
MEMBRANE
1
2
3
4
5
6
7
endo1
endo2
endo3
INTRACELLULAR
C
N
2
3
4
5
6
7
1
C

vomeronasal receptors type 2; family D is STE2 yeast pheromone receptors; family E is the yeast STE3 pheromone receptors; and family F receptors are related to slime mold cAMP receptors.

The three-dimensional structures of GPCRs – Due to the inherent difficulties in crystallizing complex membrane proteins, high resolution structural information for GPCRs was not available until crystal structure of rhodopsin has been determined at 2.8 Å resolution (11). The crystal structure of rhodopsin revealed a highly organized heptahelical transmembrane bundle with 11-cis-retinal as a key cofactor involved in maintaining rhodopsin in the ground state. The structure also gave information on the molecular mechanism of GPCR activation. A conserved set of residues on the cytoplasmic surface, where G protein activation occurs, likely undergo a conformational change upon photoactivation of the chromophore that leads to rhodopsin activation and signal transduction. Importantly, the three-dimensional structure of rhodopsin was in good agreement with the models of various GPCRs derived from low-resolution structures of rhodopsin (12-14), and from mutagenesis and biophysical studies of other classes of GPCRs (15-20). Guided by the crystal structure of rhodopsin, the models, of course, will provide a general picture of the other classes of GPCRs and thus a reliable framework within which the structure and molecular function of GPCRs can be further debated and experimentally explored.

Ligand binding domains – Numerous studies have been carried out to identify domains involved in ligand binding to various subclasses of GPCRs. The binding sites of endogenous "small-molecule" ligands in family A receptors, such

as for the retinal chromophore in rhodopsin and for catecholamines in the adrenergic receptors are perhaps the most well characterized. They have been reviewed in detail elsewhere (21-23). It is, however, only recently that we have gained insight into binding domains for other classes of ligands. Although the details of ligand binding vary between individual receptors, certain commonalties are apparent. Large ligands, such as proteins, bind to extracellular loops, while small molecules, including pharmacological agents, bind within the transmembrane region of receptor. Peptides can exhibit a mixed binding mode whereby they bind primarily to the extracellular loops while part of the structure penetrates the transmembrane region. A schematic describing different types of ligand binding is shown in Figure 2. In particular, the current knowledge about ligand-binding domains in peptide receptors will be described in further.

For the majority of peptide receptors studied, there is evidence for major interactions in the N-terminus and predicted extracellular loop regions. This includes the receptors for angiotensin (24), vasopressin/oxytosin (25), GnRH (26), opioids (27), and cholecystokin/gastrin (28), neurokinin (NK) (29), and neurotensin 1 (30). Importantly, the significance of the extracellular domains for binding of peptide ligands has been directly documented using affinity cross-linking techniques in the GnRH receptor (26), bradykinin B2 (31), secretin (32), NK-1 receptor for substance P (33), parathyroid hormone (34) and opioid receptor-like 1(ORL1) receptors (35).

Evidence indicates that some of the peptides have additional points of interactions in the TM domains and therefore, to different degrees, may enter the

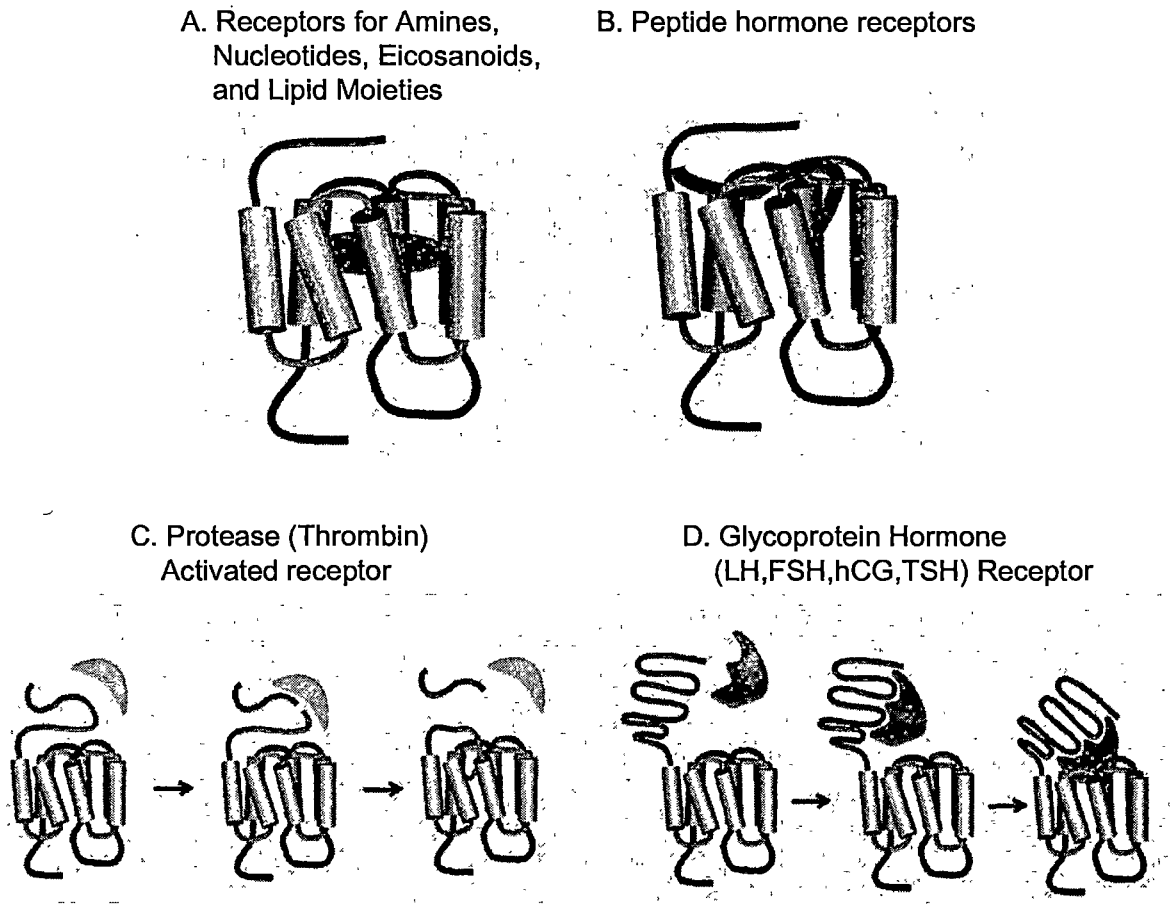

Figure 2. Schematic presentation of GPCRs-ligand interactions. Adapted and modified from (23)

TM binding crevice. These include both small tripeptides TRH (36) and fMLP (37), and larger peptides such as angiotensin (38), endothelin (39), somatostatin (40), opioids (41), bradykinin (42), oxytosin (43), and GnRH (44). The residues identified are found in the outer portions of TM2, 3, 5, 6, and 7. They differ considerably among the receptors and are, except in a very few cases, different from the key positions believed to interact with the biogenic amines (22).

Conformational changes involved in receptor activation – Several key biophysical observations have suggested that relative movements of the transmembrane helices of the GPCR accompany their receptor activation. Spin-labeling studies on cysteine-substituted mutants of rhodopsin showed that a rigid body motion of TM6 relative to TM3 accompanied by anti-clockwise rotation (as viewed from the extracellular side) (45). Additional evidence for a relative movement between TM3 and TM6 in other GPCRs was provided by direct fluorescent labeling of the β_2-adrenergic receptor (46) or by monitoring the accessibility of Cys residues to a hydrophilic sulfhydryl-specific reagent during receptor activation (47). The data imply that there are stabilizing intramolecular interactions in the tertiary structure, allowing the receptor to undergo conversion more readily between its inactive and active state (48). A stabilizing role of TM6 has been suggested from a random mutagenesis study in the muscarinic M5 receptor where substitutions on one face of the helix conveyed constitutive activity to the receptor (49). Similarly, mutation of polar residues in TM6 of the yeast α-factor pheromone receptor (Ste2p) conveyed constitutive activation to this receptor (50).

These findings, together with the mutagenesis studies indicating the presence of distinct sets of radially distributed ground state constraints, and axially distributed activating interactions centered on TM3 can be integrated into the model of receptor activation shown in Figure 3. The proposition is that TM3 acts as a rotational switch which integrates and propagates conformational changes induced by ligand binding through the transmembrane structure of the receptor. It is ideally placed to do this. Because of its high degree of tilt, it interacts, sequentially, with all of the other TM helices, with the exception on TM1 (11,12). TM1 might come into its own in stabilizing a new configuration of TM2 and TM7 in the activated state.

Mechanism of agonist activation – The currently most widely accepted model for GPCR activation is the extended ternary complex model (often referred to simply as the two-state model) (51). According to the model, the receptor exists in an equilibrium between an inactive conformation (R) and an active conformation (R*). In the absence of agonist, the inactive R state is prevailing; however, the energy barrier between the R and R* state is sufficiently low, allowing a certain fraction of the receptors spontaneously to assume the R* state. Agonists are predicted to bind with highest affinity to the R* conformation and in this way shift the equilibrium and increase the proportion of receptor in R* (conformational selection). Conversely, inverse agonists (also called negative antagonists), *i.e.*, compounds possessing the ability to stabilize the inactive R state, shifting the equilibrium away from R*. Neutral antagonists, according to the model, are defined as compounds that bind with the same affinity to both R and

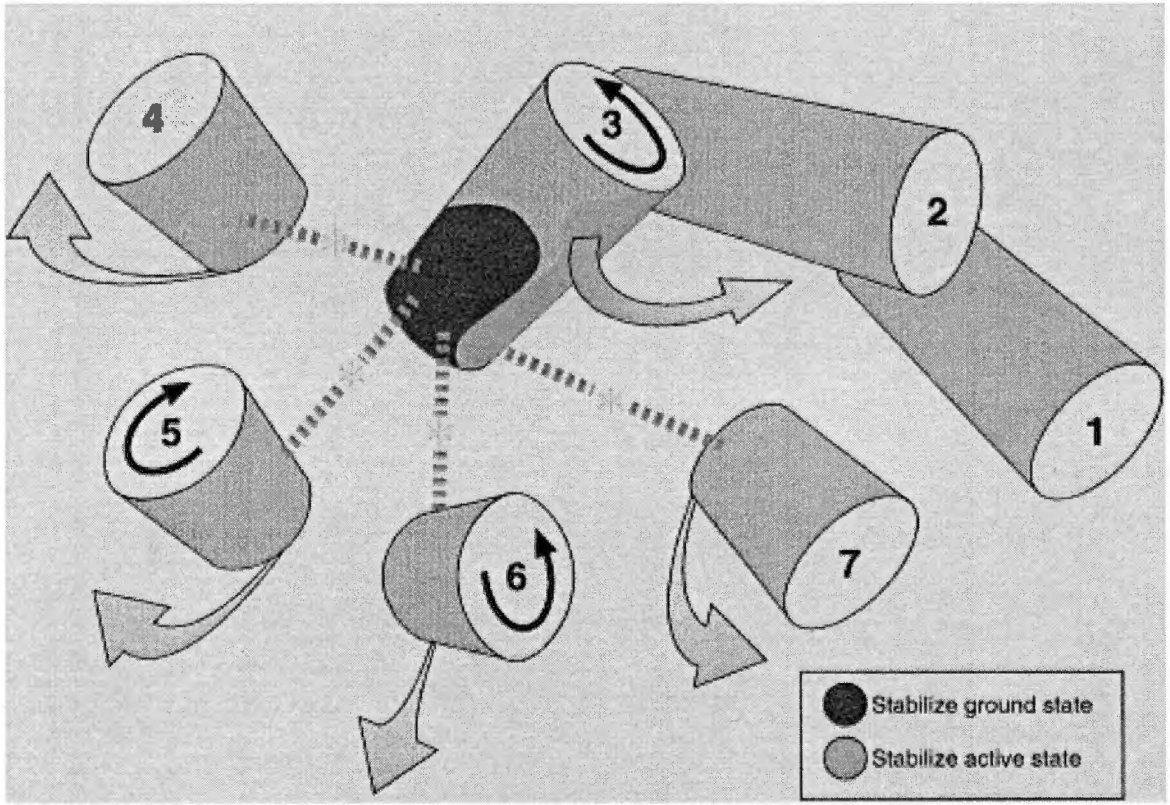

Figure 3. Cartoon of the proposed activation mechanism of the GPCRs, showing the role of TM3 as a conformational switch.

R* and thus cause no change in the equilibrium. This model can account for the basal activity of GPCRs in the absence of agonist and explains the action of inverse agonists that inhibit the activity of constitutively activated receptor.

However, it is becoming increasingly clear that the two-state model cannot sufficiently explain the complex behavior of GPCRs. Several lines of evidence have provided strong support that GPCRs may exist in possibly multiple conformational states. For example, a two-state model cannot explain how mutation of certain serines in TM5 of the dopamine D_2 receptor can lead to loss of functional coupling in response to some agonists, but not others, with only modest effect on their affinity (52). An additional interesting finding, strongly supporting the existence of more than one active receptor state, has been the observation that different constitutively active mutants of the α1b-receptor are differentially phosphorylated and internalized although they convey a similar agonist-independent activity to the receptor (53). Finally, more direct structural evidence has been obtained by fluorescence spectroscopy analysis of the purified β2-adernergic receptor, witch indicated that most ligands promote alterations in receptor structure consistent with the existence of multiple ligand-specific conformation states (54).

To explain these observations a multi-state model has been proposed (55,56). In this model the receptor is proposed to alternate spontaneously between multiple active and inactive conformations. The key element in this model in that the biological response to a given ligand is determined by the conformation to which the ligand binds with highest affinity. The important impact

of the model is, obviously, that there is no requirement for a common binding mode for agonist to trigger receptor activation. Similarly, the model does not require any overlap in binding site between agonist and a competitive antagonist. Kinetically this would be indistinguishable from a classical competitive situation with overlapping binding between the agonist and antagonists (55).

While this model is considered as an extension of conformational selection in which ligand binding depends on conformational status of receptor, various experimental evidence (mainly from peptide receptors) implicates an active role of ligand in conformational change of receptor (57,58, for review see 59). Agonist binding may involve an initial interaction between receptor and one structural group of the agonist. Following the initial binding of one structural group, binding of remaining groups occurs in a sequential manner as a result of random and spontaneous movement of TM domains to positions that permit interaction with functional groups (Sequential binding and conformational stabilization) (56). Each interaction between the receptor and the agonist stabilizes one or more TM domains until the receptor has been stabilized in the active R* state. A similar mode of binding can be envisioned for inverse agonists resulting in stabilization of R state. Partial agonists may stabilize one of the intermediate states (R' or R''), thereby increasing the chance of spontaneous isomerization to R*; or they may stabilize unique conformational states having lower affinity for the G protein.

Concluding remarks – The wealth of information gained over the last decade has substantially improved our understanding of GPCR structure and function. An extraordinary expansion in our knowledge concerning the regulation

of G protein signaling is just one example among others that was not described in this review. The information summarized here suggests that current concepts of ligand binding and GPCR activation mechanism are continuing to evolve. Importantly, it has been conceptualized that GPCRs are not simple "on/off" switches but highly dynamic structures that exist in equilibrium between active and inactive conformation. A more complete understanding of the molecular mechanism of GPCR activation will require high resolution structures, more detailed information about ligand binding sites, and the structural changes induced in the receptor by different classes of ligands. In addition, development of well-defined systems to avoid any misinterpretation of data due to high promiscuity of a GPCR for the selection of ligands and G proteins will be necessary.

CHAPTER 2

α-factor pheromone and its G protein-coupled receptor (Ste2p) in *Saccharomyces cerevisiae*

All organisms, from bacteria and yeasts to mammalian cells, respond to cues from the extracellular environment. These cues are then transduced from the cell surface to the interior of the cell, resulting in patterns of altered gene expression and protein activity, which result in a cellular response to external environment. In eukaryotic cells, the mitogen-activated protein kinase (MAPK) cascade module is a key element in mediating the transduction of many signals generated at the cell surface to the nucleus.

Mating response in yeast – One of the best-defined MAPK pathwayd is that of the *S. cerevisiae* mating signal transduction pathway (60). Yeast may exist either as haploid or diploid cells. The haploid cells have two sexual phenotypes characterized by the expression of a set of genes involved in mating that are not expressed in diploids. Two haploid cell type (**MATa** and **MAT**α) of *S. cerevisiae*, upon binding the sexual pheromone secreted by the opposite cell type (**a**-factor and α-factor), stop growing and differentiate into mating-competent cells by inducing transcription of mating genes. The G protein-coupled receptors

for the α- and **a**-factor are designated as Ste2 and Ste3, respectively because these mutation results in sterile (*ste*) phenotype.

Pheromone activation of the G protein induces activation of downstream MAPK cascade which, in turn, regulates the activity of transcription factors required for the expression of components of the mating pathway itself and genes necessary for cell cycle arrest and cell fusion (Figure 4) (61). Transmission of the signal from the G protein βγ complex to the downstream kinase cascade probably occurs through activation of the PAK kinase homologue Ste20p. Specificity of the kinases that are sequentially activated during pheromone signaling is thought to be maintained by the scaffold protein Ste5p. The ultimate response to pheromone signaling includes arrest in the G_1 phase of the cell cycle, which is mediated by the cyclin-dependent kinase inhibitor Far1p. Other responses include rearrangement of cytoskeleton and morphological changes leading to projection formation and transcriptional induction of genes involved in mating.

Structure-function analysis of α-factor pheromone – The α-factor pheromone is a tridecapeptide secreted by *MATα* cells and has the sequence of Trp^1 His^2 Trp^3 Leu^4 Gln^5 Leu^6 Lys^7 Pro^8 Gly^9 Gln^{10} Pro^{11} Met^{12} Tyr^{13}. The pheromone binds to a corresponding GPCR that is encoded by the *STE2* gene and expressed on the cell surface of *MAT**a*** cells. Extensive structure-function analyses of α-factor analogs have provided insights into the structural basis of α-factor activity. Biochemical and biophysical analysis on α-factor and its constrained analogs have provide evidence that a β-turn involving the Pro^8-Gly^9

Figure 4. *Saccharomyces cerevisiae* mating pathway. Binding of pheromone to the receptor stimulates downstream responses such as transcriptional activation of pheromone-induced genes, cell-cycle arrest, and polarization of the cytoskeleton and growth components to the site of highest pheromone pathway. Adapted from Madden and Snyder (62).

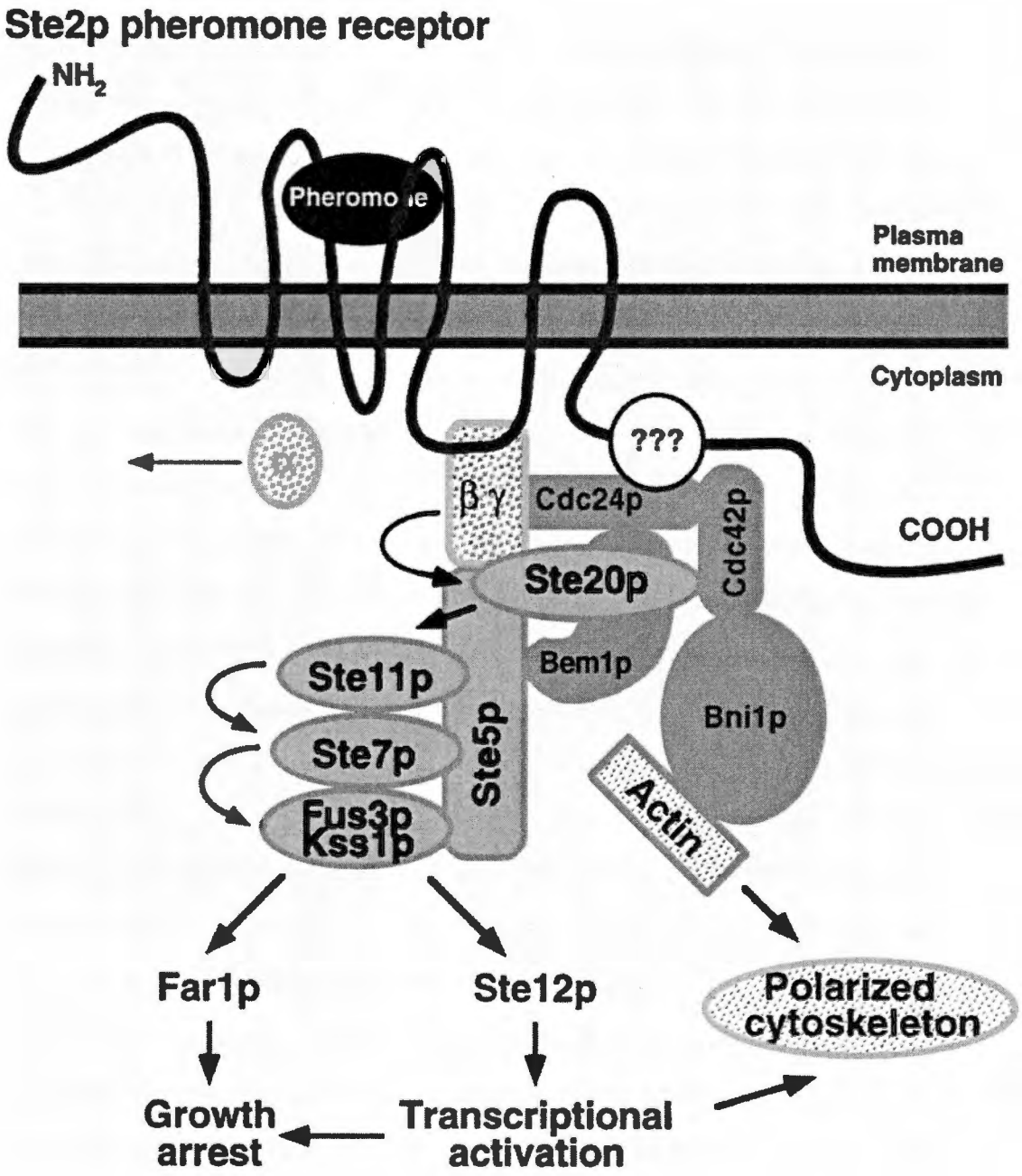
Ste2p pheromone receptor
NH2
Pheromone
Plasma membrane
Cytoplasm
???
COOH
βγ
Cdc24p
Cdc42p
Ste20p
Bem1p
Bni1p
Ste11p
Ste7p
Fus3p
Kss1p
Ste5p
Actin
Far1p
Ste12p
Polarized cytoskeleton
Growth arrest
Transcriptional activation

residues is an important determinant of the biologically active structure of the pheromone (63-67). Study of α-factor analogs modified at various positions of α-factor (deletions and substitutions) resulted in discovering antagonists and a synergist and implicated that binding and signal transduction are separable processes in the interaction between pheromone and receptor (68-71). Finally, in conjunction with those results described above, results from structure-function analysis of L- and D-Ala scanned analogs allowed assignment of general functional domains in α-factor (72).

Three functional domains are assigned in the proposed model of the functional domains of α-factor depicted in Figure 5 (72): 1) N-terminal signaling domain – The strong antagonism and relatively high binding affinity exhibited by D-Ala^3, D-Ala^4, desTrp^{1}desHis^2, and desTrp^{1}Ala^3 α-factor analogs suggested that these residues at the amino terminus play a very important role in signal transduction; 2) C-terminal binding domain – Replacement at position 10, 11, 12 and 13 with L- or D-Alanine resulted in marked reduction in binding affinity while most of alanine scan analogs at this region induced a rather efficient signal; 3) The bend region of α-factor – the center of the α-factor constitutes a bend region that orients the N-terminal signaling and C-terminal binding domains of α-factor for optimal interactions with the receptor and provides structural stability for the functionally active ends of the peptide.

The separation of functional domains for binding and activity and/or the occurrence of bend structure have been documented for other peptide hormones. Stepwise truncation from N-terminus of parathyroid hormone (PTH,

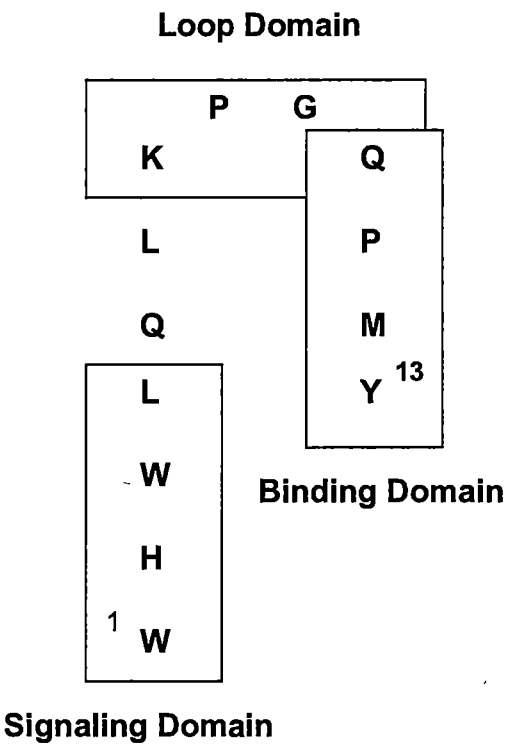

Figure 5. Functional domains of α-factor. The residues at the N-terminal region appear to mainly function in activation of receptor signaling while contributing to overall binding of α-factor. The C-terminal domain mainly functions for high affinity binding of α-factor to the receptor. The loop domain corresponds to residues which are thought to produce a turn in α-factor.

34 residues) generated an antagonist, thus defining the N-terminal 6 residues as the "principal activation domain". Detailed structure-activity studies indicated that structural features of this hormone for receptor binding are clustered in C-terminal domain, which was therefore designated as the "principal binding domain" (73). The study of a decapeptide gonadotropin-releasing hormone demonstrated that N- and C-terminal regions are the most important for binding and receptor activation, whereas the central hairpin structure are involved in conferring flexibility to the peptide (74). In angiotensin II octapeptide, the biological activity is highly dependent on C-terminal Phe^8 residue, while N-terminal residues are important for receptor binding (75). In addition, the conformation of angiotensin II suggested the presence of inverse γ-turn in the C-terminal region (76).

It is not clear yet whether the separation of domains and/or the bend structure are common features to most peptide hormones whether there is a functional significance to these structural motifs. One possible explanation may relate to the mode of receptor binding and activation by peptide ligands as suggested in Chapter 1. In the sequential binding and conformational stabilization model, one structural group of peptide ligands initially interacts with receptor. Following the initial binding of one structural group (possibly binding domain), binding of remaining groups occurs in a sequential manner as a result of random and spontaneous movement of TM domains to positions that permit interaction with functional group (possibly signaling domain). The bend region may give structural flexibility to the signaling domain so as to find or induce a

correct receptor conformation. It is possible that the same process is occurred in α-factor binding to its receptor.

Functional analysis of α-factor receptor, Ste2p – The yeast α-factor receptor is an extensively studied G protein-coupled receptor with seven hydrophobic membrane-spanning helix domains involved in sensing the mating pheromone α-factor during the process of conjugation. Although many techniques have been applied to study receptor function, much of our knowledge on the structure and mechanism of α-factor receptor activation comes from the characterization of mutant receptors (Figure 6).

The analysis of constitutively active mutants indicates that movement of TM 6 plays a key role in α-factor receptor activation (50, 77, 78). In addition, studies with chimeric receptors between *S. cerevisiae* and *S. kluyveri* α-factor receptors suggested that the specificity between *S. cervisiae* and *S. kluyveri* α-factor is determined by three small regions of receptor (79, 80). Analysis of dominant negative (DN) mutant receptors, which interfere with wild type activity by competing for the G protein, suggested that similar mutations can occur in other GPCRs and that the possible involvement of DN mutations with human disease (80). Some of these residues are also predicted to be involved in α-factor binding (81, 82). A study of mutant receptors using random mutagenesis identified residues in the receptor which response to an antagonist desTrp^{1}Ala^{3} α-factor analog. One double mutant (L255S, S288P) was able to induce *FUS1-*

Figure 6. View of the relative positions of mutations in α-factor receptor. *Circles* outlined in bold indicate the mutations in these residues lead to constitutively active receptor (50,77,78). *Black filled-circles* indicate the residues affected by dominant-negative mutations (80-82). *Squares* indicate the residues that mutations confer altered ligand specificity (83). *Triangles* indicate the mutations resulted in second-site intragenic suppressors for the loss of function mutations in TM3 (*I142N,E143K,T144P*) (84). *Arrowhead lines* indicate minimal region for ligand specificity between *S. cerevisiae* and *S. kluyveri* α-factors (79,80). *The dotted black line* between TM5 and 6 indicates the residues that where close proximity was identified by cysteine cross-linking experiment (85). *A set of dotted lines* between TM6 and 7 mark the predicted intramolecular contact that was identified by analysis of constitutive mutants (50).

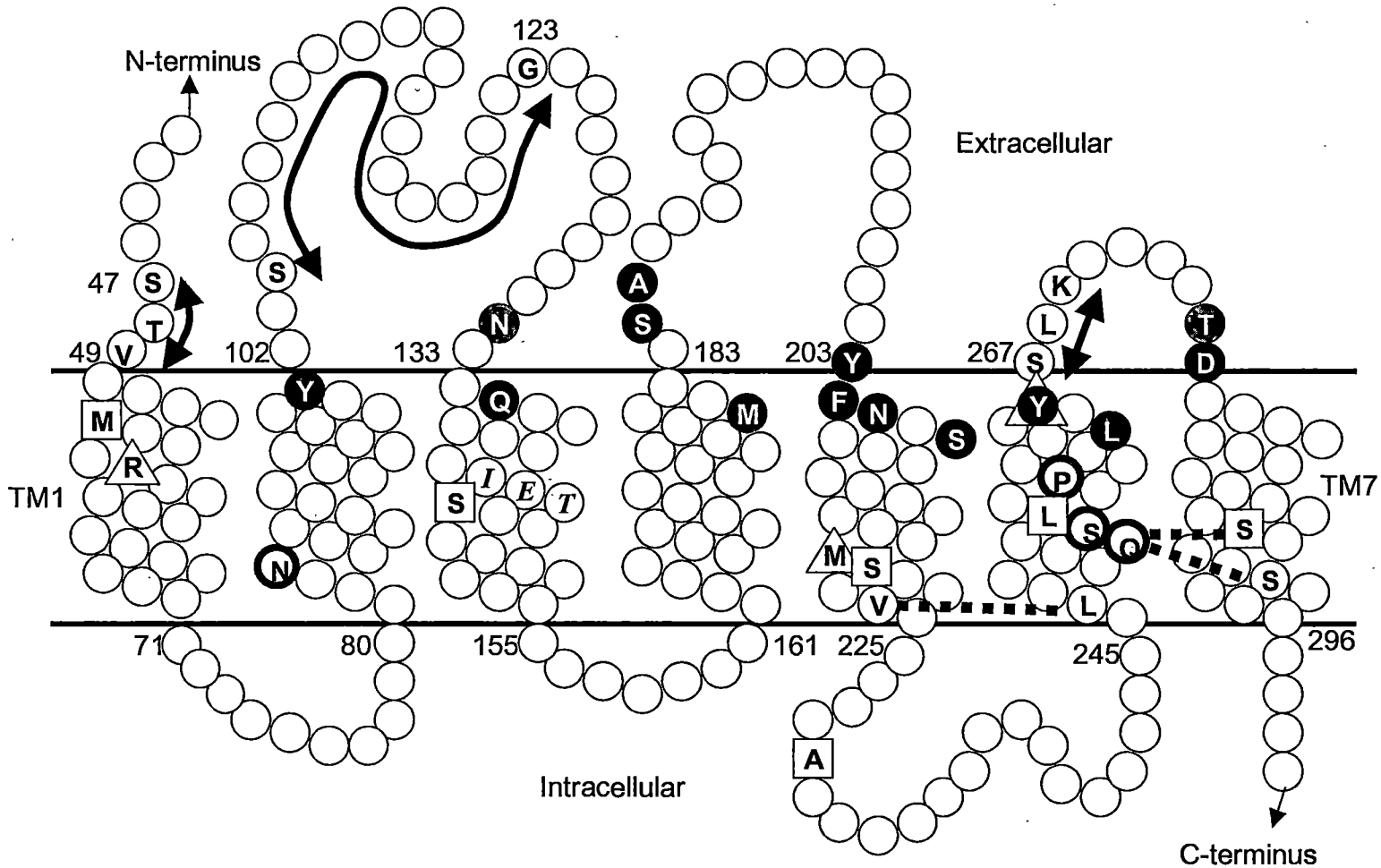
N-terminus
123
G
Extracellular
47
S
T
49
V
102
133
183
203
267
S
S
N
A
S
K
L
S
T
D
Y
Y
M
R
TM1
Y
Q
M
F
N
S
Y
L
P
L
S
Q
S
S
TM7
S
I
E
T
N
M
S
V
L
71
80
155
161
225
245
296
A
Intracellular
C-terminus

lacZ reporter but did not respond to growth arrest assay implicating G protein signaling can be separated in downstream pathway (83). Genetic interactions among TM domains of α-factor receptor were studied by selecting the second-site intragenic suppressors for the initial loss of function mutations in TM 3 (84). The results indicated that a physical interaction between TM3 and TM6, and that a role of R58 residue as a global stabilization factor of the α-factor receptor.

Two recent biophysical studies on α-factor receptor have provided an important frame work for understanding the structure and function of this receptor. Dube *et.al.,* (85) demonstrated that there is a direct interaction between TM5 and TM6 using cysteine cross-linking techniques. In another study, peptide segment of individual TM domains of α-factor receptor were examined biophysically (86). The results of both studies indicated an important role of the interactions among TM 3, 5, and 6 for receptor activation process and provided strong evidence that, despite a lack of sequence homology among the GPCR family, there is a remarkable similarity in the structure and function of these receptors.

Regulation of α-factor receptor signaling in S. cerevisiae – Three distinct processes contribute to α-factor receptor regulation: 1) rapid phosphorylation and desensitization (uncoupling of the receptor from the G protein) (87); 2) internalization and recycling (88); and 3) down-regulation and degradation (89). In most GPCRs, phosphorylation and trafficking events are associated with acute desensitization because the immediate occurrence of these events coincides with the rapid desensitization observed with most receptors. Receptor down-

regulation, which is defined as an overall reduction in receptor levels in the cell, is associated with longer term effects on signaling and occur over the course of several hours or even days (90).

In addition to the regulation processes at the receptor level, recent findings suggest that down-regulation of receptor signaling also occurs at the G protein or downstream elements. Since the pheromone response elicited by mating factors is transient, in the absence of mating, yeast cells reenter the cell cycle through a process of recovery or desensitization. One of regulators is Sst2p, a yeast homologue of regulators of G protein signaling (RGS), which attenuates G protein signaling by accelerating GTP hydrolysis and promoting subunit reassociation (91). Sst2p itself is regulated by proteolytic cleavage and this processing appears to be regulated spatially (92). An implication was the proteolytic cleavage of Sst2p occurs predominantly at the region exposed to high concentration of pheromones. Diminished Sst2p activity may result in enhanced signaling at the tip of the mating projection. Consistent with this, Zhou *et.al.*, (93) reported that, in the growth arrest assay, Sst2p is involved in recovery at low pheromone concentration, while phosphatases such as Msg5p and Mpt5p have a role in adaptive mechanism at higher concentration of pheromone. Additionally, the identification of novel regulators (Plp1 and Plp2) which selectively down-regulate early signaling events (e.g. *FUS1-lacZ* induction), but have no effect in growth arrest strongly suggest separation of these two important signaling pathways (94).

The separation in the regulation of receptor signaling may explain the discrepancy in results between early gene induction assay and growth arrest assay which occasionally observed elsewhere (79-83).

α-factor receptor as a model for GPCRs – Because of the wide array of cellular processes that are mediated by GPCRs, the study of GPCR function and regulation holds a prominent position in the field of signal transduction research. Understanding the structural basis of receptor activation is obviously crucial to any based attempt to design and to develop novel drugs targeted to this clinically important receptor family.

S. cerevisiae α-factor receptor system is an ideal system for understanding GPCRs activation mechanism for peptide hormones. The most salient properties of *S. cerevisiae* system are: 1) the availability of yeast genetic approaches to examine structure-function relationship; 2) physiological stoichiometry of receptor vs. G protein; 3) no cross-talk between GPCRs because a haploid yeast contains only one type of GPCR (Ste2p or Ste3p). Moreover, as described in this chapter, we now have substantial information about the structure and function of α-factor and its receptor.

However, one important and very critical gap for understanding α-factor receptor activation mechanism is the lack of information about binding sites of α-factor. No specific binding region between α-factor and the receptor has been proposed or tested so far. Mapping of α-factor binding regions in α-factor

receptor could give great insight for understanding receptor activation mechanisms of α-factor receptor and other GPCRs.

Part II describes development of iodinated α-factor analogs as tools for the study of α-factor binding sites. Part III describes the study of mutant α-factor receptors with altered ligand specificity. Part IV attempts to identify receptor regions which interacts with 10^{th} Gln residue of α-factor.

List of References for Part 1

1. **Bargmann, C.I.** (1998) Neurobiology of the *Caenorhabditid elegans* genome. *Science* 282:2028
2. **Horn, F., Weare, J., Beukers, M.W., Horsh, S., Bairoch, A., Chen, W., Campagne, F., Vriend, G.** (1998) GPCRDB: an information system for G protein-coupled receptors. *Nucleic Acids Res.* 26:275
3. **Aldler E., Lindemeier J., Battey J.F., Ryba Hoon MA., N.J., and Zuker C.C.** (1999) Putative mammalian taste receptors: a class of taste-specific GPCRs with distinct topographic selectivity. *Cell* 96:541
4. **Bourne, H.R., Sanders, D.A., and McCormick, F.** (1991) The GRPase super-family: conserved structure and molecular mechanism. *Nature* 349:117
5. **Hamm, H.E.** (1998) The many faces of G protein signaling. *J. Biol. Chem.* 272:669
6. **Gudermann, T., Nurnberg, B., and Schultz, G.** (1995) Receptors and G proteins as primary components of transmembrane signal transduction. *J. Mol. Med.* 73:51
7. **Flower, D.R.** (1999) Modeling G protein-coupled receptors for drug design. *Biochim. Biophys. Acta* 142:207
8. **Stadel, J.M., Wilson, S., Bergsma, D.J., and Orphan, G.** (1997) Protein-coupled receptors: a neglected opportunity for pioneer drug discovery. *Trends Pharmacol. Sci.* 18:430

9. **Littman, D.R.** (1998) Chemokine receptors: keys to AIDS pathogenesis? *Cell* 93:677

10. **Dreyer, W.J.** (1998) The area code hypothesis revisited – olfactory receptors and other related transmembrane receptors may function as the last digits in a cell surface code for assembling embryos. *Proc. Natl. Acad. Sci. USA* 95:9072

11. **Palczewski, K., Kumasaka, T., Hori, T., Behnke, C. Motoshima, H., Fox, B., Le Trong, I., Teller, D.C., Okada, T., Stenkmap, R.E., Yamamoto, M., and Miyano, M.** (2000) Crystal structure of rhodopsin: a G protein-coupled receptor. *Science* 289:739

12. **Unger, V.M., Hargrave, P.A., Baldwin, J.M., and Schertler, G.F.** (1997) Arrangement of rhodopsin transmembrane α-helices. *Nature* 389:203

13. **Krebs, A., Villa, C., Edwards, P.C., and Schertler, G.F.** (1998) Characterization of improved two-dimensional p22121 crystal from bovine rhodopsin. *J. Mol. Biol.* 282:991

14. **Davis, A., Schertler, G.F., Gowen, B.F., and Saibil, H.R.** (1996) Projection structure of an invertebrate rhodopsin. *J. Struct. Biol.* 117:36

15. **Zhou, W., Flanagan, C., Ballesteros, J.A., Konvicka, K., Davidson, J.S., Weinstein, H., Millar, R.P., and Sealfon, S.C.** (1994) A reciprocal mutation supports helix 2 and helix 7 proximity in the gonadotropin-releasing hormone receptor. *Mol. Pharmacol.* 45:165

16. **Schonberg, L.J., Rhee, M., and Wess, J.** (1995) Mutational analysis of the relative orientation of transmembrane helices I and VII in G protein-coupled receptor. *J. Biol. Chem.* 27):19532

17. **Elling, C.E., Nielsen, S.M., and Schwartz, T.W.** (1996) Connectivity and orientation of the seven helical bundle in the tachykinin NK-1 receptor probed by zinc site engineering. *EMBO J.* 15:6213

18. **Turcatti, G., Nemeth, K., Edgerton, M.D., Meseth, U., Talabot, T., Peitsch, M., Knowles, J., Vogel, H., and Chollet, A.** (1996) Probing the structure and function of the tachykinin NK-2 receptor through biosynthetic incorporation of fluorescent amino acids at specific sites. *J. Biol. Chem.* 271:19991

19. **Zeng, F.Y., Hopp, A., Soldner, A., and Wess, J.** (1999) Use of disulfide cross-linking strategy to study muscarinin receptor structure and mechanism of activation. *J. Biol. Chem.* 274:16629

20. **Altenbach, C., Klein-Seetharaman, J., Hwa, J., Khorana, H.G., and Hubbell, W.L.** (1999) Structural features and light-dependent changes in the sequence 59-75 connecting helices I and II in rhodopsin: a site-directed spin-labeling study. *Biochemistry* 38:7945

21. **Kobilka, B.** (1992) Adrenergic receptors as models for G protein-coupled receptors. *Annu. Rev. Neurosci.* 15:87

22. **Strader, C.D., Fong, T.M., Graziano, M., and Tota, M.R.** (1995) The family of G protein-receptors. *FASEB J.* 9:745

23. **Ji, T.H., Grossmann, M., and Ji, I** (1998) G protein-coupled receptors. I. Diversity of receptor-ligand interactions. *J. Biol. Chem.* 273:17299

24. **Heerding, J.N., and Yee, D.K., Jacobs, S.L., and Fluharty, S.J.** (1997) Mutational analysis of the angiotensin II type 2 receptor: contribution of conserved extracellular amino acids. *Regul. Peptides* 72:97

25. **Thibonnier, M., Coles, P., Doreen, M., Christine, L., Plesnicher, L., and Shoham, M.** (2000) A molecular model of agonist and nonpeptide antagonist binding to the human V_1 vascular vasopressin receptor. 294:195

26. **Davidson, J.S., Assefa, D., Pawson, A., Davies, P., Hapgood, J., Becker, I., Flanagan, C., Roeske, R., and Millar, R.** (1997) Irreversible activation of the gonadotropin-releasing hormone receptor by photoaffinity cross-linking: localization of attachment site to Cys residue in N-terminal segment. *Biochemistry* 36:12881

27. **Pepin, M.C., Yue, S.Y., Roberts, E., Wahlestedt, C., and Walker, P.** (1997) Novel "restoration of function" mutagenesis strategy to identify amino acids of the δ-opioid receptor involved in ligand binding. *J. Biol. Chem.* 272:9260

28. **Silvente-Poirot, S., Escrieut, C., and Wank, S.A.** (1998) Role of extracellular domains of the cholecystokinin receptor in agonist binding. *Mol. Pharmacol.* 54:364

29. **Wijkhuisen, A., Sagot, M.A., Frobert, Y., Creminon, C., Grassi, J., Boquet, D., and Couraud, J.Y.** (1999) Identification in the NK1 tachykinin receptor of a domain involved in recognition of neurokinin A and sptide but not of substance P. *FEBS Lett.* 447:155

30. **Barroso, S., Richard, F., Nicholas-Etheve, D., Reversat, J.L., Bernassau, J.M., Kitabgi, P., and Labbe-Jullie, C.** (2000) Identification of residues

involved in neurotensin binding and modeling of the agonist binding site in neurotensin receptor 1. *J. Biol. Chem.* 275:328

31. **AbdAlla, S., Jamagin, K., Muller-Esterl, W., and Quitterer, U.** (1996) The N-terminal amino group of [Tyr^{8}]bradykinin is bound adjacent to analogous amino acids of the human and rat B2 receptor. *J. Biol. Chem.* 271:27382

32. **Dong, M., Asmann, Y., Zand, M., Pinon, D., and Miller, L.** (2000) Identification of two pairs of spatially approximated residues within the carboxy-terminus of secretin and its receptor. *J. Biol. Chem.* in press

33. **Boyd, N.D., Kage, R., Dumas, J.J., Krause, J.E., and Leeman, S.E.** (1996) The peptide binding site of the substance P (NK-1) receptor localized by a photoreactive analogue of substance P: presence of disulfide bond. *Proc. Natl. Acad. Sci. USA* 93:433

34. **Piserchio, A., Bisello, A., Rosenblatt, M., Chorev, M., and Mierke, D.** (2000) Characterization of parathyroid hormone/receptor interactions: structure of the first extracellular loop. *Biochemistry* 39:8153

35. **Mouledous, L., Topham, M., Mazarguil, H., and Meunier, J.-C.** (2000) Direct identification of a peptide binding region in the opioid receptor-like 1 receptor by photoaffinity labeling with [Bpa^{10},Tyr^{14}]nociceptin. *J. Biol. Chem.* 275:29268

36. **Perlman, J.H., Laakkonrn, L., Osman, R., and Gershengorn, M.C.** (1994) A model of the thyrotropin-releasing hormone (TRH) receptor binding pocket. Evidence for a second direct interaction between transmembrane helix 3 and TRH. *J. Biol. Chem* 269:23383

37. **Mills, J.S., Miettinen, H.M., Barnidge, D., Vlases, M.J., Wimer-Mackin, S., Dratz, E.A., Sunner, J., and Jesaitis, A.J.** (1998) Identification of a ligand binding site in the human neutrophil formyl peptide receptor using a site-specific fluorescent photoaffinity label and mass spectrometry. *J. Biol. Chem.* 273:10428

38. **Monnot, C., Bihoreau, C., Conchon, S., Curnow, K.M., Corvol, P., and Clauser, E.** (1996) Polar residues in the transmembrane domains of the type1 angiotensin II receptor are required for binding and coupling. Reconstitution of the binding site by co-expression of two deficient mutants. *J. Biol. Chem.* 271:1507

39. **Webb, M.L., Patel, P.S., Rose, P.M., Liu, E.C., Stein, P.D., Lach, D.A., Fisher, S.M., Hadjilambris, O., Lee, H., Dickinson, K.E., and Krystek, S.R.** (1996) Mutational analysis of the endothelin type A recetpor (ETA): interactions and model of selective ETA antagonist BMS-182874 with putative ETA receptor binding cavity. *Biochemistry* 35:2548

40. **Kaupmann, K., Bruns, C., Raulf, F., Weber, H.P., Mattes, H., and Lubbert, H.** (1995) Two amino acids, located in transmembrane domains VI and VII, determine the selectivity of the peptide agonist SMS 201-995 for the SSTR2 somatostatin receptor. *EMBO J.* 14:727

41. **Befort, K., Tabbara, L., Kling, D. Maigret, B., and Kieffer, B.L.** (1996) Role of aromatic transmembrane residues of the δ-opioid receptor in ligand recognition. *J. Biol. Chem.* 271:0161

42. **Fathy, D.B., Mathis, S.A., Leeb, T., and Leeb-Lundberg, L.M.** (1998) A single position in the third transmembrane domains of the human B1 and B2 bradykinin receptors is adjacent to and discriminates between the C-terminal residues of subtype-selective ligands. *J. Biol. Chem.* 273:12210

43. **Fanelli, F., Barbier, P., Zanchetta, D., De Benedetti, P.G., and Chini, B.** (1999) Activation mechanism of human oxytocin receptor: a combined study of experimental and computer-simulated mutagenesis. *Mol. Pharmacol.* 56:214

44. **Flanagan, C., Rodic, V., Konvicka, K., Yuen, T., Millar, R.P., Weinstein, H., and Sealfon, S.C.** (2000) Multiple interactions of the $Asp^{2.61(98)}$ side chain of the Gonadotropin-releasing hormone receptor contribute differentially to ligand interaction. *Biochemistry* 39:8133

45. **Farrens, D.L., Altenbacetylcholine, C., Yang, K., Hubbell, W., and Khorana, H.G.** (1996) Requirement of rigid-body motion of transmembrane helices for light-activation of rhodopsin. *Science* 274:768

46. **Gether, U., Lin, S., and Kobilka, B.K.** (1997) Agonists induce confomational changes in transmembrane domains III and VI of the β_2-adrenoreceptor. *EMBO J.* 16:6737

47. **Javitch, J.A., Fu, D., Liapakis, G., and Chen, J.** (1997) Constitutive activation of the β_2 adrenergic receptor alters the orientation of its sixth membrane-spanning segment. *J. Biol. Chem.* 272:18546

48. **Rasmussen, S.G., Jensen, A.D., Liapakis, G., Ghanouni, P., Javitch, J.A., and Gether, U.** (1999) Mutation of a highly conserved aspartic acid in the β_2

adrenergic receptor: constitutive activation, structural instability, and conformational rearrangement of transmembrane segment 6. *Mol. Pharmacol.* 56:175

49. **Spalding, T.A., Burstein, E.S., Henderson, S.C., Ducote, K.R., and Brann, M.R.** (1998) Identification of a ligand-dependent switch within a muscarinic receptor. *J. Biol. Chem.* 272:21563

50. **Dube, P., and Konopka, J.B.** (1998) Identification of a polar region in transmembrane domain 6 that regulates the function of the G protein-coupled α-factor receptor. *Mol. Cell. Biol.* 18:7205

51. **Leff, P.** (1995) The two-state model of receptor activation. *Trends Pharmacol. Sci.* 16:89

52. **Wiens, B.L., Nelson, C.S., and Neve, K.A.** (1998) Contribution of serine residues to constitutive and agonist-induced signaling via the D2S dopamine receptor: evidence for multiple, agonist-specific active conformations. *Mol. Pharmacol.* 54:435

53. **Mahouty-Kodja, S., Barak, L.S., Scheer, A., Abuin, L., Diviani, D., Caron, M.G., and Cotecchia, S.** (1999) Constitutively active α-1b adrenergic receptor mutants display different phosphorylation and internalization features. *Mol. Pharmacol.* 55:339

54. **Kobilka, B., Gether, U., Seifert, R., Lin, S., and Ghanouni, P.** (1999) Characterization of ligand-induced conformational states in the beta$_2$ adrenergic receptor. *J. Recept. Signal Transduct. Res.* 19:293

55. **Schwartz, T.W., Gether, U., Schambye, H.T., and Hjorth, S.A.** (1995) Molecular mechanism of action of non-peptide ligands for peptide receptors. *Curr. Pharmacol. Design* 1:325

56. **Gether, U., and Kobilka, B.K.** (1998) G protein-coupled receptors. II. Mechanism of agonist activation. *J. Biol. Chem.* 273:17979

57. **Jarnagin, K., Bhakta, S., Zuppan, P., Yee, C., Pease, H.B., Miller, A., and Freedman, R.** (1996) Mutations in the B2 bradykinin receptor reveal a different pattern of contacts for peptidic agonists and peptidic antagonists. *J. Biol. Chem.* 271:28227

58. **Turner, P.R., Mefford, S., Bambino, T., and Nissenson, R.A.** (1998) Transmembrane residues together with the amino terminus limit the response of the parathyroid hormone (PTH) 2 receptor to PTH-related peptide. *J. Biol. Chem.* 273:3830

59. **Bourne, H.R.** (1997) How receptors talk to trimeric G proteins. *Curr. Opin. Cell Biol.* 9:134

60. **Schultz, J., Fergusson, B., and Sprague, G.F.** (1995) Signal transduction and growth control in yeast. *Curr. Biol.* 5:31-37

61. **Herskowitz, I.** (1995) MAP kinase pathway in yeast: for mating and more. *Cell* 80:187-197

62. **Madden, K., and Snyder, M.** (1998) Cell polarity and morphogenesis in budding yeast. *Annu. Rev. Microbiol.* 52:687-774

63. **Xue, C.B., Eriotou-Bargiota, E., Miller, D., Becker, J.M., and Naider, F.** (1989) A covalently constrained congener of the *Saccharomyces cerevisiae* tridecapeptide mating pheromone is an agonist. *J. Biol. Chem.*264:19161

64. **Yang, W., McKinney, A., Becker, J.M., and Naider, F.** (1995) Systematic analysis of the *Saccharomyces cerevisiae* α-factor containing lactam constraints of different ring size. *Biochemisty* 34:1308

65. **Xue, C.B., Mckinney, A., Lu, H.F., Jiang, Y., Becker, J.M., and Naider, F.** (1996) Probing the functional conformation of the tridecapeptide mating pheromone of *Saccharomyces cerevisiae* through study of disulfide-constrained analog. *Int. J. Pept. Protein Res.* 47:131

66. **Antohi, O., Marepalli, H.R., Yang, W., Becker, J.M., and Naider, F.** Conformational analysis of cyclic analogues of the *Saccharomyces cerevisiae* α-factor pheromone. *Biopolymers* 45:21

67. **Zang, Y.L., Marepalli, H.R., Lu, H.F., Becker, J.M., and Naider, F.** (1998) Synthesis, biological activity, and conformational analysis of peptidomimetic analogues of the *Saccharomyces cerevisiae* α-factor tridecapeptide. *Biochemistry* 37:12465

68. **Raths, S.K., Naider, F., and Becker, J.M.** (1988) Peptide analogues compete with the binding of α-factor to its receptor *in Saccharomyces cerevisiae. J. Biol. Chem.* 263:17333

69. **Eriotou-Bargiota, E., Xue, C.B., Naider, F., and Becker, J.M.** (1992) Antagonistic and synergistic peptide analogues of the tridecapeptide mating pheromone of *Saccharomyces cerevisiae. Biochemistry* 31:551

70. **Levin, Y., Khare, R.K., Abel, G., Hill, D., Eriotou-Bargiota, E., Becker, J.M., and Naider, F.** (1993) Histidine 2 of the α-factor *of Saccharomyces cerevisiae* is not essential for binding to its receptor for biological activity. *Biochemistry* 32:8199

71. **Zhang, Y., Lu, H.F., Becker, J.M., and Naider, F** (1997) Position one analogs of the *Saccharomyces cerevisiae* tridecapeptide pheromone. *J. Pept. Res.* 50:319

72. **Abel, M.G., Zhaing, Y.L., Lu, H.F., Naider, F., and Becker, J.M.** (1998) Structure-function analysis of the *Saccharomyces cerevisiae* tridecapeptide pheromone using alanine-scanned analogs. *J. Pept. Res.* 52:95

73. **Greenberg, Z., Bisello, A., Mierke, D.F., Rosenblatt, M., and Chorev, M.** (2000) Mapping the bimolecular interface of the parathyroid hormone (PTH)-PTH 1 receptor complex: Spatial proximity between Lys^{27} (of the hormone principal binding domain) and Leu^{261} (of the first extracellular loop) of the human PTH1 receptor. *Biochemistry* 39:8142

74. **Chauvin, S., Berault, A., Lerrant, Y., Hibert, M., and Counis, R.** (2000) Functional importance of transmembrane helix 6 Trp^{279} and exoloop 3 Val^{299} of rat gonadotropin-releasing hormone receptor. *Mol. Pharmacol.* 57:625

75. **Gasparo, M., Catt, K.J., Inagami, T., Wright, J.W., and Unger, T.** (2000) International union of pharmacology. XXIII. The angiotensin II receptors. *Pharmacol. Rev.* 52:415

76. **Carpenter, K.A., Wilkes, B.C., and Schiller, P.W.** (1998) The octapeptide angiotensin II adopts a well-defined structure in a phospholipid environment. *Eur. J. Biochem.* 251:448

77. **Konopka, J.B., Margarit, M.,and Dube, P.** (1996) Mutation of pro-258 in transmembrane domain 6 constitutively activates the G protein-coupled α-factor receptor. *Proc. Natl. Acad. Sci. USA* 93:6764

78. **Sommers, C.M., Martin, N.P., Akal-Strader, A., Becker, J.M., Naider, F., and Dumont, M.E.** (2000) A limited spectrum of mutations causes constitutive activation of the yeast α-factor receptor. *Biochemistry* 39:6898

79. **Sen, M., and Marsh, L.** (1994) Noncontiguous domains of the α-factor receptor of yeasts confer ligand specificity. *J. Biol. Chem.* 269:968

80. **Sen, M., Shah, A., and Marsh, L.** (1997) Two types of α-factor receptor determinants for pheromone specificity in the mating-incompatible *yeasts S. cerevisiae* and *S. kluyveri. Curr. Genet.* 31:235

81. **Dosil, M., Giot, L., Davis, C., and Konopka, J.B.** (1998) Dominant-negative mutations in the G protein-coupled α-factor receptor map to the extracellular ends of the transmembrane segments. *Mol. Cell. Biol.* 18:5981

82. **Leavitt, L.M., Macaluso, C.R., Kim, K.S., Martin, N.P., and Dumont, M.E.** (1999) Dominant negative mutations in the α-factor receptor, a G protein-coupled receptor encoded by the *STE2* gene of the yeast *Saccharomyces cerevisiae. Mol. Gen. Genet.* 261:917

83. **Marsh, L.** (1992) Substitutions in the hydrophobic core of the α-factor receptor of *Saccharomyces cerevisiae* permit response to *Saccharomyces kluyveri* α-factor and to antagonist. *Mol. Cell. Biol.* 12:3959

84. **Sommers, C.M., and Dumont, M.E.** (1997) Genetic interactions among the transmembrane segments of the G protein coupled receptor encoded by the yeast *STE2* gene. *J. Mol. Biol.* 266:559

85. **Dube, P., DeCostanzo, A., and Konopka, J.B.** (2000) Interaction between transmembrane domains five and six of the α-factor receptor. *J. Biol. Chem.* 275:26492

86. **Xie, H., Ding, F.-X., Schreiber, D., Eng, G., Liu, S.-F, Arshava, B., Arevalo, E, Becker, J.M., and Naider, F.** (in press) Synthesis and biophysical analysis of transmembrane domains of a *Saccharomyces cerevisiae* G protein-coupled receptor. *Biochemistry*

87. **Chen, Q., and Konopka, J.B.** (1996) Regulation of the G protein-coupled α-factor pheromone receptor by phosphorylation. *Mol. Cell. Biol.* 16:247

88. **Hicke, L., and Riezman, H.** (1996) Ubiqitination of a yeast plasma membrane receptor signals its ligand-stimulated endocytosis. *Cell* 84:277

89. **Stefan, C.J., and Blumer, K.J.** (1999) A syntaxin homolog encoded by *VAM3* mediates down-regulation of a yeast G protein-coupled receptor. *J. Biol. Chem.* 274:1835

90. **Kallal, L., and Benovic, J.L.** (2000) Using green fluorescent proteins to study G protein-coupled receptor localization and trafficking. *Trends Pharmacol. Sci.* 21:175

91. **Dohlman, H.G., and Thorner, J.** (1997) RGS proteins and signaling by heterotrimeric G proteins. *J. Biol. Chem.* 272:3871

92. **Hoffman, G.A., Garrison, T.R., and Dohlman H.G.** (in press) Endoproteolytic processing of Sst2, a multi-domain RGS protein in yeast. *J. Biol. Chem.*

93. **Zhou, J., Arora, M., and Stone, D.** (1999) The yeast pheromone-responsive Gα protein stimulates recovery from chromic pheromone treatment by two mechanisms that are activated at distinct levels of stimulus. *Cell Biochem. Biophys.* 30:193

94. **Flanary,P., Dibello, P., Estrada, P., and Dohlman, H.D.** (2000) Functional analysis of Plp1 and Plp2, two homologues of phosducin in yeast. *J. Biol. Chem.* 275:18462

PART 2

Postion 13 Analogs of he Tridecapeptide Mating Pheromone from *Saccharomyces cerevisiae*: Design of an Iodinatable Ligand for Receptor Binding[§]

[§]Part II was published in its entirety as B.K. Lee, L. K. Henry, S. Liu, S. H. Wang, B. Arshava, J.M. Becker and F. Naider. 2000. Position 13 analogs of the tridecapeptide mating pheromone from *Saccharomyces cerevisiae*: design of an iodinatable ligand for receptor binding. *J. Pep. Res.* 56: p24-34. Dr. Naider's laboratory was responsible for synthesis and purification of the peptides used in the study.

CHAPTER 1

Introduction

Hepta-helical receptors are ubiquitous sensors in living cells for a diverse array of signal molecules including peptides, alkaloids, proteins, amino acids and choline esters (1,2) . This diverse family of signal transducers currently is predicted to have more than 1000 members many of which interact with heterotrimeric G proteins located on the cytoplasmic side of the plasma membrane (3-5). Although much is now known concerning the general function of hepta-helical receptors, few studies have provided a detailed description of the atomic contacts involved in ligand receptor interaction. Furthermore, the mechanism by which ligand binding results in downstream activation of the signaling pathway is not described in detail for any member of this protein family.

The yeast *Saccharomyces cerevisiae* is a sexual organism which manifests a conjugative response when opposite mating type cells, MATa and MATα, are mixed together. The mating process is driven by exchange of diffusible mating factors, the a-factor (Tyr-Ile-Ile-Lys-Gly-Val-Phe-Trp-Asp-Pro-Ala-Cys[farnesyl]OCH_3)[1] and the α-factor (Trp-His-Trp-Leu-Gln-Leu-Lys-Pro-Gly-Gln-Pro-Met-Tyr), which interact with reciprocal receptors (Ste3p and Ste2p, respectively) on the opposite cell type (6,7). Receptor binding results in activation of G proteins which leads to a series of events including G1 growth arrest, cellular elongation, gene induction, agglutinin biosynthesis and ultimately

cell fusion. The hepta-helical receptors (Ste2p and Ste3p) have been cloned (8,9) and identified to be unique members of this family of proteins classified in subgroup D (3). Moreover, Ste2p was recently expressed in high copy number, purified to near homogeneity and reconstituted in active form in synthetic membrane vesicles (10). The availability of relatively large quantities of this receptor protein and of highly developed genetic tools for working with *S. cerevisiae* have stimulated the use of the α-factor receptor as a paradigm to learn about the biochemistry of hepta-helical receptors.

Previous investigations on α-factor - Ste2p interactions have involved both measurement of biological activities of synthetic analogs and assessment of their binding to the receptor (11-15). The receptor binding assay presently used for α-factor involves use of either tritiated pheromone prepared synthetically (16) or ^{35}S labeled α-factor prepared biosynthetically (17,18). Neither of these ligands is completely satisfactory. The tritiated pheromone is expensive to prepare and has a specific activity limited to 10-20 Ci/mmole. The biosynthetic ligand is difficult to obtain in quantity and cannot be prepared readily in forms containing amino acid analogs such as photoactivatable groups useful for receptor studies. These limitations make it problematic to use these probes in affinity labeling studies designed to determine contacts between residues of α-factor and the Ste2p binding site. An obvious alternative to the above ligands would be preparation of iodinated α-factor. However, iodination of Tyr^{13} was reported to virtually eliminate the biological activity of the pheromone (19) Moreover, structure-activity studies concluded that the phenolic OH of Tyr^{13} was important for biological activity since

substitution of Tyr by Phe resulted in nearly 10^4 decrease in activity as judged in a morphogenesis assay (20). Recently, the importance of the Tyr side chain was further indicated in an Ala scan analysis of α-factor (15). Replacement of Tyr^{13} with Ala or *D*-Ala led to a 500-fold and greater than 3000-fold decrease in receptor affinity, respectively.

The above observations stymied efforts to prepare a receptor ligand with high specific activity (>1000 Ci/mmole). Recently, however, we have reevaluated the importance of the Tyr side chain. We reasoned that the phenolic group served either as a center of electron density or a hydrogen bonding moiety. Therefore, we studied the effect of replacement with a variety of functionalized aromatic rings. In this paper we report on α-factor analogs in which Tyr was replaced with *p*-fluorophenylalanine, *p*-aminophenylalanine, *p*-nitrophenylalanine or *m*-fluorophenylalanine. Peptides containing phenylalanine or serine at position 13 served as controls. The results allowed us to design new analogs of α-factor which retain relatively high biological activity and receptor affinity after iodination. One of these analogs [$Tyr(^{125}I)^1$, Phe^{13}]α-factor gave saturable binding to the Ste2p receptor which could be specifically competed by α-factor. This probe represents the first of a new series of ligands, which can be used to study α-factor- receptor interactions.

CHAPTER 2

Materials and Methods

Strains – *S. cerevisiae* LM102 (21) [*MATa ste2-dl bar1 leu2 ura3 his4 trp1 met1 fus1::lacZ(URA3)*] transformed with pGA314[*STE2*] (22) was used for the growth arrest, gene induction, and competition binding assays of various α-factor analogs. *S. cerevisiae* DK102[*MATa ste2::HIS3 bar1 leu2 ura3 lys2 ade2 his3 trp1]* transformed with pNED1[*STE2*] (10) was used in binding studies with the radioiodinated alpha factor analogs.

Synthesis of [Nle^{12}]α-factor analogs – *L*-norleucine, which is isosteric with *L*-methionine, was incorporated at position 12 to replace the original *L*-methionine in all analogs. This replacement was shown previously to result in an analog with equal activity and receptor affinity to that of the native pheromone (16). The structures of the synthetic α-factor analogs are given in Table 1. Since all analogs have Nle in place of Met^{12} this residue is eliminated from the abbreviated names for simplicity. The replacement of Met by Nle improves the synthesis and the stability of the resulting peptide. The solid phase syntheses of all the α-factor analogs were carried out automatically on an Applied Biosystems 433A peptide synthesizer (Applied Biosystems, Foster City, California) using preloaded *N*-α-Fmoc-Phe -Wang resins[1] (0.65 mmol/gram resin, Advanced

ChemTech, Louisville, Kentucky) except for the syntheses of the *p*-NO_2-Phe ^{13}, *p*-F-Phe^{13}, *m*-F-Phe^{13} and Ser^{13} analogs. In these cases, the desired Fmoc-protected amino acid was loaded onto a Wang-resin using *p*-(*N*,*N*-dimethylamino)pyridine-catalyzed esterification with dicyclohexylcarbodiimide in NMP followed by benzoic anhydride capping. 9-Fluorenylmethoxycarbonyl (Fmoc) was employed for all *N*-α-protections while the side chain protecting groups were Trp(tBoc), His(Trt), Gln(Trt) and Lys(tBoc). The '0.1-mmol FastMoc' chemistry of Applied Biosystems was utilized for the peptide chain elongation with an HBTU/HOBt/DIEA catalyzed single-coupling using 4 equivalents of protected amino acid and a 30 min. coupling time followed by an Ac_2O/HOBt/DIEA capping (10 min). The *p*-NH_2-Phe ^{13} analog was prepared by catalytically reducing the *p*-NO_2-Phe^{13} analog using 10% Pd/C in a Parr Hydrogenenation apparatus at 30 psi of hydrogen gas for one hour. The hydrogenation was judged to be complete using HPLC and the product was purified by semipreparative HPLC as described below.

Peptide Cleavage – The *N*-α-deprotected peptide resin was washed thoroughly with NMP and dichloromethane and dried *in vacuo* for 2 hours. The cleavage was carried out in a mixture of trifluoroacetic acid (10 ml), crystalline phenol (0.75 g), ethane-1,2-dithiol (0.25 ml), thioanisole (0.5 ml) and water (0.5 ml) at room temperature for 1.5 hours. After evaporation of trifluoroacetic acid under reduced pressure, the residue was precipitated and thoroughly washed with ethyl ether and extracted into 20% aqueous acetonitrile.

Purification and Characterization – The crude peptide was purified by reversed phase HPLC (Hewlett-Packard Series 1050) on a semi-preparative Waters μBondapak C_{18} (19x300 mm) column. Wavelength set for peptide detection was 220 nm. The cleavage product (45 mg) was dissolved in about 4 ml of aqueous acetonitrile (20%) containing 0.025% TFA and applied onto the column. Elution of the peptide utilized a linear gradient from 0 to 55% acetonitrile (both the water and acetonitrile reservoirs contained 0.025% TFA) over 2 hours at a flow rate of 5 ml/min. The fractions were collected and analyzed at 220 nm by reversed phase HPLC (Hewlett-Packard Series 1050) on an analytical Waters μBondapak C_{18} column (3.9x300 mm). Fractions of over 99% homogeneity were combined and lyophilized. The peptide purity was judged with analytical HPLC using two different solvent systems. Electron spray mass spectrometry was carried out at Peptidogenics Inc. Amino acid analyses were performed by the Biopolymers Laboratory at the Brigham and Womans Hospital, Boston, Massachusetts.

Growth arrest (halo) assay – Yeast nitrogen base medium (Difco) without amino acids (SD medium) supplemented with histidine (20 μg/ml), leucine (30 μg/ml) and methionine (20 μg/ml) was overlaid with 4 ml of *S. cerevisiae* LM102 cell suspension (2.5×10^5 cells/ml of Nobel agar). Filter disks (sterile blanks from Difco), 8 mm in diameter, were impregnated with 10 μl portions of peptide solutions at various concentrations and placed onto the overlay. The plates were incubated at 30^0C for 24 -36 h and then observed for clear zones (halos)

around the disks. The data were expressed as the diameter of the halo including the diameter of the disk. Therefore, a minimum value for growth arrest is 9 mm, which represents the disk diameter (8 mm) and a small zone of inhibition. All assays were carried out at least three times with no more than a 2 mm variation in halo size at a particular amount applied for each peptide. The values reported represent the mean of these tests. Similar ranks of biological activities were obtained for these analogs within an assay as measured by growth arrest (halo) or gene induction (see below). In the latter assay cells were suspended in liquid medium thereby eliminating any contribution of diffusion through agar potentially present in the halo assay.

Effect of α-Factor Analogs on Gene Induction – S. cerevisiae LM102 carries a *FUS1* gene that is inducible by mating pheromone and which is fused to the reporter gene β-galactosidase. Cells were grown overnight in SD medium at 30°C to 5 x 10^6 cells/ml, washed by centrifugation, and grown for one doubling (hemocytometer count) at 30°C. Induction was performed by adding 0.5 ml of peptide at various concentrations to 4.5 ml of concentrated cells (1 x 10^8 cells/ml). The mixtures were vortexed and placed at 30°C with shaking for 2 h. After this time, cells were harvested by centrifugation, and each pellet was resuspended and assayed for β-galactosidase production (expressed as Miller units) in triplicate by a modified (23) standard protocol (24, 25). Each experiment was carried out at least three times with the results similar in each assay.

Binding competition assay for [^{3}H]α-factor – This assay was performed using strain LM102 and tritiated α-factor prepared by reduction of [dehydroproline^8, Nle^{12}]α-factor as described previously (16). In general, cells were grown at 30^{0}C overnight and harvested at 1 x 10^7 cells/ml by centrifugation at 5,000 x g at 4^{0}C. The pelleted cells were washed two times in ice cold YM-1 medium (15) and resuspended to 4 x 10^7 cells/ml. The binding assay was started by addition of [H^3]α-factor and various concentration of non-labeled peptide (140 µl) to a 560 µl cell suspension so that the final concentration of radioactive peptide was 6 x 10^{-9} M (20 Ci/mmole). Analog concentrations were adjusted using UV absorption at 280 nm and the corresponding extinction coefficients. After a 30 min incubation, triplicate samples of 200 µl were filtered and washed over glass fiber filtermats using the Standard Cell Harvester (Skatron Instruments, Sterling, VA) and placed in scintillation vials for counting. Each experiment was carried out at least three times with the results similar in each assay. Binding of labeled α-factor to filters in the absence of cells was less than 20 cpm. The Ki values were calculated by using the equation of Cheng and Prusoff, where $Ki = EC_{50} / (1 + [ligand] / Kd)$ (26).

Synthesis of Iodinated α-factor Peptides – Peptides were iodinated with Iodogen® tubes from Pierce, Inc. using conditions recommended by the manufacturer. Briefly, Iodogen tubes were pre-wet with Tris Iodination Buffer (TIB)(25mM Tris pH 7.5, 0.4M NaCl). TIB was decanted and 100 µl of fresh TIB was added directly to the bottom of the Iodogen tube and either 10 µl of Na^{127}I

(1.86 mg/ml) or 10 µl of $Na^{125}I$ (100 µCi/µl pH 10) was added and incubated for 6 minutes with gentle swirling every 30 seconds. Activated iodide was transferred to a siliconized microfuge tube containing 100 µl of the peptide (0.5 mmol/L in TIB) and incubated for 6 minutes with gentle mixing every 30 seconds. Scavenging buffer (50 µl at 10 mg/ml tyrosine in TIB) was added and incubated for 5 minutes with mixing at minutes 1 and 4. Following incubation, 1 ml of TIB containing 5 mM EDTA was added. The remaining unreacted iodine was separated from peptide using a Waters Sep-Pak® C18 mini-column. The eluted products were separated by HPLC using H_2O/acetonitrile/0.025% TFA with an acetonitrile percentage of 20 to 35% over 30 minutes at 1.4 ml/min on a Waters µBondapak C18 reversed phase analytical column (3.9x300mm). ^{127}I labled peptides were quantitated by UV spectrophometry using appropriate extinction coefficients. Radioiodinated peptides were labeled using carrier free $Na^{125}I$ and the resulting mono-iodinated peptides were quantitated by converting total dpm associated with the HPLC purified peptide to mmole of peptide using the specific activity of carrier free $Na^{125}I$ (2159 Ci/mmole).

Binding Assays for ^{125}I labeled α-factor – DK102 pNED1 cells (grown in MLT medium) (10) and DK102 cells (grown in MLT medium supplemented with tryptophan) were harvested at 1 x 10^7 cells/ml by centrifugation and resuspended to 6.25 × 10^7 cells/ml in 0.5M potassium phosphate buffer (PPBi) (pH6.24) containing 10mM TAME, 10mM sodium azide, 10 mM potassium fluoride, 1% BSA (fraction IV) and placed at 4°C. In competition binding assays, [$Tyr^1(^{125}I)$, Phe^{13}]α-factor (2.4 x 10^{-9} M final concentration) was pre-mixed with various

concentrations of cold competitor. In saturation binding assays, [Tyr^1(^{125}I), Phe^{13}]α-factor was diluted with cold [Tyr^1(^{127}I), Phe^{13}]α-factor to a specific activity of 12 Ci/mmole to obtain sufficient peptide concentrations. Cells in PPBi were then added to peptide solutions to a final density of 6.25 X 10^6 cells/ml and incubated for 45 minutes at room temperature. Following incubation, reaction mixes were transferred (3 x 200 μl) to wells of a 0.45 μm MultiScreen –HV, 96 well plate (Millipore MHVBN4510) pre-blocked with BSA using PPBi. Samples were vacuum filtered, washed with PPBi (2 x 200 μl) and counted on a LKB-Wallac CliniGamma 1272 gamma counter. Using this methodology non-specific binding of radiolabeled peptide to the filter was at background levels. Specific binding was determined by subtracting counts associated with the DK102 (ste2-) strain from counts bound to the DK102pNED1 ($STE2^+$) strain.

CHAPTER 3

Results

Synthesis of α-Factor Analogs – The automated solid phase synthesis of all analogs resulted in crude peptides with purities ranging from 80% - 90% except in the case of the diiodoTyr containing analogs. The synthesis of these compounds using a standard protocol resulted in very heterogeneous crude peptides with three or four major peaks. This problem was eliminated when Lys^7 of wild-type α-factor was replaced with Arg. This replacement has been previously shown to have no effect on either the biological activity or the receptor affinity of the pheromone (16, 27). The *p*-aminophenylalanine containing analog was prepared by catalytic reduction of the *p*-nitrophenylalanine containing precursor. The hydrogenation was quantitative as judged using analytical HPLC and the reduced peptide had the calculated molecular weight as judged by electrospray mass spectroscopy. All final peptides were greater than 99% homogeneous using analytical HPLC in either an acetonitrile/water/trifluoroactetic acid or methanol/water/acetonitrile/ trifluoroacetic acid gradient system. The peptides were also homogeneous on silica thin layers using a methanol/methylene chloride/acetic acid mobile phase and ninhydrin or ultraviolet light for detection. The peptides gave the expected molecular weights

within 1 dalton and had amino acid ratios within 15% of the theoretical values for all natural residues. The F-Phe residues were within 25% of theory and no attempt was made to quantify iodinated tyrosine or nitrophenylalanine substituents by amino acid analysis. The presence of Trp was qualitatively confirmed using absorbance measurements at 280 nm. In the case of the *p*-NO_2-Phe[13] analog the nitrophenyl substituent added significantly to the absorbance at this wavelength and the extinction coefficient was nearly 60% higher than that found for α-factor. The physical and analytical data on the various peptides are summarized in Table 1.

Bioactivities of Position-13 Analogs – The biological activities of the position-13 analogs were determined by growth arrest and gene induction assays (Table 2). The growth arrest activities were measured as halo size at different amounts of peptide pheromone and plotted on a semi-logarithmic plot. The plots were all linear and the slopes for all analogs were nearly parallel (Representative data shown in Fig. 1). Furthermore, the analogs were stable in all assays because we used *sst1* mutants lacking in the α-factor inactivating Bar1 protease. There are some discrepancies between the biological activities obtained with the lacZ and halo assays with a few of the peptide analogs. The differences were not due to diffusion of peptides in agar in the halo assay because results similar to those of the halo assay were obtained in growth arrest assays done in liquid medium (data not shown). Others performing similar studies (21) observed a comparable lack of relationship between these assays. The differences have been attributed to independent thresholds required to initiate the biological

Table 1. Chemical and Physical Properties of α-factor analogs

Peptide[a]	**Abbreviated Name**	**HPLC**[b] k' CH_3CN	CH_3OH	**M.W.** (Calc.)	**Mass** (Found)	**TLC**[e] (R_f)
Trp-His-Trp-Leu-Gln-Leu-Lys-Pro-Gly-Gln-Pro-Nle-Phe(*p*F)	*p*-F-Phe^{13}	5.7	5.4	1668.9	1669	0.22
Tyr-His-Trp-Leu-Gln-Leu-Lys-Pro-Gly-Gln-Pro-Nle-Phe(*p*F)	Tyr^{1}, *p*-F-Phe^{13}	4.7	3.2	1645.9	1645.5	0.25
Trp-His-Trp-Leu-Gln-Leu-Lys-Pro-Gly-Gln-Pro-Nle-Phe	Phe^{13}	5.6	5.3	1650.0	1650.9	0.20
Trp-His-Trp-Leu-Gln-Leu-Lys-Pro-Gly-Gln-Pro-Nle-Phe(*p*NH_2)	*p*-NH_2 -Phe^{13}	3.2	5.4[c]	1664.9	1664.8	0.18
Trp-His-Tyr-Leu-Gln-Leu-Lys-Pro-Gly-Gln-Pro-Nle-Phe(*p*F)	Tyr^{3}, *p*-F-Phe^{13}	3.1	5.0[c]	1645.9	1644.9	0.16
Trp-His-Trp-Leu-Gln-Leu-Lys-Pro-Gly-Gln-Pro-Nle-Ser	Ser^{13}	3.7	3.4[c]	1588.9	1589.8	0.12
Trp-His-Trp-Leu-Gln-Leu-Lys-Pro-Gly-Gln-Pro-Nle-Phe(*p*NO_2)	*p*-NO_2 -Phe^{13}	5.8	6.7[c]	1696.0	1695.9	0.11
Trp-His-Trp-Leu-Gln-Leu-Lys-Pro-Gly-Gln-Pro-Nle-Phe(*m*F)	*m*-F-Phe^{13}	5.9	4.0	1668.9	1668.7	0.12
Tyr-His-Trp-Leu-Gln-Leu-Lys-Pro-Gly-Gln-Pro-Nle-Phe	Tyr^{1}, Phe^{13}	4.7	4.6[d]	1626.9	1626.9	0.12
Trp-His-Tyr-Leu-Gln-Leu-Lys-Pro-Gly-Gln-Pro-Nle-Phe	Tyr^{3}, Phe^{13}	2.8	4.4[d]	1626.9	1626.7	0.15
Tyr(I_2)-His-Trp-Leu-Gln-Leu-Arg-Pro-Gly-Gln-Pro-Nle-Phe	Tyr^{1}(I_2), Phe^{13}	6.3	5.2[d]	1906.5	1906.5	0.15
Trp-His-Tyr(I_2)-Leu-Gln-Leu-Arg-Pro-Gly-Gln-Pro-Nle-Phe	Tyr^{3}(I_2), Phe^{13}	5.6	5.3[d]	1906.5	1906.9	0.12

[a]The structure of the native α-factor is: Trp-His-Trp-Leu-Gln-Leu-Lys-Pro-Gly-Gln-Pro-Met-Tyr. [b]HPLC was run on a C_{18} reversed-phase column. The gradient used with CH_3CN (CH_3CN:H_2O: 0.025% CF_3COOH) was from 20% - 40% CH_3CN in 20 min. The gradient used with CH_3OH (CH_3OH:H_2O: 0.025% CF_3COOH) was from 50-80% CH_3OH in 30 min.

[c]The gradient was from 30-80% CH_3OH in 30 min. [d]The gradient was from 30-100% CH_3OH in 30 min. [e]TLC - was run on silica thin layers. The mobile phase was $CH_3OH/CHCl_3$/AcOH (2:1:2).

Table 2. Biological activities and binding affinities of α-factor analogs

Peptide	Halo Assay (ug peptide for a 15mm halo)	β-galatosidase Assay (% activity at 10^{-7} M)	Binding Assay (Ki; nM)
α-factor	0.26 ± 0.03	100	11 ± 3
p-F-Phe^{13}	0.46 ± 0.04	110 ± 5	16 ± 3
Tyr^{1}, *p*-F-Phe^{13}	1.45 ± 0.22	69 ± 0	94 ± 8.5
p-NH_2-Phe^{13}	0.47 ± 0.03	95 ± 8	36 ± 3
Tyr^{3}, *p*-F-Phe^{13}	0.19 ± 0.04	79 ± 5	127 ± 25
Ser^{13}	1.49 ± 0.11	55 ± 4	>1000
p-NO_2-Phe^{13}	0.36 ± 0.03	94 ± 6	58 ± 7
m-F-Phe^{13}	0.38 ± 0.02	86 ± 3	59 ± 6
Phe^{13}	0.29 ± 0.05	120 ± 8	22 ± 3.5
Tyr^{1}, Phe^{13}	3.30 ± 0.25	13 ± 2	181 ± 26
Tyr^{3}, Phe^{13}	0.60 ± 0.12	28 ± 2	200 ± 25
Tyr^{1}(I_2), Phe^{13}	1.10 ± 0.15	38 ± 2	330 ± 32
Tyr^{3}(I_2), Phe^{13}	1.02 ± 0.13	97 ± 9	30 ± 4
Tyr^{1}(I_1), Phe^{13}	0.90 ± 0.10	33 ± 3	81 ± 9

Figure 1. Growth arrest of *S. cerevisiae* by α-factor and various analogs. The halo of growth arrest is plotted in response to various amounts of peptide as indicated in the figure. Fig. 1A shows α-factor (■) and the diiodinated analogs: Tyr^1 (I_2), Phe^{13} (Δ), Tyr^3(I_2), Phe^{13} (O). Fig 1B shows α-factor (■) and the analogs: Tyr^1, Phe^{13} (O), Tyr^3, Phe^{13} (Δ) and Phe^{13} (▲).

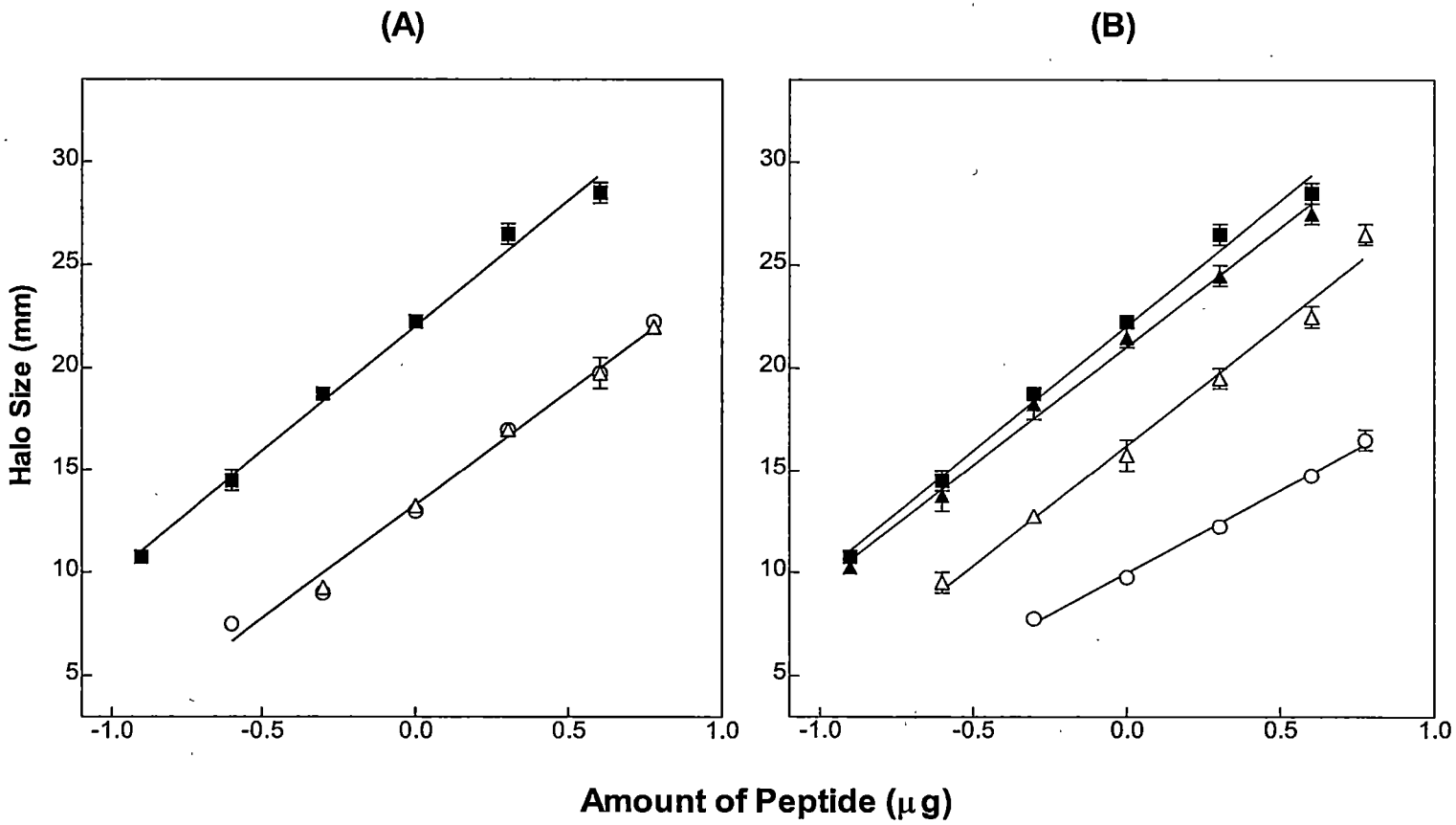
(A)
(B)
Halo Size (mm)
30
25
20
15
10
5
-1.0
-0.5
0.0
0.5
1.0
Amount of Peptide (μg)

responses of growth inhibition (halo assay) versus gene induction (*lacZ*) probably due to differences regulation of the two pathways. As summarized in Table 2, replacement of Tyr^{13} with *p*-F-Phe, *m*-F-Phe, *p*-NO_2-Phe, *p*-NH_2-Phe, or Phe resulted in peptides which caused a 15 mm growth arrest halo from 0.29 μg peptide to 0.47 μg in the growth arrest assay compared to 0.26 μg for the parent α-factor. These same analogs exhibit 80%-120% of the activity of the α-factor in the gene induction assay. Thus the OH of Tyr is clearly not necessary for high biological activity as it can be eliminated completely or it can be replaced by a variety of groups including F and NH_2. Even the relatively large NO_2 moiety did not markedly decrease the biological activity of this analog. The analog containing Ser^{13} had the lowest biological activity of any of the singly-substituted position 13 analogs tested in both the growth arrest and gene induction assays (Table 2).

Bioactivities of Multiple Replacement Analogs – A principal goal of this study was the development of probes for the α-factor receptor. Having learned that Tyr^{13} could be replaced with Phe we wished to determine whether Tyr could be placed at other positions in [Phe^{13}]α-factor. Accordingly we synthesized two analogs in which Trp^1 or Trp^3 were replaced by Tyr. As indicated in Table 2, Figure 1b, and Figure 2 these analogs had significantly lower activity than [Phe^{13}]α-factor exhibiting 2-10 fold lower activity than α-factor in the growth arrest assay and only 13-28 % potency in the gene induction assay. Interestingly, the $Tyr^1(I_2)$, Phe^{13}, and $Tyr^3(I_2)$, Phe^{13} analogs exhibited higher potency than the

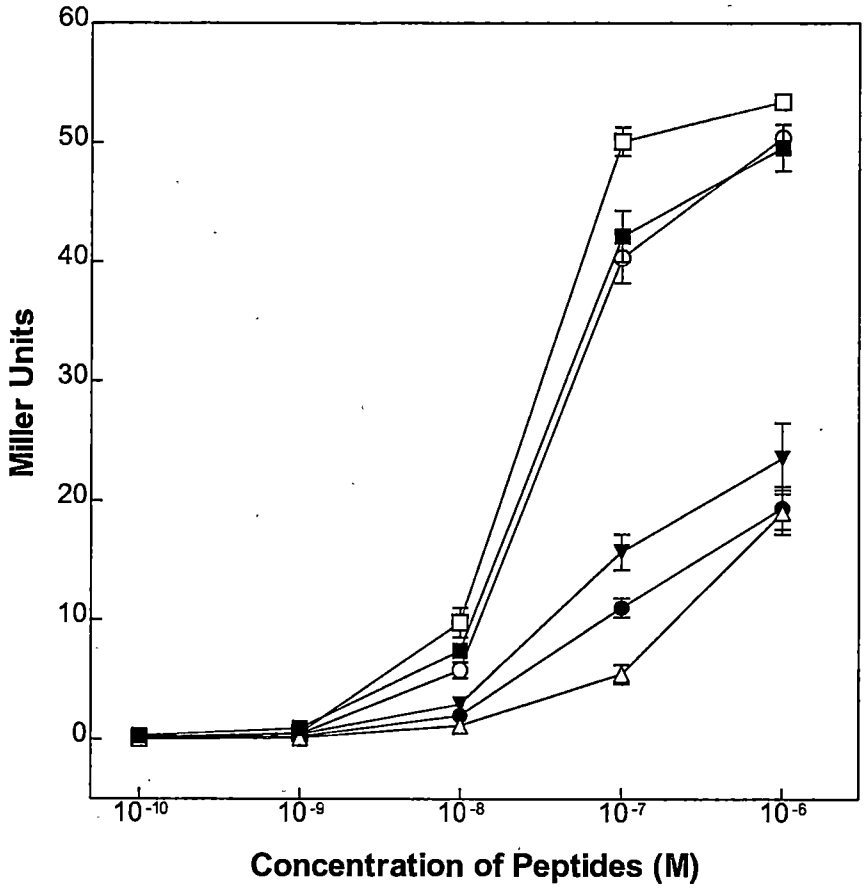

Figure 2. Dose response to α-factor and analogs determined by reporter gene *lacZ* (β-Galactosidase). β-galactosidase activity in Miller Units was measured in cultures incubated with various amounts of peptide as shown: α-factor (■), Tyr^1, Phe^{13} (Δ), $Tyr^1(I_2)$, Phe^{13} (▼), Tyr^3, Phe^{13} (●),$Tyr^3(I_2)$, Phe^{13} (O), Phe^{13} (□).

Tyr^1, Phe^{13} and Tyr^3, Phe^{13} analogs, respectively, in the gene induction assay. In fact the latter compound is nearly as active as α-factor in this assay. However, whereas iodination of Tyr^1 also increased activity in the growth arrest assay iodination of Tyr^3 resulted in a decrease in activity in this same assay. There is some indication in the data that the biological response of the Tyr^1,Phe^{13}, the Tyr^3, Phe^{13} and the Tyr^1 (I_2),Phe^{13} analogs have not reached a plateau at the highest concentrations tested. However, due to the poor solubility of these peptides, higher concentrations were not tested. Whether these peptides are capable of fully stimulating a biological response is not known.

Receptor Affinities of α-Factor Analogs – The affinity of the position 13 and multiple position analogs for the Ste2p receptor was determined by measuring the relative abilities of these compounds to compete with [^{3}H]α-factor. As exemplified in Figure 3 the pheromones were able to eliminate more than 80% of the binding of the radioactive α-factor. This result is similar to that found when cold α-factor is used as the competitor. The binding competition resulted in sharp curves whose slopes were parallel to each other. The concentration of competitor causing 50% displacement of α-factor was determined from these curves and converted to K_i values using the approach of Cheng and Prusoff (26). The results show that replacement of Tyr^{13} with Phe or *p*-F-Phe had almost no

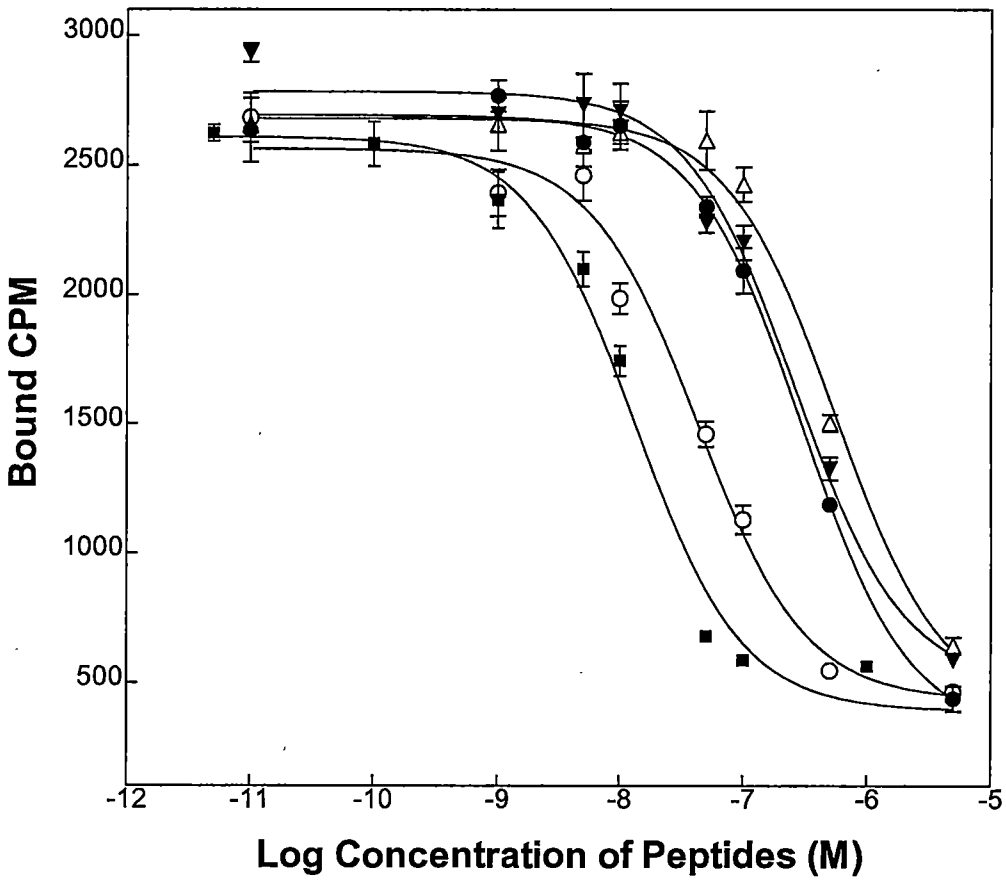

Figure 3. Competition binding assay. Binding of the analogs was performed in competition with [^{3}H]α-factor. The binding curves are for α-factor (■), Tyr^1, Phe^{13} (●), Tyr^1(I$_2$), Phe^{13} (Δ), Tyr^3, Phe^{13} (▼), Tyr^3(I$_2$), Phe^{13} (O).

effect on receptor affinity (Table 2). Incorporation of NH_2 in place of the Tyr OH caused about a three-fold decrease in affinity while a nitro group at the para position resulted in approximately a five-fold decrease. When the fluorine group was placed in the *meta* position of the phenyl ring the affinity was also about five-fold lower than when it was in the *para* position. In contrast to the analogs containing a substituted phenyl ring at position 13, incorporation of Ser at this position resulted in a large decrease (>100-fold) in receptor affinity.

The high affinity of Phe^{13} and *p*-F-Phe^{13} analogs encouraged us to place Tyr at positions 1 and 3 in place of the Trp residues of these pheromones. In both the Phe and the *p*-F-Phe series the incorporation of Tyr at positions 1 or 3 resulted in a drop in affinity of about 6-10 fold. This still represented receptor affinities in the 100 nM range. Thus, these compounds were potential substrates for radioiodination. Prior to preparing radioactive substrates we synthesized diiodinated standards containing ^{127}I. During the synthesis we experienced problems when Lys was in position 7. This problem was eliminated when Arg was placed in this position (See peptide synthesis). Interestingly, diiodination of Tyr^1 resulted in a two-fold decrease whereas diiodination of Tyr^3 resulted in a large increase in receptor affinity (Table 2).

Synthesis and Binding of Radioiodinated ([Tyr^1(^{125}I),Phe^{13}]α-Factor – Based on the significant receptor affinities and bioactivities of the diiodinated analogs of α-factor we attempted to radioiodinate the Tyr^1, Phe^{13} and Tyr^3, Phe^{13} analogs. All attempts with the latter compound resulted in multiple products as judged by HPLC and we were not able to isolate pure labeled receptor probes.

However, the Tyr^1, Phe^{13} analog could be successfully monoiodinated using IODOGEN® tubes. The monoiodinated compound exhibited a retention time intermediate to those for the underivatized and doubly derivatized compound (data not shown) . This non-radioactive monoiodinated peptide moved at the same retention time as the radiolabeled compound and had the expected molecular weight as determined by mass spectrometry. Its biological activities are indicated in Table 2.

The [Tyr^1(^{125}I), Phe^{13}]α-factor specifically bound to the α-factor receptor and showed saturation binding with a K_D = 81 nM in a whole cell binding assay (Fig. 4a). A similar K_D of 108 nM was found when cell membranes were used for binding (data not shown). The binding of monoiodinated α-factor could be displaced by both the unlabelled diiodinated pheromone and α-factor (Figure 4b). The K_I determined for α-factor in this experiment was 7.7 nM which is consistent with the affinity of α-factor that we normally find in our receptor binding analyses. A known α-factor antagonist [Trp-Leu-Gln-Leu-Lys-Pro-Gly-Gln-Pro-Nle-Tyr] also displaced labeled [Tyr^1(^{125}I), Phe^{13}]α-factor from the receptor (Fig 4b) whereas Trp-His-Trp-Leu-Gln-Leu-Lys-Pro-Gly-Gln-Pro, an α-factor analog that does not bind to Ste2p (28), could not release the iodinated ligand from this protein (data not shown).

Figure 4. Saturation and competition binding assays with [Tyr^1(^{125}I), Phe^{13}]α-factor. Cells were incubated with increasing amount of [Tyr^1(^{125}I), Phe^{13}]α-factor as described in the Experimental Procedures and the dpm associated with the Ste2p receptor were plotted against the pheromone concentration. The inset represents the total counts bound to cells with receptor (DK102pNED1, ■) and total counts bound to cells without receptor (DK102, ▲) [Panel A]. Competition for binding of [Tyr^1(^{125}I), Phe^{13}]α-factor to Ste2p receptor was performed using α-factor (■), Tyr^1(^{127}I$_2$), Phe^{13} (▲), and Trp-Leu-Gln-Leu-Lys-Pro-Gly-Gln-Pro-Nle-Tyr (▼) as competitors (Panel B). The concentration of the radioactive pheromone was 2.4 x 10^{-9} M and the concentration of the competitors is indicated in the figure.

(A)

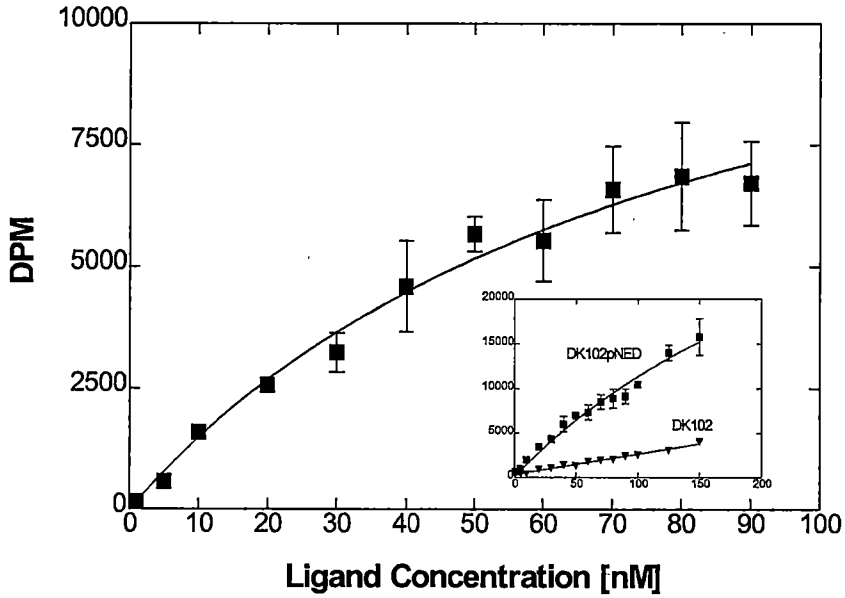
DPM
Ligand Concentration [nM]
DK102pNED
DK102

(B)

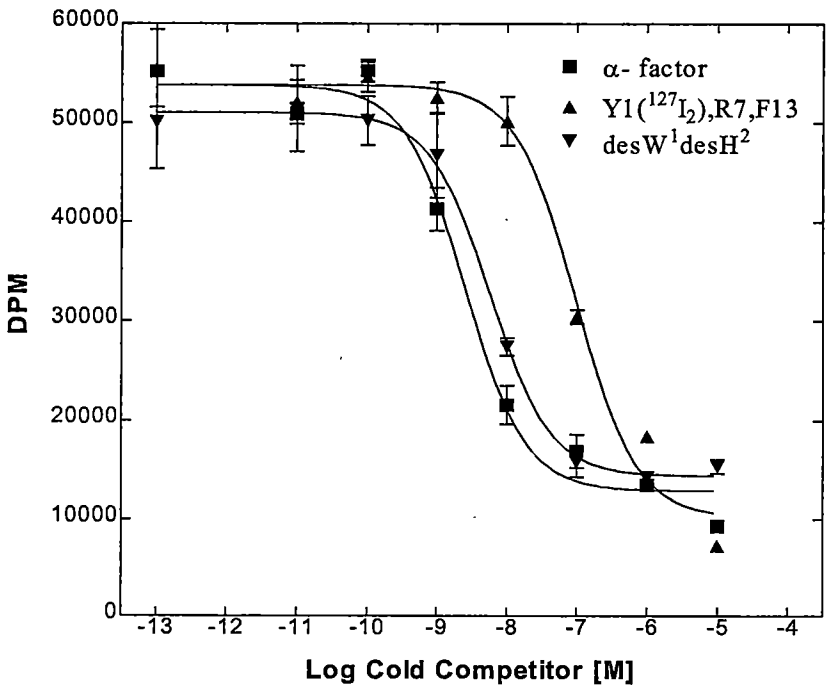
DPM
Log Cold Competitor [M]
α- factor
Y1($^{127}I_2$),R7,F13
desW^{1}desH^2

CHAPTER 4

Discussion

The α-factor receptor from the yeast *S. cerevisiae* is a representative of Class D within the GPCR family of heptahelical receptors (3-5). This subgroup consists solely of fungal receptors which are characterized by the absence of disulfide bridges in the functional protein. Very little work has been done on this family of receptors and its characterization is of interest in defining distinguishing features of the different subgroups and the relationship between receptor structure and function.

Although Ste2p has been subjected to a variety of mutagenesis studies (21, 22, 29-35) there is little knowledge on the pheromone binding site. Structure -activity relationship studies combined with conformational analysis on the α-factor suggest that the two termini of the pheromone are important for receptor binding and that the pheromone is bent when it binds to its receptor (12, 15, 36-38). However, there is no direct evidence for contacts between residues of the peptide ligand and residues of the receptor. At present a method of choice for discerning such contacts is photoaffinity crosslinking of bound agonist into the receptor and characterizing the crosslinking site using biochemical techniques (39-45). This approach requires the availability of a photoactivatable ligand with a

tag that can be used to follow ligand incorporation by subsequent analytical procedures. Although biotin has been suggested as one approach for such a tag, the sensitivity of its detection is two to three orders lower than that of ^{125}I. Recent reports indicated that biotin was not useful in receptor analysis of the integrin receptor $\alpha_v\beta_3$ (46). Studies on α-factor - Ste2p interactions have previously been stymied by the lack of an iodinatable agonist. Therefore, design and characterization of such a probe was the principal goal of the present study.

Can Tyr^{13} of α-factor be replaced by other residues? – Since iodination of α-factor results in an inactive ligand with low receptor affinity, we evaluated replacement of Tyr^{13} with amino acids containing other aromatic side chains. In contrast to previous reports (20), we found that incorporation of a variety of aromatic amino acids including Phe at position 13 resulted in pheromones with high biological activity and high receptor affinities. An analog with Ser^{13} exhibited poor activity and more than a 100-fold drop in receptor affinity. In a previous study it was noted that [Alà^{13}]α-factor had low biological activity and did not bind well to Ste2p (15). These results suggest that the phenolic hydroxyl group of residue 13 is not involved in a direct interaction with the receptor and that an aromatic side chain at this position seems to be required for high affinity binding to Ste2p. Interestingly, even the Ser^{13} and Ala^{13} analogs, which bind poorly, can trigger biological responses. Thus, the aromatic side chain at residue 13 is not necessary for downstream signal transduction from the α-factor receptor. At present very little is known about the nature of the binding site for α-factor. The fact that aromatic residues in both positions 1 and 13 have been associated with

a high receptor affinity (12, 15), taken together with the hypothesis of a bent pheromone, suggests that an aromatic cluster between residues near the chain ends might occur on binding to Ste2p. This cluster would likely interact with a hydrophobic surface in the receptor. In addition, it is possible that there may be contacts between Arg or Lys side chains in the extracellular receptor loops with the aromatic rings of the pheromone forming cation - π interactions. Such cation-π interactions have been suggested to supply significant stabilization energies in proteins and in protein ligand interactions (47).

Are multiple substitutions at the N and C termini of the pheromone accepted by Ste2p – To obtain an iodinatable ligand one strategy would be to remove Tyr from position 13 and place it at other positions of α-factor. Therefore, starting with the Phe^{13} or *p*-F-Phe^{13} analogs we determined whether it would be possible to substitute Tyr for the Trp residues in positions 1 and 3 and still retain high receptor affinity. We found that substitution of Tyr at position one or three of either [Phe^{13}]α-factor or [*p*-F- Phe^{13}]α-factor resulted in a 6-10-fold reduction in receptor affinity and that diiodination of these compounds did not lead to a significant further reduction in the binding constant. These observations suggest that α-factor analogs with multiple changes in the aromatic residues at position 13 and positions 1 or 3 would be potential ligands for use in a receptor binding assay. Most importantly, the cold diiodinated pheromone still had a binding affinity in the 100 nM range indicating that it could be used directly to develop a radioactive probe.

Can iodinated α-factor analogs bind specifically to Ste2p – Attempts to use iodinated α-factor in a radioactive binding assay started with [$Tyr^1(I_2)$]α-factor prepared by exhange from the ^{127}I containing peptide (48). Specific binding of iodinated α-factor to receptor was masked by high levels of non-specific binding of iodinated α-factor to filters used in the binding assay. In previous studies such sticking to filters was not encountered with tritiated α-factor. For binding studies with iodinated α-factor we developed methods that eliminated non-specific binding of the iodinated peptide. We switched to a charged, low-protein binding filter (Durapore membranes, Millipore Corp.) and incorporated BSA (1% w/v) into the binding medium.

In another report significant differences in specific binding were observed for a peptide hormone containing a monoiodinated as compared to a diiodinated tyrosine derivative (49). In order to obtain a monoiodinated receptor probe we used IODOGEN® to radiolabel the Tyr^1, Phe^{13} analog and isolated [$Tyr^1(^{125}I)$, Phe^{13}]α-factor. This ligand gave saturable binding to Ste2p. Binding was competed by α-factor and an antagonist, but not by an α-factor analog known not to bind to Ste2p. The K_D values determined with whole cells (81 nM) and membranes (108 nM) as calculated by fitting the binding isotherm indicated that the monoiodinated pheromone binds to the receptor as well as or better than either Tyr^1,Phe^{13} or $Tyr^1(I)_2$,Phe^{13} (Table 2).

In a previous study with [Bpa^3, Arg^7]α-factor we found that replacement of Trp^1 with diiodoTyrosine resulted in a peptide with an approximately 20-fold

decrease in affinity for Ste2p compared to α-factor (50). Moreover, this latter peptide had nearly the same growth arresting activity as [Bpa^{3}, Arg^{7}]α-factor. These findings are consistent with the results found for the [Phe^{13}]α-factor and [*p*-F-Phe^{13}]α-factor series. They suggest that peptides containing Phe^{13}, Bpa and an iodinateable tyrosine should retain reasonably high (100 nanomolar) receptor affinities and therefore should be potential photoaffinity labels for Ste2p.

In conclusion, we have successfully prepared a new radioligand for the α-factor receptor which has very high specific activity. This peptide can be radiolabeled by a simple procedure that is employed in many laboratories. This iodinatable α-factor analog will be a useful tool for researchers interested in studying wildtype and mutant Ste2p.

List of References for Part 2

1) **Wess, J.** (1997) G protein-coupled receptors: molecular mechanisms involved in receptor activation and selectivity of G protein recognition. *FASEB J.* 11, 346-354.

2) **Hall, R.A., Premont, R.T. and Lefkowitz RJ** (1999) Heptahelical receptor signaling: beyond the G protein paradigm. *J. Cell. Biol.* 145, 927-32.

3) **Kenakin, T.** (1996) The classification of seven transmembrane receptors in recombinant expression systems. *Pharmacol. Rev.*, 48, 413-463.

4) **Strader, C.D., Fong. T.M., Graziano, M. P., and Tota, M.R.** (1995) The family of G protein-coupled receptors. *FASEB J.* 9, 745-754.

5) **Strader, C.D., Fong, T.M., Tota, M.R., Underwood, D., and Dixon, R. A. F.** (1994) Structure and function of G protein-coupled receptors. *Annu. Rev. Biochem.* 63, 101-132.

6) **Blumer, K. J., and Thorner, J.** (1991) Receptor G protein signaling in yeast. *Annu. Rev. Physiol.* 53, 37-57.

7) **Dohlman, H. G., Thorner, J., Caron, M. G. and Lefkowitz, R. J.** (1991) Model systems for the study of seven-transmembrane-segment receptors. *Annu. Rev. Biochem.* 60, 653-688.

8) **Burkholder, A. C. and Hartwell, L. H.** (1985) The yeast α-factor receptor: structural properties deduced from the sequence of the *STE2* gene. *Nucleic Acids Res.* 13, 8463-8475.

9) **Nakayama N., Miyajima, A. and Arai, K.** (1985) Nucleotide sequences of *STE2* and *STE3*, cell type-specific sterile genes from *Saccharomyces cerevisiae*. *EMBO J.* 4, 2643-2648.

10) **David, N. E., Gee, M., Andersen, B., Naider, F., Thorner, J. and Stevens, R. C.** (1997) Expression and purification of the *Saccharomyces cerevisiae* α-factor receptor (Ste2p), a 7-transmembrane-segment G protein-coupled receptor. *J. Biol. Chem.* 272, 15553-15561.

11) **Naider, F. and Becker, J.M.** (1986) Structure-function relationships of the Saccharomyces cerevisiae α-factor. *CRC Critical Reviews in Biochemistry* 21, 225-248.

12) **Zhang, Y. L., Lu, H.-F., Becker, J. M. and Naider, F.** (1997) Position one analogs of the *Saccharomyces cerevisiae* tridecapeptide pheromone. *J. Peptide Res.* 50, 319-328.

13) **Manfredi, J. P., Klein, C., Herrero, J. J., Byrd, D. R., Trueheart, J., Wiesler, W. T., Fowlkes, D. M. and Broach, J. R.** (1993) Yeast α mating factor structure-activity relationship derived from genetically selected peptide agonists and antagonists of Ste2p. *Mol. Cell. Biol.* 16, 4700-4709.

14) **Levin, Y., Khare, R. K., Able, G., Hill, D., Eriotou-Bargiota, E., Becker, J. and Naider, F.** (1993) Histidine2 of the α-factor of *Saccharomyces cerevisiae* is not essential for binding to its receptor or for biological activity. *Biochemistry,* 32, 8199-8206.

15)**Abel, M.G., Zhang, Y.L., Lu, H.F., Naider, F. and Becker, J.M.** (1998) Structure-function analysis of the *Saccharomyces cerevisiae* tridecapeptide pheromone using alanine-scanned analogs. *J. Peptide Res.* 52, 95-106.

16)**Raths, S. K., Naider, F. and Becker, J. M.** (1988) Peptide analogues compete with the binding of α-factor to its receptor in *Saccharomyces cerevisiae. J. Biol. Chem.* 263, 17333-17341.

17)**Jenness, D.D., Burkholder, A.C., and Hartwell, L.H.** (1983) Binding of α-factor pheromone to yeast a cells: Chemical and genetic evidence for an α-factor receptor. *Cell* 35, 521-529.

18)**Blumer, K. J., Reneke, J. E. and Thorner, J.** (1988) The *STE2* gene product is the ligand-binding component of the α-factor receptor of *Saccharomyces cerevisiae. J. Biol. Chem.* 263, 10836-10842.

19)**Lipke, P.N.** (1976) Morphogenetic effects of α-factor on *S. cerevisiae* a-cells. Ph.D. Thesis University of California, Berkeley.

20)**Masui,Y., Chino, N., Kita, H., and Sakakibara, S.** (1979) Amino acid substitution of mating factor of *Saccharomyces cerevisiae* structure-activity relationship. *Biochem. Biophys. Res. Comm.* 86, 982-987.

21)**Marsh, L.** (1992) Substitutions in the hydrophobic core of the α-factor receptor of *Saccharomyces cerevisiae* permit response to *Saccharomyces kluyveri* α-factor and to antagonist. *Mol. Cell. Biol.* 12, 3959-3966.

22)**Abel, M.G., Lee, B.K., Naider, F. and Becker, J.M.** (1998) Mutations affecting ligand specificity of the G-protein-coupled receptor for the

Saccharomyces cerevisiae tridecapeptide pheromone. *Biochim. Biophys. Acta* 1448, 12-26.

23)**Kippert, F.** (1995) A rapid permeabilization procedure for accurate quantitative determination of beta-galactosidase activity in yeast cells. *FEMS Microbiol. Lett.* 128, 201-206.

24)**Guarente, L.** (1983) Yeast promoters and lacZ fusions designed to study expression of cloned genes in yeast. *Meth. Enzymol.* 101, 167-180.

25)**Miller, J.H.** (1972) Experiments in Molecular Genetics, Cold Spring Harbor Laboratory, Cold Spring Harbor, New York.

26)**Cheng, Y. and Prusoff, W.H.** (1973) Relationship between the inhibition constant (K1) and the concentration of inhibitor which causes 50 percent inhibition (I50) of an enzymatic reaction. *Biochem. Pharmacol.* 22, 3099-3108.

27)**Samokhin, G.P., Lizlova, L.V., Bespalova, J.D., Titov, M.I., and Smirnov, V.N.** (1979) Substitution of Lys7 by Arg does not affect biological activity of α-factor, a yeast mating pheromone. *FEMS, Microbiol. Lett.* 5, 435-438.

28)**Eriotou-Bargiota, E., Xue, C.-B., Naider, F., and Becker, J.M.** (1992) Antagonistic and synergistic peptide analogues of the tridecapeptide mating pheromone of *Saccharomyces cerevisiae*. *Biochemistry* 31, 551-557.

29)**Clark, C. D., Palzkill, T. and Botstein, D.** (1994) Systematic mutagensis of the yeast mating pheromone receptor third intracellular loop. *J. Biol. Chem.* 269, 1-11.

30)**Sen, M. and Marsh, L.** (1994) Noncontiguous domains of the alpha-factor receptor of yeasts confer ligand specificity. *J. Biol. Chem.* 269, 968-973.

31)**Stefan, C. J. and Blumer, K. J.** (1994). The third cytoplasmic loop of a yeast G-protein-coupled receptor controls pathway activation, ligand discrimination, and receptor internalization. *Mol. Cell. Biol.* 14, 3339-3349.

32)**Konopka, J. B., Margarit, S. M. and Dube, P.** (1996) Mutation of Pro-258 in transmembrane domain 6 constitutively activates the G protein-coupled alpha-factor receptor. *Proc. Natl. Acad. Sci. USA,* 93, 6764-6769.

33)**Sen, M., Shah, A., and Marsh, L.** (1997) Two types of alpha-factor receptor determinants for pheromone specificity in the mating-incompatible yeasts *S. cerevisiae* and *S. kluyveri. Curr. Genet.* 31, 235-240.

34)**Sommers, C.M. and Dumont, M. E.** (1997) Genetic interactions among the transmembrane segments of the G protein coupled receptor encoded by the yeast STE2 gene. *J. Mol. Biol.* 266, 559-575.

35)**Martin, N.P., Leavitt.L.M., Sommers, C.M., and Dumont, M. E.** (1999) Assembly of G protein-coupled receptors from fragments: identification of functional receptors with discontinuities in each of the loops connecting transmembrane segments. *Biochem.* 38, 682-695.

36)**Jelicks, L.A., Naider, F., Shenbagamurthi, P., Becker, J.M., and Broido, M.S.** (1988) A type II beta-turn in a flexible peptide proton assignment and conformational analysis of the alpha-factor from *Saccharomyces cerevisiae* in solution. *Biopolymers* 27, 431-449.

37)**Naider, F., Jelicks, L.A., Becker, J.M., and Broido, M.S.** (1989) Biologically significant conformation of the *Saccharomyces cerevisiae* alpha factor. *Biopolymers* 28, 487-497.

38)**Zhang, Y.L., Marepalli, H.R., Lu, H.F., Becker, J.M., and Naider. F.** (1998) Synthesis, biological activity, and conformational analysis of peptidomimetic analogues of the *Saccharomyces cerevisiae* alpha-factor tridecapeptide. *Biochemistry* 37, 12465-12476.

39)**Williams, K.P and Shoelson, S.E.** (1993) Bpa^{B25} insulins: photoactivatable analogues that quantitatively crosslink, radiolabel, and activate the insulin receptor. *J. Biol. Chem.* 268, 5361-5364.

40)**Zhou, A.T., Besalle, R., Bisello, A., Nakamoto, C., Rosenblatt, M., Suva, L.J., and Chorev, M.** (1997) Direct mapping of an agonist-binding domain within the parathyroid hormone/parathyroid hormone-related protein receptor by photoaffinity crosslinking. *Proc. Natl. Acad. Sci. USA.* 94, 3644-3649.

41)**Bisello, A., Adams, A., Mierke, D., Pellegrini, M., Rosenblatt, M., Suva, L. and Chorev, M.,** (1998) Parathyroid hormone-receptor interactions identified directly by photocrosslinking and molecular modeling studies. *J. Biol. Chem.* 273, 22498-22505.

42)**Dong, M., Wang, Y., Pinon, D., Hadac, E. and Miller, L.** (1999) Demonstration of a direct interaction between residue 22 in the carboxyl terminal half of secretin and the amino terminal tail of the secretin receptor using photoaffinity labeling. *J. Biol. Chem.* 274, 903-909.

43)**McNicoll, N., Gagnon, J., Rondeau, J.J., Ong, H. and DeLean, A.** (1996) Localization by photoaffinity labeling of natiuretic peptide receptor - A binding domain. *Biochemistry* 35, 12950-12956.

44)**Blanton, M.P., Li, Y.M., Stimson, E.R., Maggio, J.E. and Cohen, J.B.** (1994) Agonist induced photoincorporation of a *p*-benzoylphenylalanine derivative of substance P into membrane-spanning region 2 of the torpedo nicotinic acetylcholine receptor ε subunit. *Mol. Pharmacol.* 46, 1048-1055.

45)**Anders, J., Bluggel, M., Meyer, H.E., Kuhne, R., ter Laak, A.M., Kojro, E. and Fahrenholz, F.** (1999) Direct identification of the agonist binding site in the human brain choecystokinin B receptor. *Biochemistry* 38, 6043-6055.

46)**Bitan, G., Scheibler, L.,Greenberg, Z.,Rosenblatt, M., and Chorev, M.** (1999) Mapping the Integrin $\alpha_v\beta_3$-Ligand Interface by Photoaffinity Cross-Linking. *Biochemistry*; 38, 3414-3420.

47)**Dougherty, D.A.** (1996) Cation-pi interactions in chemistry and biology: a new view of benzene, Phe, Tyr and Trp. *Science* 271, 163-168.

48)**Breslav, M., McKinney, A., Becker, J.M., and. Naider . F.** (1996) A New Method for Radioiodination of Peptides. *Analytical Biochemistry* 239, 213-217.

49)**Goldman, M.E., Chorev, M., Reagan, J.E., Levy, J.J., and Rosenblatt M.** (1988) Evaluation of novel parathyroid hormone analogs using a bovine renal membrane receptor binding assay. *Endocrinology* 123, 1468-1475.

50)**Jiang, Y., Breslav, M., Khare, R.K., McKinney, A., Becker, J.M., and Naider, F.** (1995) Synthesis of alpha-factor analogues containing photoactivatable and labeling groups. *Int. J. Peptide Protein Res.* 45, 106-115.

PART 3

Mutations affecting ligand specificity of *Saccharomyces cerevisiae* α-factor receptor.[§]

[§] Part 3 was published in a modified form as **Abel, M.G., Lee, B.-K., Naider, F., and Becker, J.M.** (1998) Mutations affecting ligand specificity of the G protein-coupled receptor for the Saccharomyces cerevisiae tridecapeptide pheromone. *Biochim. Biophys. Acta* 1448:12. Synthesis of α-factor analogs used in this study were carried out in the laboratory of Dr. Fred Naider, Department of Chemistry, C.U.N.Y., College of Staten Island, NY 10314

CHAPTER I

Introduction

The G protein-coupled receptors (GPCRs) constitute a large family of transmembrane proteins that mediate cellular responses to diverse extracellular stimuli, including light, neurotransmitters, peptide and glycoprotein hormones and ordorants (1). Through selective ligand binding, the GPCRs discriminate between these multiple external signals. The GPCRs amplify and transduce the information inherent in ligand binding to the cell interior via interaction with intracellular heterotrimeric G proteins. After activation by agonist-bound GPCR, the α subunit and $\beta\gamma$ complex are free to modulate the activity of a variety of effector proteins, including adenylyl cyclase, phospholipase, G protein-gated Ca^{2+} and K^{+} channels, and membrane-proximal elements of mitogen-activated protein kinase (MAPK) signal transduction pathway (for review see 2). Their integral role in cell signaling makes the GPCRs an important class of therapeutic targets for pharmaceutical research.

Many of the elements of GPCR-mediated signal transduction pathways in mammalian cells closely resemble comparable pathway *in Saccharomyces cerevisiae*. Haploid yeast cells employ GPCRs to signal the beginning of the mating process (3). Secreted mating type specific peptide pheromones are detected by cells of the opposite mating type through binding to G protein-coupled mating-pheromone receptors (i.e. mating type **a** cells produce the **a**

factor and express the α-factor receptor, Ste2; mating type α cells secrete the α-factor and express the **a**-factor receptor, Ste3).

The structure of GPCRs is based partially on the low-resolution structure of the transmembrane core of bacteriorhodopsin as proposed by Baldwin (4, 5). This model is used by many workers as a point of reference in model building for other GPCR structures and ligand binding sites and has shown to be consistent, in general, with the recent crystal structure of rhodopsin at 2.8 Å resolution (6). However, the structure of no single GPCR for peptide hormones is known at atomic resolution. Although all GPCRs share the common topologic feature of 7 TMs, subfamilies of GPCRs differ markedly in the strategies used to maintain ligand affinity and selectivity (7-10). At one extreme, determinants of affinity and selectivity may reside exclusively in the TMs (*e.g.* opsin and adrenergic receptor subfamilies). At the other extreme, agonist affinity and selectivity may be largely a function of residues in the receptors' N-terminal extracellular domains (*e.g.* luteinizing hormone/thyrotropin receptor subfamily). For many peptide receptors it is assumed that some extracellular loops and the extracellular portions of certain TMs are critical for ligand binding whereas the intracellular portions of the receptor are involved in G protein recognition.

Functional analysis of peptide hormone receptors has been carried out using receptor chimeras and site-directed mutagenesis with selective agonistic and antagonistic ligands. Analysis of B2 bradykinin mutant receptors with peptidic antagonists provided a unifying view that peptide hormones bind to their receptors using the extracellular sequences to gain most of their binding energy

(affinity) and specificity while a small part of the ligand interacts with helical regions near TM5, TM6, and TM7 (11). Xue (12) constructed receptor chimeras between the μ and κ opioid receptors and identified binding regions of the receptor that differentiated between peptide and non-peptide ligands. Site-directed mutagenesis of a single tyrosine residue on the 7th transmembrane domain of $AT1_A$ angiotensin II receptor had no effect on agonist binding but severely impaired association of the receptor with phospholipase C identifying a linkage between receptor activation and signal transduction (13).

A number of α-factor receptor mutants have been generated that contribute to our knowledge of pheromone binding and G protein coupling. Linker insertion mutants (14), single residue substitution mutations (15-19), and receptor chimeras between *S. cerevisiae* and *S. kluyveri STE2* genes (20,21) all indicate that the α-factor binding site might include determinants contributed by side chains from several transmembrane segments and from extracellular loops. In another study, a very interesting mutant (P258L) caused the receptor to be active in the absence of pheromone: i.e., constitutively activated (16)

Ligand binding to GPCR is thought to cause a conformational change which is propagated to an associated G protein. The concept of receptor isomerization has been demonstrated in many systems (22, 23) and described by a two-state model of receptor activation (24). In order to understand the molecular mechanism governing ligand-induced receptor activation, structural information about the conformational differences between the receptor resting and activated states must be obtained. A recent study using the yeast α-factor-

Ste2p model system indicated that agonist binding led to an increased trypsin-accessibility of the I3 loop, whereas an antagonist led to a reduction of proteolytic cleavage within this loop (25). This analysis clearly indicated that agonists and antagonists induced distinct conformational states that differ from the unbound form of the receptor. Although the binding of agonists and structurally related antagonists to the receptor is competitive, there is obviously a critical difference in that occupancy by agonists generates an intracellular signal whereas binding of antagonists does not (for reviews see 26, 27). Defining the differences at the molecular level between the receptor:agonist complex and receptor:antagonist complex is central to our understanding of GPCR activation and to the rational design of receptor-specific agonists and antagonists. However, our understanding of the molecular interactions between ligands and the receptor protein and, particularly, of the structural correlates of receptor activation or inhibition by agonists and antagonists, respectively, is still rudimentary.

Because the α-factor receptor is thought to be organized in similar functional domains as other GPCRs, information gleaned from the study of interaction between α-factor and its receptor may be able to contribute to the understanding of the function of the whole family. One approach we pursued involved the search for mutant receptors that responded to α-factor analogs that did not activate the wild-type receptor. A number of antagonists were available in our stocks of synthetic α-factor analogs that were candidates for use in such a screen. Therefore, in following with the previously described investigations and to add to the understanding of this family of receptors, Part 3 is a study, using

random and site-directed mutagenesis, of those residue(s) of α-factor receptors affecting ligand specificity as well as residue(s) involved in receptor activation for the mating signal transduction.

CHAPTER 2

Materials and Methods

Strains – *S. cerevisiae* LM23-16az (16) [*MAT***a** *ste2-i4 bar1 leu2 ura3 his4 lys5 met1 FUS1-lacZ::URA3*] from Lorraine Marsh, Albert Einstein College of Medicine, New York, NY, was used as the recipient for transformation with the *STE2* randomly-mutated library and *S. cerevisiae* LM102 (16) [*MAT***a** *ste2-dl bar1 leu2 ura3 his4 trp1 met1 FUS1::lacZ*] from Lorraine Marsh was used as the recipient of the *STE2* site-directed mutants and to measure pheromone-induced growth arrest (halo assay), pheromone-induced gene expression (*lacZ* assay) and to determine pheromone binding. Strain LM23-16az carried a mutation in the receptor gene rendering it inactive, whereas strain LM102 was deleted for the receptor gene. Both strains carried the *bar1* mutant allele, thus inactivating the BAR1 protease responsible for degradation of α-factor, and both strains contained a *fus1:lacZ* gene serving as a pheromone-inducible reporter.

Primers and Sequencing – All primers were purchased from BioServe BioTechnologies (Laurel, MD). Sequencing was carried out manually using a dideoxy DNA sequencing kit from United States Biochemical according to manufacturer's instructions (Sequenase Version 2.0) or by the DNA sequencing facility located on the campus of the University of Tennessee.

Random mutagenesis of STE2 using a modified PCR – Random mutations were introduced into *STE2* by use of a modified version of a PCR

based random mutagenesis protocol (28) as described below. *STE2* was amplified using the primers XHOIA (CATATCCA AGACTCGAGAATGTCTGATGCG) and XHOIB (CTACCACTACTCTCGAGAT GTTTATTATG) using the following conditions: 50ng of pAB539 (29) as template; 50nM each of XHOIA and XHOIB primers; 200μM $MnCl_2$; 200μM each of dCTP, dGTP, dTTP, and 40μM dATP; 1X PCR buffer (50mM Tris, 500μg/ml BSA, 0.5% Ficoll, 1mM Tartrazine, 2mM $MgCl_2$); 2.5 Units of *Taq* DNA polymerase (Promega) in 25μl total volume. Hot start PCR was used for amplification by heating the reaction mix (without *Taq* polymerase) to 94°C for 5 min., transferring to ice for 5 min., and then adding 2.5 Units of *Taq* polymerase and cycling 25 times at 94°C for 30 sec., 58°C for 2 min., and 72°C for 1.5 min. Point mutations in primer sequences (underlined) introduced flanking *Xho*I restriction sites that allowed for subcloning of mutagenic PCR products into the unique *Sal* I site of the vector pAD54 (30) to produce a series of yeast expression vectors (pSTEAD) containing a library of mutant receptor genes.

FUS1-lacZ screen for antagonist responsive mutant receptors – The pSTEAD library of plasmids was transformed according to standard protocol (31) into yeast strain LM23-16az, plated on synthetic dextrose minimal medium supplemented with lysine and methionine (SD+KM) and grown at 30°C for 72 hrs. *LacZ* induction was assayed as previously described (16). Transformant colonies were replica plated onto SD+KM plates overlayed with filters (Whatman no. 50) and with or without 10 μg/ml desTrp^{1}desHis^2[Nle^{12}]α -factor antagonist

incubated for 6 hrs. at 30°C. Filters were quick frozen in liquid nitrogen for 20 sec. and transferred to a second filter (Whatman no. 3) that had been soaked with 2.5 ml Z-buffer (60mM $Na_2HPO_4 \cdot 7H_2O$, 40mM $NaH_2PO_4 \cdot H_2O$, 10mM KCl, 1mM $MgSO_4 \cdot 7H_2O$, 50mM β-mercaptoethanol, pH 7.0) containing 0.03% X-gal. The filters were incubated at 30°C for 1-3 hrs. to allow for any blue color development from β-galactosidase production. Filters were aligned with the original transformant plates and colonies corresponding to replicated colonies that turned blue were isolated for further testing. Plasmids from the transformed yeast colonies that demonstrated unusual phenotype(s) to [Nle^{12}]α-factor and/or antagonist were isolated (32), amplified in *E. coli,* and purified using a plasmid maxiprep kit (Qiagen, Inc.) as per manufacturer's instructions.

Construction of expression vector for site-directed mutagenesis – A yeast/bacterial shuttle vector (pGA314.WT) was constructed by starting with the vector pRS314 (33) linearized with *Spe*I (New England Biolabs, NEB) and purified with the Wizard DNA clean-up kit according to manufacturers protocol (Promega). A 1.8 Kb PCR fragment containing the *STE2* ORF plus 316 bp upstream promoter region from the start ATG and 163 bp downstream region from the stop codon was amplified from the vector template pAB539 (29) using the primers SPEIA (GCTTTGCAATGAAACACTAGTATCCGCTAAG) and SPEIB (GTGGTTTCTAC CACTAGTTACGAGATGTTTATTATG). The PCR conditions used were as follows: 40ng pAB539, 100nM each primers SPEIA and SPEIB, mix of 200μM each of dNTP, 1X DeepVent polymerase buffer (10mM KCl, 10mM

$(NH_4)_2SO_4$, 20mM Tris-HCl (pH 8.8), 2mM $MgSO_4$, 0.1% Triton X-100), 1 Unit DeepVent DNA polymerase (NEB), for 25 cycles of 94°C (1 min.), 46°C (2 min.), 72°C (3 min.) with a final extension of 72°C for 10 min. Point mutations (underlined in primer sequence) introduce *Spe*I restriction sites into the ends of the PCR fragment. PCR fragments were subsequently digested with *Spe*I and purified with the Wizard PCR preps DNA purification system (Promega). PCR fragment and linear pRS314 vector were ligated together using the standard protocol accompanying the Ligator rapid DNA ligation and screening kit (Epicenter Technologies) producing the vector pGA314.WT. The entire *STE2* gene and flanking regions was sequenced and confirmed that the subcloned region was wild-type sequence with no spurious mutations. In this plasmid, the *STE2* gene was under control of its own promoter, and the plasmid replicated under control of the CEN6/ARSH4 element.

Site-directed mutagenesis of STE2 – Site-directed mutagenesis of *STE2* was carried out using a modified version of overlap extension PCR (34). The first round of amplification required 200 ng pGA314.WT DNA, 5 μM dNTPs, 1 μM primer A or B, 1 μM of each mutagenic primer, 1X *Taq* DNA polymerase buffer (50mM KCl, 10mM Tris-HCl, 0.1% Triton X-100, 2mM $MgCl_2$, NEB), and 2.5 Units *Taq* DNA polymerase (NEB) in a total volume of 100μl for 25 cycles of 94°C (1 min.), 50°C (2 min.), and 72°C (3 min.). Fragments generated during the first round of PCR were gel purified using the Geneclean I kit (Bio101) and used as template DNA for a second round of PCR-overlap extension

mutagenesis. The second round of amplification was performed using 200ng of the 5'-half mutagenic fragment, 200ng of the 3'-half mutagenic fragment, 1X *Taq* DNA polymerase buffer, 100μM dNTPs, and 1 Unit *Taq* DNA polymerase in a total volume of 10μl for 10 cycles of 94°C (1 min.), 55°C (2 min.), and 72°C (3 min.). A third round of amplification was performed to produce the full length *STE2* gene with point mutations (underlined in primer sequences below) that introduce single amino acid substitutions in the translated protein product. Conditions for the third round of amplification were 1 μl of round 2 reaction mix, 1.0 μM primer A, 1.0 μM primer B, 1X *Taq* DNA polymerase buffer, 5 μM dNTPs, and 2.5 Units *Taq* DNA polymerase in a total volume of 100 μl for 30 cycles of 94°C (1 min.), 50°C (2 min.), and 72°C (3 min.).

Full length third round PCR reaction products were subcloned into the vector pCR2.1 (Invitrogen TA cloning kit) and amplified in *E. coli* strain DH5α. Bacterial transformants were randomly chosen and plasmid DNA was isolated from each (35). Insert-containing plasmids were digested with *Eco*RI and the 1.8Kb *STE2* gene fragment was isolated using the Geneclean I DNA purification kit and subcloned into the unique *Eco*RI site of pRS314 to produce the plasmids pGA314.F55V, pGA314.S219P, and pGA314.S259P (pGA314.WT vector with *TRP* and *URA* as selectable markers that now contains a *STE2* gene with the designated mutation).

Primer pairs used for the initial round of amplification reactions to introduce single point mutations were primer A (GGATAACAATTTCACA

CAGG) with primer F55VF (GGCCATTATGGTTGGTGTCAG), primer A with primer S259PF (GTTGGTTCCACCGATAAT ATT), primer A with primer S219PF (GCATCCT CAATAAACTTTATGCCATTTGTCCTGGTAGTTAAATTGATTTTAGC), primer B (TCGCTATTACGCCAGCTGG) with primer F55VR (CTGACACCAACCATA ATGGCC), primer B with primer S259PR (AATATTATCGGTGGAACCAAC), primer B with primer S219PR (GCTAAAATCAATTTAACTACCAGGACAAA TGGCATAAAGTTTATTGAGGATGC). All of the mutant receptor genes were sequenced twice to ensure that the sequences were identical to the published wild type sequence of *STE2* with the exception of the designed mutant nucleotide changes.

Growth arrest (halo) assay – SD medium (36) supplemented with histidine (20μg/ml), leucine (30μg/ml) and methionine (20μg/ml) was overlayed with 4 ml of *S. cerevisiae* LM102 (2.5×10^5 cells/ml of Nobel agar) transformed with various plasmids containing wild-type or mutant *STE2*. Filter disks (sterile blanks from Difco), 8 mm in diameter, were placed on the overlay, and 10 μl portions of peptide solutions at various concentrations were placed on the disks. The plates were incubated at 30°C for 24-36 hours and then observed for clear zones (halos) around the disks. The data were expressed as the diameter of the halo including the diameter of the disk. The minimum value for growth arrest is 9 mm, which represents the disk diameter (8 mm) and a small zone of inhibition. [Nle^{12}]α-factor, an isosteric analog that is equally active (37) to the wild-type pheromone was used as a control in all bioactivity assays and in receptor

binding. All assays were repeated at least three times with no more than a 2 mm variation in halo size for a particular amount of peptide. The data were plotted as halo size versus the amount of pheromone added to the lawn and linearized by regression analysis. To compare the relative activities of different peptides with different receptors, the amount of peptide causing a halo size of 15 mm was determined from the regression line. At least two dose response values were above and below the point intersecting 15 mm zone with the amount of peptide making extrapolation of the data unnecessary. In addition, the slopes of dose response curves for the different receptors were nearly identical validating the comparisons among receptors for different analogs. Differences in diffusion of the various analogs in the agar medium did not contribute to the differences in the biological activities in the halo assay. Similar trends were obtained for these analogs when activities were ranked within an assay as measured by the halo or gene (*FUS1-LacZ*) induction. In the *FUS1-LacZ* assay, cells were suspended in liquid medium and diffusion through agar played no role in the activity of the soluble pheromones. Further evidence that diffusion rates do not determine bioactivity in the halo assay is given by the fact that there is no correlation between bioactivity and peptide hydrophobicity as measured by K' values on HPLC columns (38).

Effect of α-Factor Analogs on Gene Induction – S. cerevisiae LM102 carries a *FUS1* gene that is inducible by mating pheromone and fused to the gene encoding β-galactosidase as a reporter. Cells were grown overnight in SD at 30°C to 5 x 10^6 cells/ml, harvested by centrifugation, resuspended in fresh

medium, and grown for one doubling at 30°C. Induction was performed by adding 0.5 ml of peptide at various concentrations to 4.5 ml of concentrated cells (1×10^8 cells/ml). The suspensions were vortexed and placed at 30°C with shaking for 2 h. After this time, cells were harvested by centrifugation, each pellet was resuspended, and assays were carried out for β-galactosidase in triplicate by a recently modified (39) standard protocol (40, 41). The experiments were repeated at least twice for each analog with the values plotted representing an average of these determinations.

Antagonism and Synergism Assays – The halo assay was used to determine whether analogs that had no growth arrest activity by themselves were capable of antagonizing (interfering with activity by agonists) or synergizing (enhancing activity of agonists) activity of [Nle^{12}]α-factor (38). Lawns of LM102 were overlaid onto SD plates as described in the growth arrest assay. Sterile disks were placed adjacent to each other so that the disk containing the test peptide would lie at the periphery of the halo formed by [Nle^{12}]α-factor. One disk was impregnated with 1 μg of [Nle^{12}]α-factor in 10 μl H_2O, and the other disk was impregnated with various amounts of the test peptide in 10 μl H_2O. Plates were incubated as described in the growth arrest assay and the effects on halo formation noted.

Peptide synthesis – [Nle^{12}]α-factor, and all antagonists and a synergist used in this study were synthesized using solid phase peptide synthesis as described in detail previously (38, 42, and 43). All peptides used were >98%

homogeneous as judged by reversed-phase HPLC in two eluent systems and capillary zone electrophoresis. The [Nle^{12}] α-factor analogs were devoid of the parent compound as judged using HPLC analysis.

HPLC purification of [^{3}H]α-factor – Synthetic [Nle^{12}]α-factor was labeled by reduction of dehydroproline containing α-factor by the TR3 hydrogenation procedure of Amersham International as described previously (37). Unpurified, labeled peptide (dissolved in ethanol/water 1:1) was dried *in vacuo,* redissolved in sterile water and purified by HPLC using a Waters μBondapak C_{18} column (3.9 mm×300 mm) on a Beckman System Gold HPLC. The peptide solution was injected into the HPLC and eluted with a water/acetonitrile gradient from 0-40% acetonitrile. Fractions containing peptide eluting from the column similarly to unlabeled α-factor (elution at 32.3% CH_3CN) were collected and counted for radioactivity in a scintillation counter. All collected fractions were dried, resuspended in storage buffer (1mM methionine, 0.03% trifluoroacetic acid, 20% ethanol), combined, and the concentration and specific activity of the purified labeled peptide was determined.

Binding competition assay – This assay was performed using membranes of strain LM102 and HPLC-purified H^3[Nle^{12}]α-factor (see above) as described previously (44). Binding of labeled α-factor to filters in the absence of membranes was less than 20 cpm. Specific binding is defined as (mean bound cpm/total mean cpm) x 100. Mean bound cpm is the average of 4 determinations for each binding point for each analog and total mean cpm is the average of 4 determinations of the total counts incubated with each analog. Results for each

analog were expressed as a percent of total binding in the absence of the analog. Each binding assay was carried out at least two times with virtually identical curves obtained. The *Ki* values were calculated by dividing the experimentally determined concentration giving 50% binding displacement by [1 + H_T/K_D] where H_T = concentration of radiolabel and K_D = dissociation constant of radiolabeled α-factor (45).

Western blot – Equal amounts of solublized membrane proteins (5 mg) were resolved by SDS-PAGE (10%), electrophoretically transferred to immobilon P membrane (Millipore) and probed with anti-N-terminal-Ste2p antibodies provided by James Konopka, SUNY Stony Brook (46). The resulting immune complexes were detected by incubation with 1:3,000 dilution of horseradish peroxidase-conjugated goat anti-rabbit antibodies, and visualized by chemiluminescence (ECL kit, Amersham).

CHAPTER 3

Results

Random mutagenesis of STE2 and sequence analysis – The plasmid pAB539 was used as the template DNA for PCR-based, random mutagenesis of the *STE2* gene. *Saccharomyces cerevisiae* strain LM23-16az (a *MAT**a*** yeast strain that expresses a non-functional α-factor receptor) was transformed with the library of mutant *STE2*-containing plasmids and screened for ligand-dependent biological response to desTrp^{1}desHis^{2}[Nle^{12}]α-factor, an antagonist peptide (42), by *FUS1*-lacZ induction. Approximately 40,000 colonies were screened and a total of 144 *FUS1-lacZ* positive clones were isolated. These clones were re-tested for *FUS1*-lacZ induction and 83 false positive clones that did not respond to antagonist identified and discarded. The high number of false positive colonies isolated during the first screening round was due to the inexact selection of positively responding colonies; the close proximity of colonies on the plates did not allow for the specific identification of positive clones. The remaining 61 β-galactosidase-positive colonies were individually plated as lawns on selective medium and tested for growth arrest response to 3 μg of [Nle^{12}]α-factor, 10 μg of the antagonist desTrp^{1}desHis^{2}[Nle^{12}]α-factor, and 10μg of the antagonist desTrp^{1}[Ala^{3},Nle^{12}]α-factor (47). Eighteen colonies demonstrated varying degrees of growth arrest (zones of growth inhibition from 9mm to 21mm)

to both antagonists and [Nle^{12}]α-factor (e.g. MR007 and MR012, Table 1), and 20 colonies (e.g. MR 097, Table 1) demonstrated no growth arrest response to either of the antagonists or [Nle^{12}]α-factor. The remaining isolates responded only to [Nle^{12}]α-factor to varying degrees (9mm to 25mm diameter zones of growth inhibition), but did not respond to either antagonist (e.g. MR 019 and MR 025, Table 1) or respond only to antagonists (e.g. MR 131, Table 1). Plasmid DNA from representatives of each phenotype class was purified and *STE2* sequenced to identify the mutated residues (Table 1). Each of the mutated *STE2* genes contained between 10-19 bp changes that translated into 5-10 residue mutations per receptor protein. Due to the difficulties in interpreting phenotypic changes in pheromone response with receptors containing multiple mutations, we decided to generate site-specific mutants based on results obtained in the multiply mutated receptors produced by PCR mutagenesis.

Site-directed mutagenesis of STE2 – Specific residues identified during the random mutagenesis of the *STE2* gene were targeted for site-directed mutagenesis based on three criteria: 1) The residue was observed to be changed in receptors with an antagonist-responsive growth arrest phenotype; 2) The residue was located in a transmembrane domain; and 3) The residue was in close proximity to previously described receptor mutations demonstrating phenotypes of altered ligand (15,16). PCR based site-directed mutagenesis (see Chapter 2) of wild-type *STE2* was carried out to produce 3 mutant receptors each expressing one of the following mutations: F55V (TM domain 1), S219P (TM domain 5), or S259P (TM domain 6) (Figure 1).

TABLE 1: Sequence and growth arrest response of mutant α-factor receptors selected from random mutagenesis screen.

Mutant	Mutation			Halo response to:	
	N-terminal domain (residues 1-50)	Middle domain (residues 51-299)	C-terminal domain (residues 300-431)	Antagonist[a]	α-factor
MR007	None	N84D M165T F182L N216S I230T D242G	I308G F327S E403G	+	+
MR012	None	S259P I263V	A369G M409T D417G	+	+
MR019	E40G	L93F Q149R	N375S D417G K422E F423S	-	+
MR025	F38L	R76G G156S M165I L255M S267G T278S	N301S T354R K374N G402A	-	+
MR097	S28F N46D	F116L L284P	K304I K374E L380S T382A	-	-
MR131	None	F55V N132S I142N S219P	T313S R318G L324P N334D R343S D357G	+	-

(***a***) desTrp^{1}desHis^2[Nle^{12}]α-factor and desTrp^1[Ala^3, Nle^{12}]α-factor were the antagonist used in the screening.

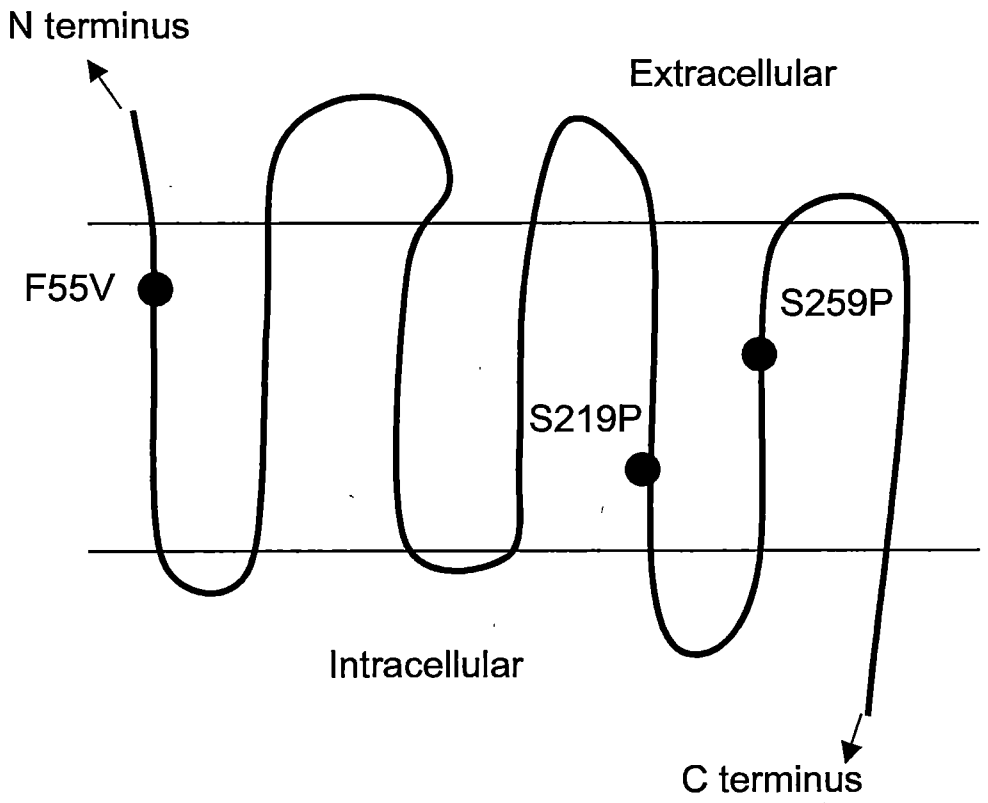

Figure 1: Site-directed mutations introduced into the α-factor receptor. Mutations were introduced individually using a modified PCR protocol (See Material and Method). Relative locations of each residue (black circle) are indicated based on predicted membrane topology of the α-factor receptor (55).

Growth arrest response of mutant α-factor receptors to [Nle^{12}]α -factor and various analogs – The three mutant receptors were expressed in LM102 and tested for their growth arrest response to [Nle^{12}]α-factor and α-factor analogs (Table 2). Three peptides previously demonstrated to be antagonists (38,42,47) desTrp^{1}desHis^{2}[Nle^{12}]α-factor, desTrp^{1}[Ala^{3},Nle^{12}]α-factor, and [D-Ala^{3},Nle^{12}]α-factor, and one synergistic peptide (38), [D-Ala^{10},Nle^{12}]α-factor were used to challenge mutant receptors (Figure 2). As previously shown, none of these analogs elicited a growth arrest response from a cell expressing a wild-type receptor. All responses to all peptides were ligand-dependant (constitutively responding mutant receptors were not isolated or observed).

Each of the strains carrying mutant receptors was induced to form 15 mm halo by less α-factor than that needed to induce 15 mm halo in the wild type receptor strain. Thus, the mutant receptor responded better than the wild type receptor to α-factor itself in this assay (Table 2). The largest increase in sensitivity (~2-fold) was found with S259P. The response of the mutants was greater to α-factor at each amount tested from 0.05 to 10 μg/ml of α-factor (data not shown). Receptor F55V did not respond to any antagonist, but the synergist analog [*D*-Ala^{10}Nle12]α-factor became a weak agonist for this mutant receptor; it took 1.38 μg of analog to produce a 15 mm halo in F55V, whereas only 0.33 μg of α-factor was required to induce this size halo in the wild type receptor.

Table 2: Growth arrest response to α-factor and α-factor analogs in cells expressing various receptors.

Ste2p expressed	Amount of peptide (μg) for 15 mm halo[a]				
	α-factor	desW^{1}desH^2	desW^{1}A^3	D-A^3	D-A^{10}
Wild type	0.33 (1.0)	> 20 [b]	> 20	> 20	> 20
F55V	0.26 (1.27)	> 20	> 20	> 20	1.38 (0.24)
S219P	0.17 (1.94)	> 20	1.84 (0.18)	> 20	0.45 (0.73)
S259P	0.15 (2.2)	5.75 (0.06)	2.5 (0.13)	1.96 (0.17)	3.55 (0.09)

(***a***) The number in parentheses is the ratio of the amount of peptide required for a 15 mm halo compared to the amount (0.33 μg) of α-factor required for a 15 mm halo in the wild type receptor.

(***b***) 20 μg was highest amount of peptide tested.

		Abbreviation
Agonist		
[Nle^{12}]α-factor –	WHWLQLKPGQP[Nle]Y	α-factor
Antagonists		
desTrp^{1}desHis^{2}[Nle^{12}]α-factor –	WLQLKPGQP[Nle]Y	desW^{1}desH^{2}
desTrp^{1}[Ala^{3},Nle^{12}]α-factor –	H(A)LQLKPGQP[Nle]Y	desW^{1}A^{3}
[D-Ala^{3},Nle^{12}]α-factor –	WH(D-A)LQLKPGQP[Nle]Y	D-A^{3}
Synergist		
[D-Ala^{10},Nle^{12}]α-factor –	WHWLQLKPG(D-A)P[Nle]Y	D-A^{10}

Figure 2: List of α-factor and its analogs.

The primary structure of α-factor and α-factor analogs used in this study is compared. Abbreviations of each peptide are used in the figures and tables throughout the study.

Receptor S219P responded well to the synergist and poorly to one of the antagonists (desTrp^1[Ala^3,Nle^{12}]α-factor), but not at all to the other two antagonists tested. Receptor S259P, which was the most responsive to α-factor, responded, to all the antagonists and synergists tested, albeit rather poorly. The failure of F55V to respond to any of the antagonists, despite the fact that the screen implicated this as a potential residue for antagonist responsiveness, indicates that other mutations of the receptor, or a combination of these other mutations and F55V, caused the antagonist response in the screen.

When a peptide showed no agonist activity to an expressed receptor, the peptide was tested for antagonistic activity against peptides that were agonist for that receptor. The results of these assays are summarized in Table 3. For clarity, the table also reflects the results of Table 2 as to the activity of active peptides. The pattern of cross antagonism is complex. For example, desTrp^{1}desHis^2[Nle^{12}]α-factor is antagonistic to [D-Ala^{10},Nle^{12}]α-factor but not α-factor in the F55V receptor whereas it is antagonistic to all agonists in the S219P receptor. DesTrp^{1}Ala^3[Nle^{12}]α-factor and [D-Ala^{3}Nle^{12}]α-factor are not antagonists in the F55V receptor, but [D-Ala^{3}Nle^{12}]α-factor was an antagonist to all agonists in the S219P receptor. As indicated by the competition binding assays, the above characteristics are closely related to the relative changes in affinities of these peptides for the various receptors (see below).

Expression of receptor protein in mutants – A direct measurement of receptor was carried out to determine whether any of the mutations affected receptor biosynthesis or transport to the membrane. Cells expressing the various

Table 3: Profile of peptide activities in wild type and mutant receptors [a]

Receptors	Activities of peptides tested				
	α-factor	desW^{1}desH^2	desW^{1}A^3	D-A^3	D-A^{10}
Wild type	Agonist	Antagonist	Antagonist	Antagonist	Synergist
F55V	Agonist	Antagonist to D-A^{10} but not to α-factor	Not antagonistic to α-factor or D-A^{10}	Not antagonistic to α-factor or D-A^{10}	Agonist
S219P	Agonist	Antagonist to all agonist	Agonist	Antagonist to all agonist	Agonist
S259P	Agonist	Agonist	Agonist	Agonist	Agonist

(***a***) The agonist activity is seen in both the growth arrest (Table 2) and *Fus1-lacZ* assay (Table 4).

mutant Ste2p constructs were grown, membranes prepared, and proteins separated by SDS-PAGE according to standard conditions for measurement of Ste2p expression in *S. cerevisiae*. Ample amounts of receptor were detected in Western blots of the wild type and mutant receptors F55V and S219P (Figure 3). The apparent doublet form of the receptor has been observed by others using various antibody preparations (15,25,41,45) implying different levels of glycosylation. In contrast to visualization of Ste2p in mutant F55V and S219P, the S259P receptor was practically undetectable despite the good α-factor response in cells expressing S259P receptor. The data represented in Figure 3, along with the inability to obtain a measurable binding of α-factor to cells expressing S259P, may be attributed to the instability of the S259P receptor or other factors as discussed below.

Mutant receptor signaling as indicated by induction of pheromone-responsive gene to α-factor and α-factor analogs – LacZ activity was measured in response to a single concentration (10 μM) of various peptides added to cultures expressing wild type and mutant receptors (Table 4). At this concentration α-factor induced near maximal activity in cell expressing wild type receptor. In general, the pattern of *FUS1-lacZ* gene induction is similar to that of the growth arrest response for all receptors and peptides. In all cases, peptides exhibiting no activity in the growth arrest assay induce less than 3% of the *lacZ* activity induced by α-factor. Where activity was observed in the growth arrest assay, gene induction was also observed. For example, the D-Ala^{10} analog was an agonist against all mutant receptors in both assays. However, some subtle

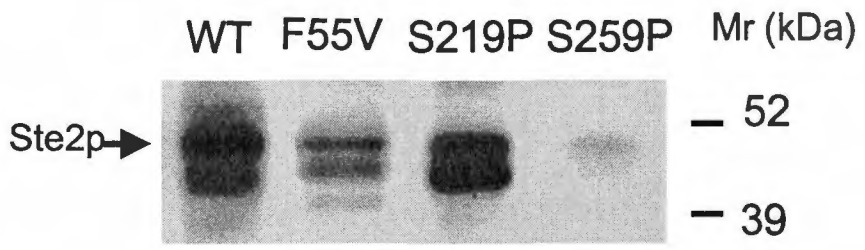

Figure 3: Western blots of cells expressing wild type and mutant receptors. WT, wild type cells; F55V, S219P, and S259P, cells expressing Ste2p carrying the F55V, S219P, and S259P mutations, respectively. The molecular weight markers are shown for proteins of 52 and 39 kDa, and the position where Ste2p is predicted to migrate is indicated by an arrow.

Table 4: Gene Induction by various peptides in wild type and mutant receptors. All peptides were added at 10 μM and the *lacZ* activity in Miller units was determined as in Section 2. The standard error of the mean is indicated, and the number in parentheses is the ratio of the activity of *lacZ* compared to the amount (24 Miller units) induced by α-factor in the wild type receptor. The basal activity for all peptides and mutant was less than 0.2 Miller units.

Ste2p	Gene induction activity of peptides tested				
expressed	α-factor	desW^{1}desH^2	desW^{1}A^3	D-A^3	D-A^{10}
Wild type	24.0 ± 1.9 (1.0)	0.3 (<0.03)	0.2 (<0.03)	0.1 (<0.03)	0.35 (<0.03)
F55V	19.2 ± 1.8 (0.8)	0.3 (<0.03)	0.5 (<0.03)	0.3 (<0.03)	20.0 ± 2.8 (0.83)
S219	15.0 ± 1.5 (0.63)	0.6 (<0.03)	6.0 ± 0.8 (0.25)	0.6 (<0.03)	13.0 ± 1.1 (0.54)
S259P	24.0 ± 2.2 (1.0)	15.5 ± 2 (0.65)	17.0 ± 1.6 (0.7)	14.9 ± 1.8 (0.62)	18.0 ± 1.3 (0.75)

differences between the growth arrest assay and the gene induction assay are noted: (1) in the growth arrest assay, α-factor was more active in the mutant receptors than in the wild type receptor, whereas α-factor was most active for the wild type receptor in the gene induction assay.; (2) all analogs appeared to be more active in the gene induction assay than in the growth arrest assay for the S259P receptor; and (3) the D-Ala10 analog was more active for the F55V and S259P receptor mutants in the gene induction assay as compared to the growth arrest assay. In order to carry out a more detailed study, a dose response of *lacZ* activity to various amounts of peptides were determined (Figure4). The wild-type receptor did not transduce the signal to the reporter gene at any concentration of antagonist or synergist (Figure. 4, Panel A). Furthermore, the response curves of F55V and S219P indicated only partial induction of the lacZ gene even at pheromone concentrations as high as 10 μM. Thus, while the mutant receptors respond to certain compounds that were inactive with wild type Ste2p, these receptors cannot trigger a complete signal upon activation by these compounds or α-factor.

The maximal response to all peptides appeared to peak at 10^{-6}M for F55V and S219P, whereas the response of S259P did appear to peak at concentrations of 10^{-5} M.

Binding competition assays----Binding of peptides to the wild-type and two mutant receptors was determined by competition assays on isolated membrane. The binding curves for the α-factor analogs demonstrate that many analogs do this study. This is likely due to the poor binding affinity of these peptides at the

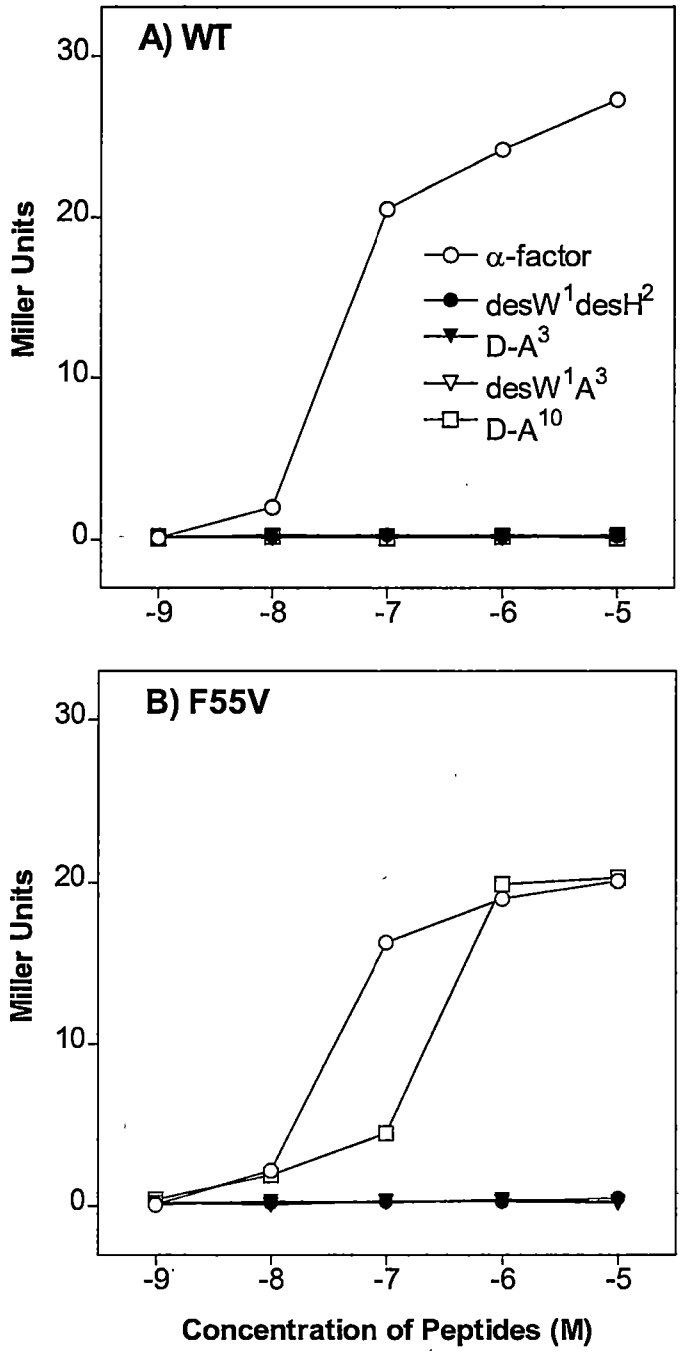

Figure 4: Dose response to α-factor and α-factor analogs in wild type and mutant receptors determined by reporter gene *lacZ*. The wild type (A), F55V (B), S219P (C), and S259P (D) receptors are shown in separate panels indicated on the figure.

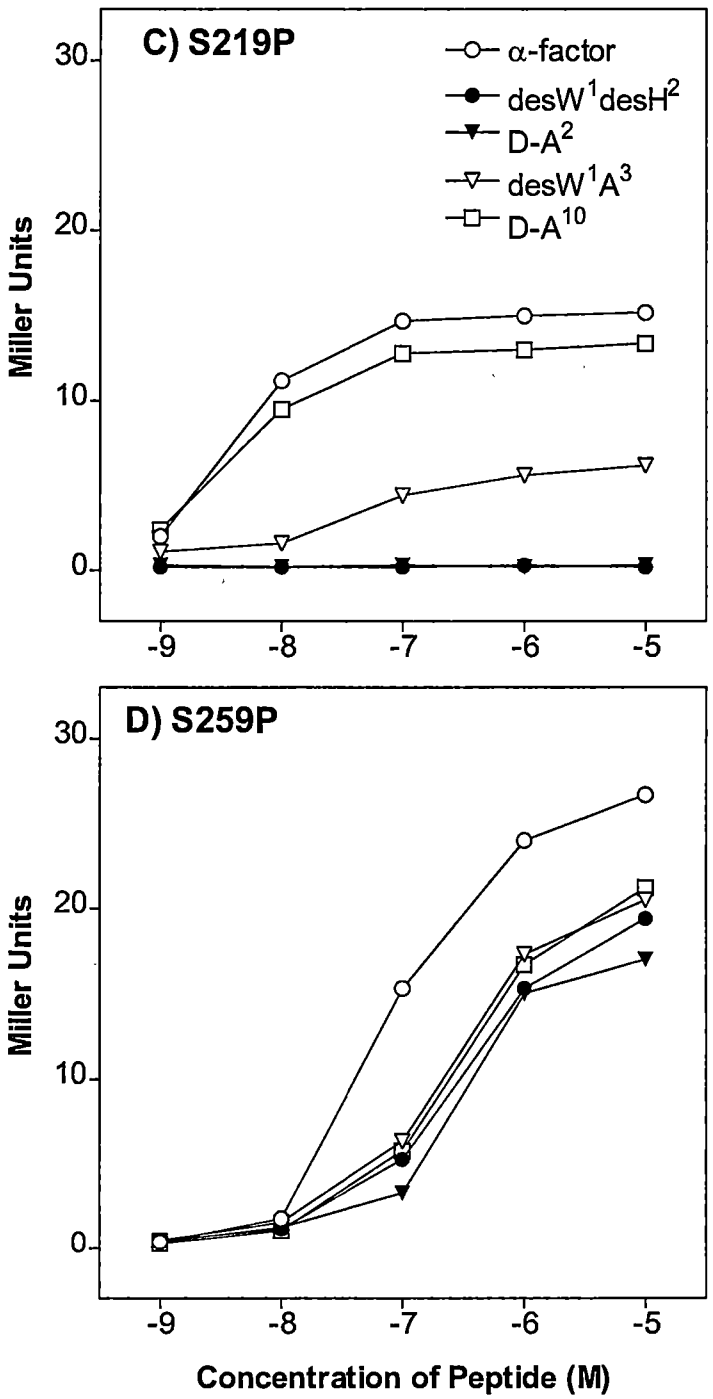
C) S219P
α-factor
desW1desH2
D-A2
desW1A3
D-A10
Miller Units
30
20
10
0
-9
-8
-7
-6
-5
D) S259P
Miller Units
30
20
10
0
-9
-8
-7
-6
-5
Concentration of Peptide (M)

this study. This is likely due to the poor binding affinity of these peptides at the concentrations attainable for testing (Figure 5).

The calculated *Ki* values indicate that binding of α-factor to the F55V and S219P receptors was about 10-fold less than its binding to the wild type receptor (Table 5). As seen in previous reports (38,42), the competition of the synergist for α-factor binding to the wild type receptor was not detectable, but the synergist did compete with the α-factor binding site in F55V. The synergist had a 10-fold lower affinity than α-factor for the F55V receptor. We were not able to measure binding to the S259P receptor. Even at high concentrations of [^{3}H]α-factor, the amount of radioactive α-factor associated with membranes from cells expressing the S259P receptor was not above background levels. Attempts to measure binding with whole cells were unsuccessful as well using methods previously employed by us and others (37,48). The inability to measure binding to the S259P receptor may be related to the instability of this receptor as reflected by the barely detectable amount of Ste2p in Western blot (Figure 3). The *Ki* values for the antagonists to the wild-type receptor were similar to values obtained for measurements using whole cells and *STE2* expressed from its natural chromosomal site under its natural promoter (37,38). This was despite the fact that several of these peptides were either weak agonists or antagonists for these mutant receptors in the halo or gene induction assays (Table 2 and 4).

Figure 5: Competition binding assays of wild type and mutant receptors to α-factor and α-factor analogs. The wild type (A), F55V (B) and S219P (C) receptors are shown in separate panels indicated on the figure.

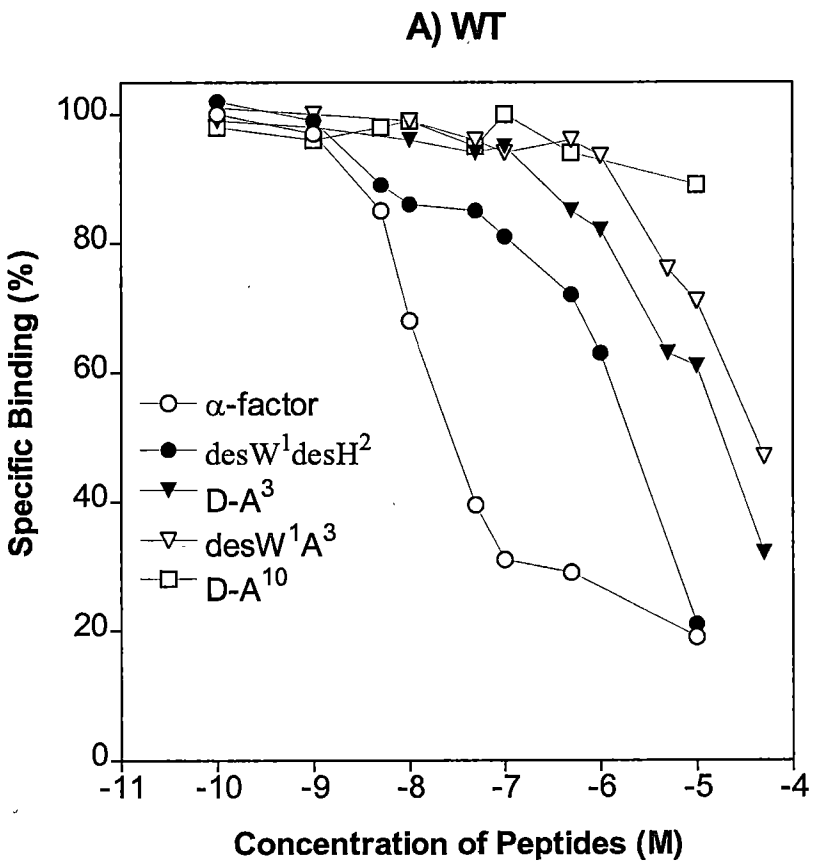
A) WT
Specific Binding (%)
100
80
60
40
20
0
-11
-10
-9
-8
-7
-6
-5
-4
α-factor
desW1desH2
D-A3
desW1A3
D-A10
Concentration of Peptides (M)

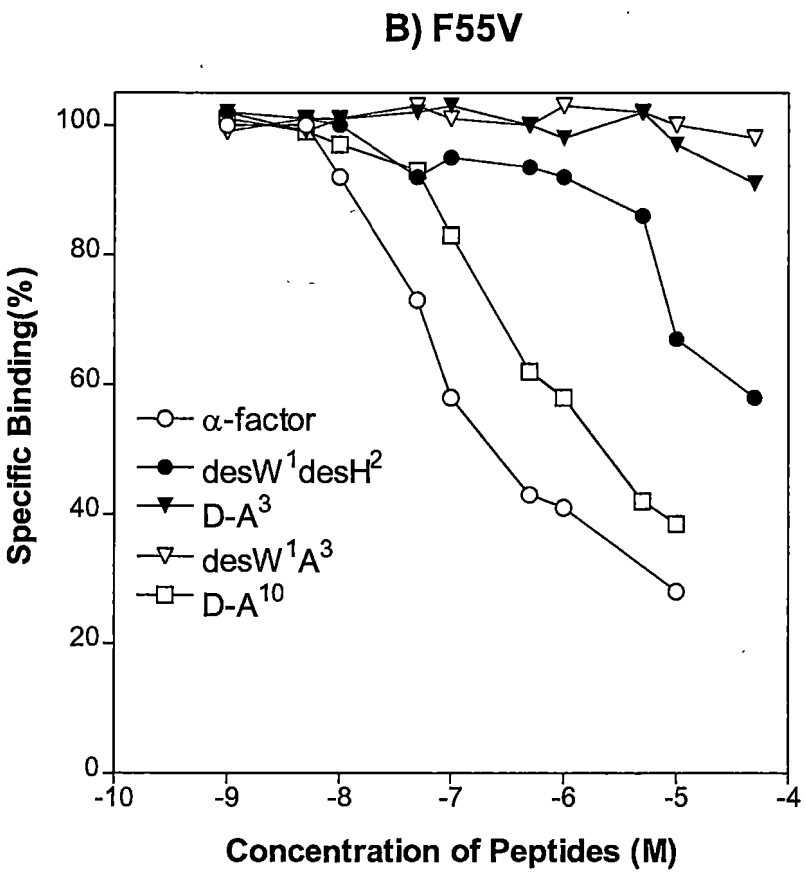
B) F55V
Specific Binding(%)
100
80
60
40
20
0
-10
-9
-8
-7
-6
-5
-4
Concentration of Peptides (M)
α-factor
desW1desH2
D-A3
desW1A3
D-A10

C) S219P

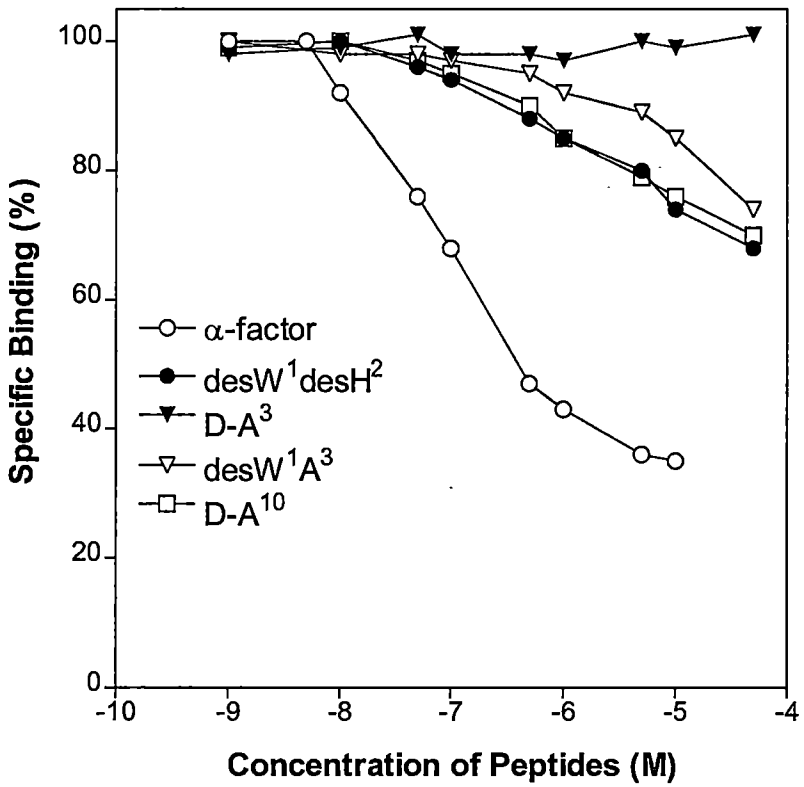
Specific Binding (%)
100
80
60
40
20
0
-10
-9
-8
-7
-6
-5
-4
α-factor
desW1desH2
D-A3
desW1A3
D-A10
Concentration of Peptides (M)

Table 5: Competition binding assay

Ste2p expressed	Binding constants of peptides tested[a]				
	α-factor	desW^{1}desH^2	desW^{1}A^3	D-A^3	D-A^{10}
Wild type	1.8 ± 0.2	125 ± 10	1750 ± 100	1050 ± 50	> 10000
F55V	19.4 ± 0.4	~ 10000	> 10000	> 10000	210 ± 10
S219P	14.6 ± 2.6	> 10000	> 10000	> 10000	> 10000
S259P	No detectable binding under the conditions tested				

(***a***) The values shown in the table are the *Ki* values (x 10^{-8} M). The standard error of the mean is indicated for quadruplicate assays.

CHAPTER 4

Discussion

We have generated mutant α-factor receptors altered in their response to various α-factor analogs using PCR-based random mutagenesis and site directed mutagenesis. Three receptors containing mutations F55V (TM1), S219P (TM5), and S259P (TM6) were analyzed for their biological responses to α-factor antagonists and a synergist and for their ligand binding profiles. Analysis of these mutant receptors implicates the first, fifth and sixth transmembrane regions of Ste2p as important for ligand interaction, ligand specificity, and/or receptor activation to initiate the signal transduction pathway. Change in binding affinity of pheromone analogs to wild type and mutant receptors indicate that residue 55 of Ste2p is involved with both ligand binding and signal transduction.

Initially, the α-factor receptor was mutated utilizing the intrinsic error rate of the *Taq* DNA polymerase in a modified PCR protocol (29) in an attempt to introduce single mutations randomly throughout the gene. The screen was successful in that we were able to introduce random mutations in the *STE2* gene yielding antagonist-responsive receptors, but the mutant *STE2* genes recovered from colonies responding to an α-factor antagonist contained 5-10 residue

substitutions per receptor. While information concerning the roles of specific residues of the receptor could not be elucidated from mutant receptors containing multiple mutations, these experiments provided guidance for the subsequent generation of site-directed, single-residue mutants.

The F55V mutation found in the random screen was chosen for further study due its proximity to a mutaion in the adjacent methionine (M54I) residue described by Marsh (16). The M54I receptor responded poorly to desTrp^{1}[Ala^{3}]-α-factor in comparison to its response to α-factor in the *FUS1-lacZ* assay and growth arrest assat, and this receptor (M54I) responded equally as well as the wild-type receptor to α-factor in both assays. These and other results (16) allowed Marsh to conclude that the M54I mutation appeared to affect ligand specificity only. In our studies, the F55V mutant receptor responded to the synergistic analog [*D*-Ala^{10},Nle^{12}]α -factor and also to [Nle^{12}]α -factor, but there was no response to any of three antagonists tested including desTrp^{1}[Ala^{3}]-α-factor. It is interesting, and perhaps indicative of subtle interactions between ligand residues and receptor residues that are adjacent in the primary sequence, that the analog desTrp^{1}[Ala^{3}]-α-factor, an antagonist to the wild type receptor, was an agonist to M54I, but not to F55V. In the wild-type receptor the D-Ala^{10} analog did not have any activity in the growth arrest assay or *FUS1-lacZ* on its own, but did enhance the potency of [Nle^{12}]α-factor in both assays when incubated together (38). The nature of this specificity reversal for the D-Ala^{10}

analog might be explained by a mutation in receptor residue 55 that normally interacts directly with the native ligand.

Although the binding of α-factor itself is decreased in the F55V mutant, the binding of the D-Ala^{10} analog is greatly increased over its binding to the wild type receptor (Table 5). According to the previous (38) and present results, it is reasonable that the D-Ala^{10} analog does not bind to wild type Ste2p. Change in chirality of residue 10 would result in a major change in the orientation of the carboxyl terminus of α-factor relative to the remainder of the pheromone. In contrast to the 10 to over 100 fold decrease in binding affinity of α-factor and all antagonists tested, D-Ala^{10} α-factor showed a dramatic increase in binding affinity to F55V receptor and this binding results in signal transduction. Considering the primary sequence of α-factor and analogs (Figure 1), it is interesting that the binding affinity of peptides with intact C-terminal region (α-factor and all antagonists tested) was decreased to F55V receptor while the affinity of a peptide modified at C-terminal region (D-Ala^{10}) was increased. This may indicate that the replacement of valine for phenylalanine causes a change in the local environment of receptor which interacts with C-terminal part of α-factor.

Previous results indicated that the carboxyl terminus of α-factor is extremely important for binding (38). Changing Tyr^{13} to Ala^{13} resulted in almost a 500-fold decrease in affinity for wild type Ste2p. In addition, results with chimeric receptors from *S. cerevisiae* and *S. kluyveri* indicated that residues 45-47 of the receptor are important in ligand specificity between α-factors of two closely

related species (21). These results allow us to hypothesize that one aspect of the binding of α-factor to Ste2p involves interactions of the carboxyl terminus of the pheromone (residues 10-13) with residues near the interface between extracellular N-terminus and the first transmembrane helix of Ste2p. If this hypothesis is correct, then the side chain of F55 might directly interact with Tyr^{13} of α-factor via aromatic stacking or might be a part of a binding pocket.

The S219P and S259P mutations in the TM 5 and 6, respectively, were interesting because of the nature of the mutation (a serine to a proline residue) and the locations in the protein (TM domains contiguous with the 3rd cytoplasmic loop). *In vitro* mutagenesis studies with several GPCRs provided compelling evidence for the existence of intramolecular constraining determinants between TM3, TM5, and TM6 which stabilize an inactive receptor conformation (Figure 6) (49). It is widely believed that agonist binding (Figure 6A) and activating point mutations (Figure 6B) may lead to a relative movement of TM6 versus TM5, thus enabling critical transmembrane sequences to interact with the G protein (50-53).

Ste2p with mutations in TM5 have been identified previously (16). One such receptor had the mutation of A229V and another contained the two mutations S145L (TM3) and S219L. These mutant receptors responded to both α-factor and an antagonist $desTrp^1[Ala^3]$-α-factor. In our studies, cells expressing the S219P receptor responded to $desTrp^1[Ala^3]$-α-factor and a synergist in the growth arrest and *FUS1-LacZ* assays. In the *lacZ* assay, the EC_{50} values of α-factor and $D\text{-}A^{10}$ were shifted leftward compared to wild type

Figure 6: Proposed activation mechanism of GPCRs. The inactive state of the receptor is stabilized by interhelical hydrogen bond networks, by electrostatic and by hydrophobic interactions. Agonist-induced receptor activation (A) destabilizes these interactions resulting in a relative movement of TMs (for instance TM5 and TM6 to render the N-terminal portion of TM6 accessible for the G protein. Naturally occurring activating mutations or those introduced by *in vitro* mutagenesis may also entail the disruption of stabilizing structures (B) thus mimicing active receptor states (54).

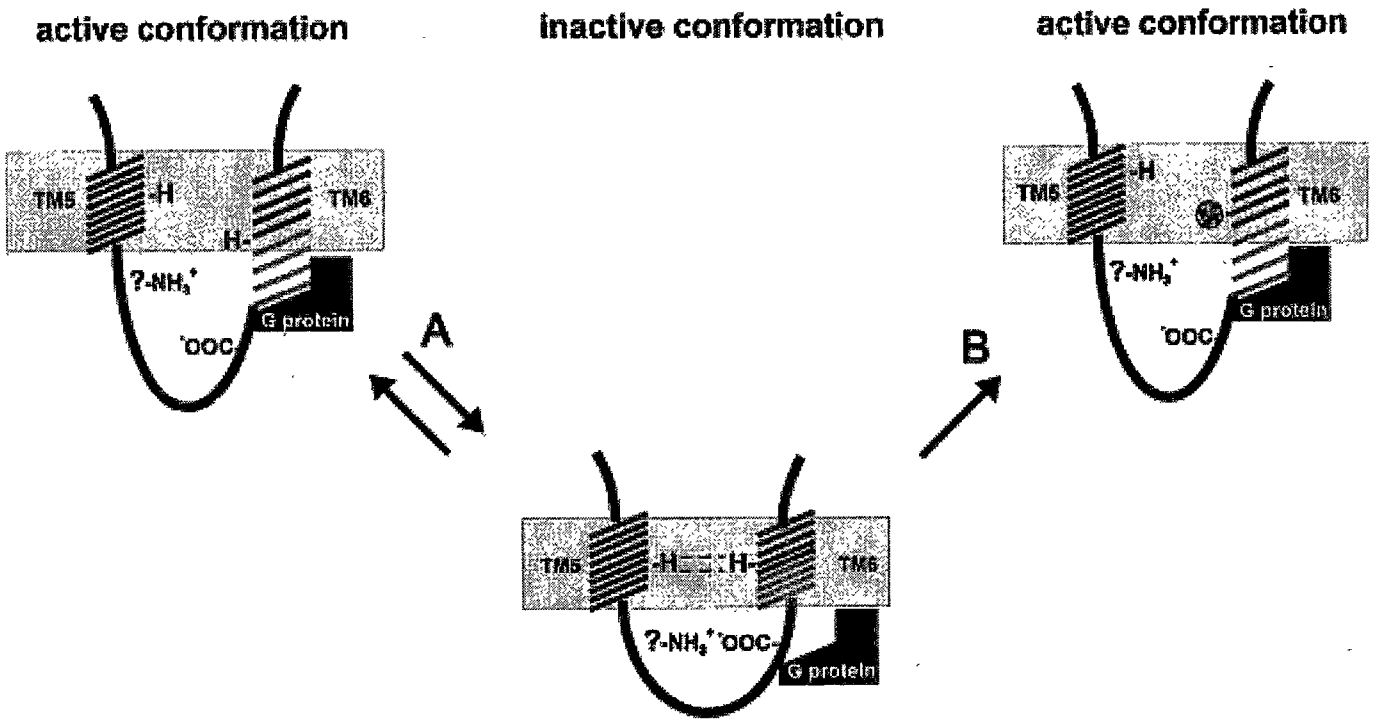
active conformation
inactive conformation
active conformation
TM5
TM6
G protein
A
B

or F55V receptors while maximum responses were just 50-60% of the α-factor response to wild type receptor (Figure3). S219 residue is predicted face TM 6 (55). S219P mutation may induce altered helix packing of TM5 and interactions with TM6 in a way that increases the potency of agonists but the interaction of this mutant receptor and G protein is not stable enough for full activation of G proteins. Of the antagonistic analogs tested, S219P receptor responded only to desTrp^{1}[Ala^{3}]-α-factor implying the conformation of this mutant receptor still discriminate structural differences in N-terminal region of α-factor.

The S259P mutation produces a receptor that responds to all antagonists and the synergist peptide tested as if they were agonists. Residue 259 is adjacent to another proline at 258 and the introduction of two prolines in the TM6 domain may confer a drastic conformational change allowing normally weakly binding ligands to occupy the binding site of the receptor and trigger a response. A constitutively active receptor mutant was reported that contains a mutation changing P258 to leucine (15). The introduction of the leucine residue may have locked the receptor in the "on" conformation and thus cause the constitutive phenotype observed. Although the S259P mutant is not a constitutively active receptor in our strain background, in other strain backgrounds, it does appear to be constitutive (M. Dumont. personal communications). The introduction of a proline at residue 258 might remove some stabilizing conformational restraints allowing receptors to be sensitized by antagonists and a synergist without strict structural requirement of ligand.

The changes of specificity in activity of antagonists to agonist shown in the present study are a rare phenomenon in GPCR family. Partial agonist activity for certain antagonists has been described in mutated GPCR which do not display constitutive activity. The inverse agonist 11-cis-retinal behaves as a partial agonist at the G121L mutation in TM3 of rhodopsin (56). Claude *et.al.*(57) hypothesized that antagonists with high structural homology to agonists are capable of agonist activity if the receptor is permissive. This was based on the observation that the mutation of conserved serine residues (S177L or S196L) in transmembrane 4 of μ-opioid receptors confers full agonistic properties to peptide and alkaloid antagonists. A similar explanation may also account for antagonists and a synergist in our study since their structures resemble cognate agonist α-factor.

The inability to determine a measurable binding of α-factor to the S259P receptor may be attributable to the instability of this receptor. Although the receptor is stable enough to be responsive to peptides in various biological assays, when cells or membranes are subjected to the treatment used for binding studies or for gel electrophoresis, the protein is apparently not stable enough to be detected. Recently structural instability of a constitutively active G protein-coupled receptor was reported (52). In this study, the β_2 adrenergic receptor showed a 4-fold increase in the rate of denaturation at 37°C as compared to the wild-type receptor. In contrast to the above explanation, it is possible that the Western blot and binding analyses provide a semi-quantitative assessment of the number of S259P receptor molecules in these cells. If this is

correct, it appears that only a very small number of S259P receptor molecules are required for induction of the mating pathway. Furthermore, this may indicate that triggering of only a small fraction of the wild type receptors is necessary for signal transduction.

Ligand specific conformational changes of the α-factor receptor have been recently investigated using limited trypsin digestion of the receptor in the presence of agonist and antagonist peptides (25). In the native receptor, the α-factor peptide seems to promote a distinct conformational state that favors interaction of the third cytoplasmic loop with the G-protein while an antagonist peptide promotes a different conformation than the signal inducing isomerization state. This and results of our present study with S219P and S259P receptors can not be easily explained by the simple two-step model of receptor activation (24). Indeed, emerging evidence indicate there are multiple activation steps in GPCRs (58,59). Antagonists used in this study may form intermediate receptor-ligand complexes which could not overcome energy barrier between the unativated and activated receptor-agonist complex due to the lack of correct interactions with TM5 and TM6 and probably TM3 regions. The S219P and S259P mutations in the receptor may lower energy barrier and increase the rate of receptor transition to the active state.

Clearly, we are still far from mapping the binding domain of Ste2p and understanding how the pheromone-receptor interaction leads to initiation of signal transduction. Biochemical and biophysical characterization of mutant

receptors described here may lead to a better understanding of activation of the α-factor receptor and other GPCRs.

List of References for Part 3

1) **Dohlman, H.G., Thorner, J. Caron, M.G., and Lefkowitz, R.J.** (1991) Model systems for the study of seven-transmembrane-segment receptors. *Annu. Rev. Biochem.* 60:653

2) **Neer, E.J.** (1995) Heterotrimeric G proteins: organizers of transmembrane signals. *Cell* 80:249

3) **Sprague, G.G., and Thorner, J.W.** (1992) *In* the molecular biology of the Yeast *Saccharomyces*: Gene expression (Vol. 2) (Pringle, J.R., Jones, E.W. and Broach, J.R., eds), pp. 675-674, Cold Spring Harbor Laboratory Press. Cold Spring Harbor, NY.

4) **Baldwin, J.M.** (1993) The probable arrangement of the helices in G protein-coupled receptors. *EMBO J.* 12:1693

5) **Unger, V.M., Hargrave, P.A., Baldwin, J.M., and Schertler, G.F.X.** (1997) Arrangement of rhodopsin transmembrane alpha-helices. *Nature* 389:203

6) **Palczewski, K., Kumasaka, T. Hori, T. et. al.,** 2000 Crystal structure of rhodopsin: a G protein-coupled receptor. *Science* 289:739

7) **Kobilika, B.** (1992) Adrenergic receptors as models for G protein-coupled receptors. *Annu. Rev. Neurosci.* 15:87

8) **Savarese, T.M., and Fraser, C.M.** (1992) In vitro mutagenesis and the search for structure-function relationships among G protein-coupled receptors. *Biochem. J.* 283:1

9) **Strader, C.D., Fong, T.M., Graziano, M.P., and Tota, M.R.** (1995) The family of G protein-coupled receptors. *FASEB J.* 9:745

10) **Ji, T.H., Grossmann, M., and Ji, I.** (1998) G protein-coupled receptors. I. Diversity of receptor-ligand interactions. *J. Biol. Chem.* 273:17979

11) **Jarnagin, K., Bhakta, S., Zuppan, P., Yee, C., Ho, T., Phan, T., Tahilramani, R., Pease, H.B., Miller, A., and Freedman, R.** (1996) Mutation in the B2 bradykinin receptor reveal a different pattern of contacts for the peptidic agonists and peptidic antagonists. *J. Biol. Chem.* 271:28227

12) **Xue, J.C., Chen, C., Zhu, J., Kunapuli, S., DeReil, J.K., Yu, L., and L.-Chen, L.Y.** (1994) Differential binding domains of peptide and non-peptide ligands in the cloned rat κ opioid receptor. *J. Biol. Chem.* 269:30195

13) **Marie, J., Maigret, B., Joseph, M.P., Larguier, R., Nouet, S., Lombard, C., and Bonnafous, J.C.** (1994) Tyr^{292} in the seventh transmembrane domain of the AT_{1A} angiotensin II receptor is essential for its coupling to phospholipase C. *J. Biol. Chem.* 269:20815

14) **Konopka, J.B. and Jenness, D.D.** (1991) Genetic fine-structural analysis of the *Saccharomyces cerevisiae* alpha-pheromone receptor. *Cell Regul.* 2:439

15) **Konopka, J.B., Margarit, S.M., and Dube, P.** (1996) Mutation of Pro-258 in transmembrane domain 6 constitutively activates the G protein-coupled alpha-factor receptor. *Proc. Natl. Acad. Sci. USA* 93:6764

16) **Marsh, L.** (1992) Substitutions in the hydrophobic core of the α-factor receptor of *Saccharomyces cerevisiae* permit response to *Saccharomyces kluyveri* α-factor and to antagonist. *Mol. Cell. Biol.* 12:3959

17)**Clark, C.D., Palzkill, T., and Boststein, J.** (1994) Systematic mutagenesis of the yeast mating pheromone receptor third intracellular loop. *J. Biol. Chem.* 269:1

18)**Weiner, J.L., Guttierez-Steil, G., and Blumer, K.J.** (1993) Disruption of receptor-G protein coupling in yeast promotes the function of an *SST2*-dependent adaptation pathway. *J. Biol. Chem.* 268:8070

19)**Stefan, C.J., and Blumer, K.J.** (1994) The third cytoplasmic loop of a yeast G-protein-coupled receptor controls pathway activation, ligand discrimination, and receptor internalization. *Mol. Cell. Biol.* 14:3339

20)**Sen, M., and Marsh, L.** (1994) Noncontiguous domains of the alpha-factor receptor of yeasts confer ligand specificity. *J. Biol. Chem.* 269:968

21)**Sen, M., Shah, A., and Marsh, L.** (1997) Two types of alpha-factor receptor determinants for pheromone specificity in the mating-incompatible *yeasts S. cerevisiae* and *S. kluyveri. Curr. Genet.* 31:235

22)**Lefkowitz, R.J., Cotecchia, S., Samama, P., and Costa, T.** (1993) Constitutive activity of receptors coupled to guanine nucleotide regulatory proteins. *Trends Pharmacol. Sci.* 14:303

23)**Hwa, J., Graham, R.M., and Perez, D.M.** (1996) Chimeras of α1-adrenergic receptor subtype identify critical residues that modulate activate state isomerization. *J. Biol. Chem.* 271:7956

24)**Leff, P.** (1995) The two-state model of receptor activation. *Trends Pharmacol. Sci.* 16:89

25)**Bukusoglu, G., and Jenness, D.D.** (1996) Agonist-specific conformation changes in the yeast α-factor pheromone receptor. *Mol. Cell. Biol.* 16:4818

26)**Kenakin, T., Morgan, P., and Lutz, M.** (1995) On the importance of the "antagonist assumption" to how receptors express themselves. *Biochem. Pharmacol.* 50:17

27)**Schoneberg, T., Schultz, G., and Gudermann, T.** (1999) Structural basis of G protein receptor function. *Mol. Cell. Endocrinol.* 151:181

28) **Muhlrad, D., Hunter, R., and Parker, R.** (1992) A rapid method for localized mutagenesis of yeast genes. *Yeast* 8:79

29)**Burkholder, A.C., and Hartwell, L.H.** (1985) The yeast alpha-factor receptor: structural properties deduced from the sequence of the STE2 gene. *Nucleic Acids Res.* 13:8463

30)**Colicelli, J., Birchmeier, C., Michaeli, T., O'Neil, K., Riggs, M., and Wigler, M.** (1989) Isolation and characterization of a mammalian gene encoding a high-affinity cAMP phosphodiesterase. *Proc. Natl. Acad. Sci. USA* 86:3599

31)**Gietz, D., St. Jean, A., Woods, and R.A., Schiestl, R.H.** (1992) Improved method for high efficiency transformation of intact yeast cells. *Nucleic Acids Res.* 20:1425

32)**Ward, A.C.** (1990) Single-step purification of shuttle vectors from yeast for high frequency back-transformation into E. *coli. Nucleic Acids Res.* 18:5319

33)**Sikorski, R.S., and Hieter, P.** (1989) A system of shuttle vectors and yeast host strains designed for efficient manipulation of DNA *in Saccharomyces cerevisiae. Genetics* 122:19

34)**Ho, S.N., Hunt, H.D., Horton, R.M., Pullen, J.K. and Pease, L.R.** (1989) Site-directed mutagenesis by overlap extension using the polymerase chain reaction. *Gene* 77:51

35)**Sambrook, J., Fritsch, E.F., and Maniatis, T.** (1989) Molecular Cloning: A Laboratory Manual, 2nd ed., Cold Spring Horbor Laboratory Press, Cold Spring Harbor, NY.

36)**Rose, M.D., Winston, R., and Hieter, P. (**1990) Methods in yeast genetics, a laboratory course manual. Cold Spring Harbor Laboratory Press, Cold Spring Harbor, NY.

37)**Raths, S.K., Naider, F., and Becker, J.M.** (1988) Peptide analogues compete with the binding of alpha-factor to its receptor *in Saccharomyces cerevisiae. J. Biol. Chem.* 263:17333

38)**Abel, M.G., Zhang, Y.L., Lu, H.-F., Naider, F., and Becker, J.M.** (1998) Structure-function analysis of the *Saccharomyces cerevisiae* tridecapeptide pheromone using alanine-scanned analogs. *J. Peptide Res.* 52:95

39)**Kippert, F.** (1995) A rapid permeabilization procedure for accurate quantitative determination of beta-galactosidase activity in yeast cells. *FEMS Microbiol. Lett.* 128:201

40)**Guarente, L.** (1983) Yeast promoters and *lacZ* fusions designed to study expression of cloned genes in yeast. *Methods Enzymol.* 101:181

41)**Miller, J.H.** (1975) Experiments in Molecular Genetics, Cold spring Harbor Laboratory, Cold Spring Harbor, NY.

42)**Eriotou-Bargiota, E., Xue, C.-B., Naider, F., and Becker, J.M.** (1992) Antagonistic and synergistic peptide analogues of the tridecapeptide mating pheromone of *Saccharomyces cerevisiae. Biochemistry* 31:551

43)**Xue, C.-B., Eriotou-Bargiotta, E., Miller, D., Becker, J.M., and Naider, F.** (1989) A covalently constrained congener of the *Saccharomyces cerevisiae* tridecapeptide mating pheromone is an agonist. *J. Biol. Chem.* 264:19161

44)**Davie, N.E., Gee, M., Anderson, B., Naider, F., Thorner, J., and Stevens, R.C.** (1997) Expression and purification of the *Saccharomyces cerevisiae* alpha-factor receptor (Ste2p), a 7-transmembrane-segment G protein-coupled receptor. *J. Biol. Chem.* 272:15553

45)**Linden, J.** (1982) Calculating the dissociation constant of an unlabeled compound from the concentration required to displace radiolabel binding by 50%. *J. Cyclic Nuleot. Res.* 8:163

46)**Konopka, J.B., Jenness, D.D., and Hartwell, L.H.** (1988) The C-terminus of the *S. cerevisiae* alpha-pheromone receptor mediates an adaptive response to pheromone. *Cell* 54:609

47) **Shenbagamurthi, P., Baffi, R., Khan, S.A., Becker, J.M., and Naider, F.** (1983) Structure-activity relationships in the dodecapeptide alpha factor of *Saccharomyces cerevisiae. Biochemistry* 22:1298

48)**Blumer, K.J., Reneke, J.E., and Thorner, J.** (1988) The *STE2* gene product is the ligand-binding component of the alpha-factor receptor of *Saccharomyces cerevisiae. J. Biol. Chem.* 263:10836

49)**Gether, U.** (2000) Uncovering molecular mechanisms involved in activation of G protein-coupled receptors. *Endocrine Review* 21:90-118

50)**Kosugi, S., Mori, T., and Shenker, A.** (1998) An anionic residue at position 546 is important for maintaining the inactive conformation of the human lutropin/choriogonadotropin receptor. *Mol. Pharmacol.* 53:894.

51)**Javitch, J.A., Fu, D., Liapakis, G., and Chen, J**. (1997) Constitutive activation of β-adrenergic receptor alters the orientation of its sixth membrane-spanning segment. J. Biol. Chem. 272:18546

52)**Gether, U., Lin, S., Ghanouni, P., Ballesteros, J., Weinstein, H., and Koblika, B.** (1997) Agonists induce conformational changes in transmembrane domins III and VI of the β_2 adrenoceptor. *EMBO J.* 16:6737

53)**Spalding, T., Burstein, E.S., Henderson, S.C., Ducotes, K.R., and Brann, M.** (1998) Identification of a ligand-dependent switch within a muscarinic receptor. J. Biol. Chem. 273:21563

54)**Schoneberg, T., Schultz, G., and Gudermann, T.** (1999) Structural basis of G protein-coupled receptor function. *Mol. Cell. Endocrinol.* 151:181

55)**Dube, P., DeCostanzo, A., and Konopka, J.B.** (2000) Interaction between transmembrane domains five and six of the α-factor receptor. *J. Biol. Chem.* 275:26492

56)**Han, M., Lou, J., Nakanishi, K., Sakamar, T.P., and Smith, S.O.** (1997) Partial agonist activity of 11-cis-retinal in rhodopsin mutants. *J. Biol. Chem.* 272:23085

57)**Claude, P.A., Wotta, D.R., Zhang, X.H., Prather, P.L., McGinn, T.M., Erickson, L.J., Loh, H.H., and Law, P.Y.** (1996) Mutation of a conserved serine in TM4 of opioid receptors confers full agonistic properties to classical antagonists. *Proc. Natl. Acad. Sci. USA* 93:5715-5719

58) **Surya A., Stadel, J., and Knox, B.E.** (1998) Evidence for multiple, biochemically distinguishable states in the G protein-coupled receptor, rhodopsin. *Trends Pharmacol. Sci.* 19:243

59)**Prossnitz, E.R., Gilbert, T.L., Chiang, S., Campbell, J.J., Qin, S., Newman, W., Sklar, L., and Ye, R.D.** (1999) Multiple activation steps of *N*-formyl peptide receptor. *Biochemistry* 38:2240

PART 4

Identification of ligand binding region in *Saccharomyces cerevisiae* α-factor receptor[§]

[§] Synthesis of α-factor analogs used in this study were carried out in the laboratory of Dr. Fred Naider, Department of Chemistry, C.U.N.Y., College of Staten Island, NY 10314

CHAPTER 1

Introduction

G protein-coupled receptors (GPCRs) comprise a broadly distributed class of transmembrane proteins that mediate cellular responses to extracellular signals such as physical stimuli, hormones, and neurotransmitters. Upon activation, each receptor in this class interacts with a cytoplasmic heterotrimeric G protein, leading to release of bound GDP, binding of GTP, and dissociation of the subunits, which in turn activate diverse pathways such as protein kinases, adenlyate cyclase, phospholipases, and ion channels (1,2).

GPCRs contain a common structural pattern consisting of seven hydrophobic segments that are predicted to form transmembrane helices. A detailed knowledge of the structure of GPCRs will be required to understand the determinants of ligand binding and the mechanism by which binding leads to activation of the cytoplasmic G protein. Except for a recent crystallographic structure of rhodopsin (3), the difficulty of obtaining, purifying, solubilizing, and crystallizing integral membrane proteins has hindered the application of X-ray crystallography and NMR to all other GPCRs. Therefore, the insights into the structural basis underlying the biological function of the GPCRs have come from the analysis of mutant receptors: either site-directed or chimeric, where large stretches of residues are swapped for those of a related receptor. Mutant receptors have been used to examine several aspects of receptor functions,

including post-translational modifications, G protein coupling, and, of most relevance to us, ligand binding.

GPCRs bind ligands of widely diverse origins, and are unsurpassed as therapeutic targets. Consequently, much effort has been devoted to mapping of the binding sites for agonist and antagonist ligands in these receptors (4). Even though peptides are the most common class of ligands for GPCRs, few peptide GPCRs have been investigated thus far, and in most of those cases the identity of the peptide-binding epitopes remains elusive.

The tridecapeptide α-factor pheromone (WHWLQLKPGQPMY) of *Saccharomyces cerevisiae* induces conjugation in yeast by binding to its cognate GPCR, Ste2p, that activates a G protein signal pathway that is highly conserved with mammalian signaling pathways (5). This peptide has been studied extensively as a model for understanding the biochemistry of mammalian peptide hormones. ^{1}H NMR studies on this peptide indicate that the Lys7-Gln10 residues assume a β-turn structure and that this conformational feature is an important factor in the bioactive state of the molecule (6,7). This structural feature has been supported by further studies of covalently constrained (8) and peptidomimetic analogs (9). In addition, a recent systematic investigation of the importance of the side-chain functionality of α-factor using L-Ala and D-Ala scanning analogs pinpoints residues or segments with dominant roles in forming biologically active pheromone conformation (residue 7-10), in receptor binding (residue 10-13), and in receptor activation and signal transduction (residue 1-4) (10).

The function and structure of the α-factor receptor (Ste2p) have been extensively studied as well. The analysis of constitutively active mutants indicates that movement in the sixth transmembrane domain (TM 6) plays a key role in receptor activation (11,12) (See Figure 6 in Part 1). Analysis of the intracellular domains of the receptor has demonstrated that the third intracellular loop is important for G protein activation (13). Mutagenesis studies also indicate that the cytoplasmic C terminus is involved in down-regulation of receptors by endocytosis (14) and desensitization of receptors by phosphorylation (15). Importantly, results from cysteine cross-linking experiment between TM5 and TM6 (16) and from a biophysical study of synthetic peptides of each TM (17) indicate that, despite a lack of sequence similarity among the GPCR family, there is a remarkable similarity in the structure and function of these receptors.

Despite numerous studies concerning the structure and function of α-factor pheromone or of its receptor, very few studies have focused on the identification of the ligand binding sites. Although no information has yet been published on determinants involved in ligand binding to the α-factor receptor, few recent studies provided valuable information for searching the α-factor binding sites. In a mutation in TM 1 (F55V) of α-factor receptor, D-Ala10-α-factor analog showed an agonist activity with a good binding affinity while the affinities of α-factor and antagonists were decreased by 10 to 100 fold (PART 3). Since D-Ala^{10}-α-factor does not bind to wild type receptor, we hypothesized that that one aspect of the binding of α-factor to the receptor involves interactions of the

carboxyl terminus of the pheromone (residues 10-13) with TM1 of the receptor. Other important information for identifying α-factor binding sites has come from the study of chimeric receptors between *S. cerevisiae* and *S. kluyveri* α-factor receptors. The α-factor receptors from these two related species exhibit 50% overall identity each other (18). The *S. kluyveri* α-factor pheromone (WHWLSFSKGEPMY) shows identity to the *S. cerevisiae* α-factor at 8 of 13 residues (19). Using chimeric receptors of the two α-factor receptors, Sen *et al.* (20,21) Identified limited regions in α-factor receptor determining ligand specificity. Especially, residues 47-49 (STV in *S. cerevisiae* and KKI in *S. kluyveri* α-factor receptor) at the junction between the N-terminal domain and TM1 were proposed to be a potential contact region with the five variant residues of the two α-factors (residues 5-8 and residue 10).

In light of a turn structure in residues 7-10 of α-factor and potential interactions between the C-terminus of α-factor and TM1 as proposed in PART3, we hypothesized that 10^{th} residue of α-factor interacts with residues 47-48 of the receptor. To test this hypothesis, we constructed mutant receptors at this region. The binding affinities of these constructs and their biological activities were then determined by α-factor and its analogs in which the 10^{th} residue was substituted by various functional groups.

CHAPTER 2

Materials and Methods

Strain and plasmid – The yeast strain used in the study, LM102, has been described by Sen and Marsh (20). The relevant genotype is: *MAT**a**, bar1, leu2, ura3, FUS1-lacZ::URA3, ste2-dl* (the α-factor receptor coding region deletion). LM102 strain was used as the recipient of the *STE2* site-directed mutants and to measure pheromone-induced growth arrest (halo assay), pheromone-induced gene expression (*lacZ* assay) and to determine pheromone binding. The strain carried the *bar1* mutant allele, that inactivating BAR1 protease responsible for degradation of α-factor. A yeast/bacterial shuttle vector (pGA314.WT) described in Part 3 was used as a template for the site-directed mutagenesis of α-factor receptor gene.

Primers and sequencing – All primers were purchased from Sigma/Genosys (The Woodlands, Texas) as a phosphorylated form at the 5' end to facilitate ligation reaction during mutagenesis. Sequences of primers are; 5'-GCAAGGTTTAGTTAACAAGACTGTTACTCAGGCC for S47K mutation, 5'-GCAAGGTTTAGTTAACAGTAAGGTTACTCAGGCC for T48K mutation, 5'-GCAAGGTTTAGTTAACAAGAAGGTTACTCAGGCC for S47K, T48K double mutation, and 5'-GCAACCTTTAGTTAACGAGGAGGTTACTCAGGCC for S47E, T48E double mutation. DNA sequencing was carried out in the DNA sequencing facility located on the campus of the University of Tennessee.

Site-directed mutagenesis – Single-stranded phagemid DNA of pGA314.WT was prepared by infecting *E.coli* strain CJ236 (*ung*$^-$,*dut*$^-$) carrying the pGA314.WT with the helper phage M13KO7 (22). Oligonucleotide-directed mutagenesis of single-stranded phagemid DNA was constructed as described by Kunkel *et al.* (23). After annealing mutagenic primer with the isolated single-stranded pGA314.WT, second-strand synthesis was performed in the presence of T4 DNA polymerase and T4 DNA ligase with synthesis buffer (0.4mM each dNTP, 0.75mM ATP, 17.5mM Tris, 3.75mM $MgCl_2$, 0.5mM DTT). The product of mutagenesis reaction mixture was transformed into *E. coli* strain DH5α and transformants were selected in ampicillin-containing plates. Plamids were then isolated from transformants using the Wizard protocol from Promega Corp. After sequence confirmation, constructs were transformed into yeast strain LM 102 (*ste2*-deletion strain) (24) and transformants were selected by their growth in media lacking tryptophane.

Synthesis and purification of peptides – L-Norleucine, which is isosteric with L-methionine, was incorporated at position 12 to replace L-methionine in all of the analogs. This replacement was previously shown to result in an analog with activity and binding affinity equal to that of native pheromone (25). The solid-phase synthesis of all the analogs were carried out in the laboratory of Dr. F. Naideron, CUNY, NY on an Applied Biosystems 433 peptide synthesizer (Applied Biosystems, Foster City, CA) starting with *N*-α-Fmoc-Tyr(OtBu)-Wang resin (0.65 mmol/g resin, Advanced ChemTech, Louisville, KY). The "0.1-mmol FastMoc" chemistry of Applied Biosystems was used for the peptide chain elongation with

an HBTU/HBOt/DIEA-catalyzed single-coupling using 4 equiv of protected amino acid and a 30-min coupling time followed by an Ac_2O/HOBt/DIEA capping (10 min). The *N*-α-protected peptide resin was washed thoroughly with 1-methyl-2-pyrrolidinone and dichloromethane and dried *in vacuo* for 2h. The cleavage was carried out in a mixture of trifluoroacetic acid, crytalline phenol, ethane-1,2-dithiol, thioanisole and water at room temperature for 1.5 h. After evaporation of trifluoroacetic acid under reduced pressure, the residue was precipitated and thoroughly washed with ethyl ether and extracted into 20% aqueous acetonitrile. The crude peptide was purified by reversed phase HPLC (Hewlett-Packard Series 1050) on a semipreparative Waters Bondapak C_{18} (19 x 300mm) column. The cleavage product was applied to the column and eluted with a linear gradient of water and acetonitrile both containing 0.025% TFA from 0 to 55% acetoitrile. The fractions were collected and analyzed on an analytical Waters μBondapak C_{18} column (3.9 x 300mm). The fraction of more than 99% homogeneity were combined and lyophilized and purity was judged with analytical HPLC using two different solvent systems and with high performance capillary electrophoresis (Hewlett-Packard 3D-CE model G1600A). Molar extinction coefficient of 13,500 at 280 nm was used for measuring peptide concentration throughout the study.

HPLC purification of [^{3}H]α-factor – Synthetic [Nle^{12}]α-factor was labeled by reduction of dehydroproline containing α-factor by the TR3 hydrogenation procedure of Amersham International as described previously (25). Unpurified, labeled peptide (dissolved in ethanol/water 1:1) was dried *in vacuo,* redissolved in sterile water and purified by HPLC using a Waters μBondapak C_{18} column (3.9

mm×300 mm) on a Beckman System Gold HPLC. The peptide solution was injected into the HPLC and eluted with a water/acetonitrile gradient from 0-40% acetonitrile. Fractions containing peptide eluting from the column similarly to unlabeled α-factor (elution at 32.3% CH_3CN) were collected and counted for radioactivity in a scintillation counter. All collected fractions were dried, resuspended in storage buffer (1mM methionine, 0.03% trifluoroacetic acid, 20% ethanol), combined, and the concentration and specific activity of the purified labeled peptide was determined.

Membrane preparation and Western blot – All steps for membrane preparation were performed at 4 °C, and all buffers were supplemented with protease inhibitor cocktail (AEBSF, pepstatin A, trans-epoxysuccinyl-L-leucylamido(4-guanidino)butane (E-64), and 1,10-phenanthroline, Sigma). Approximately 10g of yeast cell paste were suspended in 15 ml of 10% (w/v) sucrose in buffer (50mM HEPES (pH 7.5), 5 mM EDTA, protease inhibitors). The cells were lysed by vigorous shaking with glass beads for three 2-min pulses in a Braun Scientific (Allentown, PA) cell homogenizer. Unlysed cells were removed by centrifugation at 700 x g, and the membrane fraction was collected by centrifugation at 186,000 x g for at least 1 h. Equal amounts of solubilized membrane proteins were resolved by SDS-PAGE (10%), electrophoertically transferred to immobion P membrane (Millopore) and probed with anti-N-terminal-Ste2p antibodies provided by James Konopka, SUNY, Stony Brook. The resulting immune complexes were detected by incubation with 1:3,000 dilution of

horseradish peroxidase-conjugated goat anti-rabbit antibodies, and visualized by chemiluminescence (ECL kit, Amersham).

Growth arrest (halo) assay – Yeast nitrogen base medium (Difco) without amino acids (SD medium) supplemented with histidine (20 μg/ml), leucine (30 μg/ml) and methionine (20 μg/ml) was overlaid with 4 ml of cell suspension (2.5 x 10^5 cells/ml of Nobel agar). Filter disks (sterile blanks from Difco), 8 mm in diameter, were impregnated with 10 μl portions of peptide solutions at various concentrations and placed onto the overlay. The plates were incubated at 30^0C for 24 -36 h and then observed for clear zones (halos) around the disks. The data were expressed as the diameter of the halo including the diameter of the disk. Therefore, a minimum value for growth arrest is 9 mm, which represents the disk diameter (8 mm) and a small zone of inhibition. All assays were carried out at least three times with no more than a 2 mm variation in halo size at a particular amount applied for each peptide. The values reported represent the mean of these tests. Similar ranks of biological activities were obtained for these analogs within an assay as measured by growth arrest (halo) or gene induction (see below). In the latter assay cells were suspended in liquid medium thereby eliminating any contribution of diffusion through agar potentially present in the halo assay. NaCl (1M) was added to the media and peptide solution to test the effect of high salt on growth arrest assay.

Effect of α-Factor Analogs on Gene Induction – S. cerevisiae LM102 carries a *FUS1* gene that is inducible by mating pheromone and which is fused to the reporter gene β-galactosidase. Cells were grown overnight in SD medium at

30°C to 5 x 10^6 cells/ml, washed by centrifugation, and grown for one doubling (hemocytometer count) at 30°C. Induction was performed by adding 0.5 ml of peptide at various concentrations to 4.5 ml of concentrated cells (1 x 10^8 cells/ml). The mixtures were vortexed and placed at 30°C with shaking for 2 h. After this time, cells were harvested by centrifugation, and each pellet was resuspended and assayed for β-galactosidase production (expressed as Miller units) in triplicate by a modified (26) standard protocol (27, 28). EC_{50} and E_{max} values were calculated with a 95% confidence interval using GraphPad Prism software (sigmoidal dose-response curve fitting, variable slope). Each experiment was carried out at least three times with the results similar in each assay.

Binding assays – Saturation and competition binding assays were performed using tritiated α-factor prepared by reduction of [dehydroproline^8, Nle^{12}]α-factor as described previously (25). In general, cells were grown at 30^{0}C overnight and harvested at 1 x 10^7 cells/ml by centrifugation at 5,000 x g at 4^{0}C. The pelleted cells were washed two times in ice cold YM-1 medium (10) and resuspended to 4 x 10^7 cells/ml. The competition binding assay was started by addition of [H^3]α-factor and various concentration of nonlabeled α-factor analogs (140 μl) to a 560 μl cell suspension so that the final concentration of radioactive peptide was 6 x 10^{-9} M (20 Ci/mmole). Analog concentrations were adjusted using UV absorption at 280 nm and the corresponding extinction coefficients. After a 30 min incubation, triplicate samples of 200 μl were filtered and washed

over glass fiber filtermats using the Standard Cell Harvester (Skatron Instruments, Sterling, VA) and placed in scintillation vials for counting. NaCl (1M) was added all the solutions and media to test the effect of high salt on the binding affinity of α-factor analogs. In saturation binding assays, various concentrations of radioactive α-factor was added to cell suspension. Specific binding was determined by subtracting counts associated with the LM102 (*ste2* deletion) strain from counts bound to the strains harboring wild type or mutant receptors. Each experiment was carried out at least three times with the results similar in each assay. Binding of labeled α-factor to filters in the absence of cells was less than 20 cpm. Data curves were fitted from at least 8 triplicate data points with GraphPad Prism software (nonlinear regression, one site competition or saturation). The Ki values were calculated by using the equation of Cheng and Prusoff, where $Ki = EC_{50} / (1 + [ligand] / Kd)$ (29).

CHAPTER 3

Results

In order to determine if residues at 47 and 48 of the α-factor receptor interact with the 10th residue of α-factor and contribute to the ability to discriminate between the two closely related *S. cerevisiae* and *S. kluyveri* α-factors, we created mutant receptors in which Ser47 and Thr48 residues at the junction between the N-terminal extracellular domain and transmembrane domain 1 (TM1) of the α-factor receptor. The location of mutations in the receptor and the sequence comparison of two α-factor receptors are schematically represented in Figure1. The nomenclature used for these constructs was KK for S47K,T48K double mutant and EE for S47E, T48E double mutants. To directly address the possible interaction between this region in the receptor and 10th residue of α-factor, we synthesized a number of α-factor analogs which were specifically modified at 10th residue (Table 1) and tested their binding affinities and biological activities for wild type and mutant receptors.

Binding properties of mutant and wild type α-factor receptor – The [^{3}H]α-factor binding properties of wild type and mutant receptors were analyzed by saturation binding assay using whole cells. As shown in Table 2 and Figure 2, the *Kd* value for EE mutant receptor was equivalent to that of wild type receptor

Figure 1. Schematic representation of the receptor region targeted in this study. A) The location of the residues mutated in this study (region47-49) and two other regions (104-123, 267-269), which are reportedly involved in ligand specificity between *S. cerevisiae* and *S. kluveri* α-factors, were filled with black color. A black circle indicates F55. Valine substitution at this site confers increased binding affinity to D-A^{10}-α-factor. B) Primary sequence comparison at the junction between N-terminal extracellular domain and TM1 of *S. cerevisiae and S. kluyveri* α-factor receptors is shown. Boldface indicates residues mutated in this study.

A)

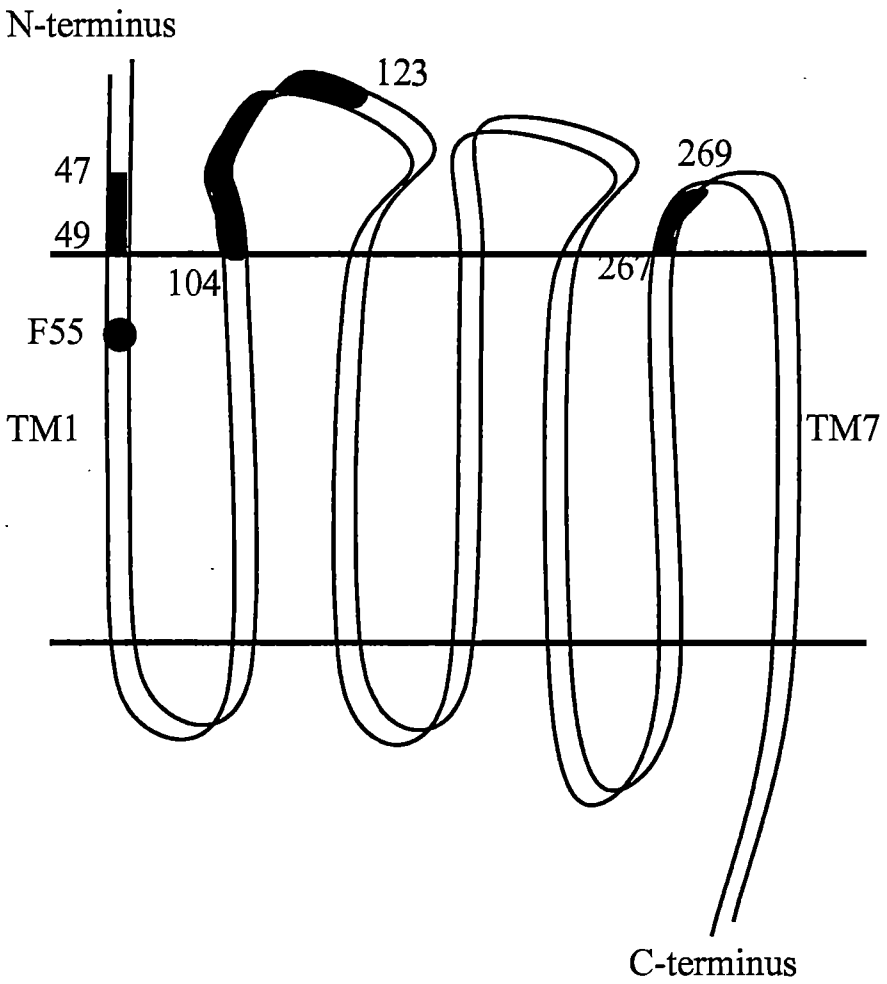

B) *S. cerevisiae* α-factor receptor

41 LQGLVN**ST**VT QAIMFGVRCG 60

S. kluyveri α-factor receptor

40 SQIFVN**KK**IT QGISFGTRIG 59

Table 1. List of α-factor analogs used in this study. The primary sequences are compared and the residues that are different from the wild type α-factor are marked as boldface.

Name	Structure	Amino acid at position 10
S. cerevisiae α-factor(α-factor)	WHWLQLKPGQPMY	Glutamine
S. kluyveri α-factor(k-α-factor)	WHWL**SFSK**G**E**PMY	Glutamic acid
K^{10}-α-factor	WHWLQLKPG**K**PMY	Lysine
Orn^{10}-α-factor	WHWLQLKPG**(Orn)**PMY	Ornithine
E^{10}-α-factor	WHWLQLKPG**E**PMY	Glutamic acid
D^{10}-α-factor	WHWLQLKPG**D**PMY	Aspartic acid
N^{10}-α-factor	WHWLQLKPG**N**PMY	Asparagine
S^{10}-α-factor	WHWLQLKPG**S**PMY	Serine

Table 2. Binding parameters for wild type and mutant α-factor receptors with [^{3}H]α-factor. Saturation binding curves were determined using whole cells carrying wild type or mutant receptors, as described in Materials and Methods. *Kd* and *Bmax* values, calculated using a one-site model, are shown as means ± standard errors of at least two experiments. Each determination was performed in triplicate.

Receptor	*Kd* (nM)	*Bmax* (Binding sites per cell)
WT	6.8±1.5	44408±3360
KK	37.0±4.2	37503±1464
EE	6.5±1.4	36404±2564
S47K	20.5±3.3	50825±2873
T48K	15.7±2.7	46384±2013

Figure 2. Saturation binding isotherms of [^{3}H]α-factor wild type and mutant α-factor receptors. Cells harboring wild type, KK, S47K, T48K, and EE receptors were incubated with increasing concentrations of [^{3}H]α-factor and assayed as described under Materials and Methods. The data shown are mean ± S.E. from three individual experiments, each of which was performed in triplicate. The calculated Kd and Bmax values are presented in Table 2.

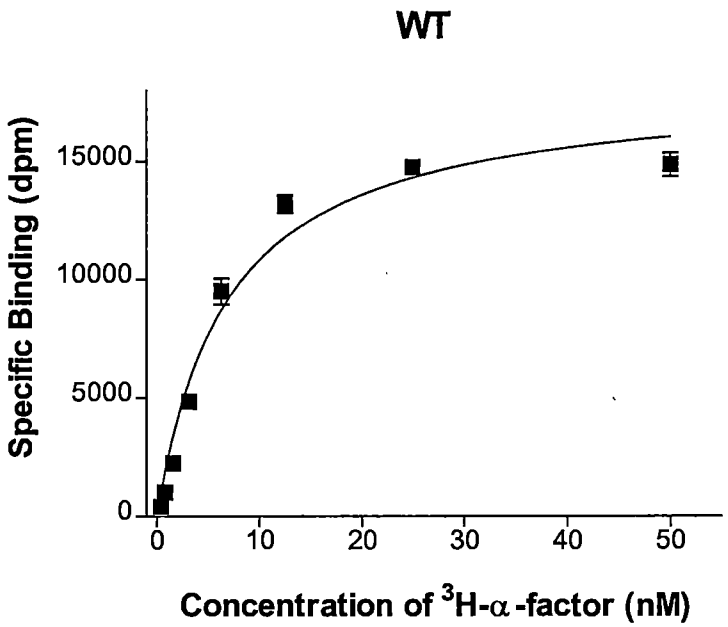
WT
Specific Binding (dpm)
15000
10000
5000
0
0
10
20
30
40
50
Concentration of ^{3}H-α-factor (nM)

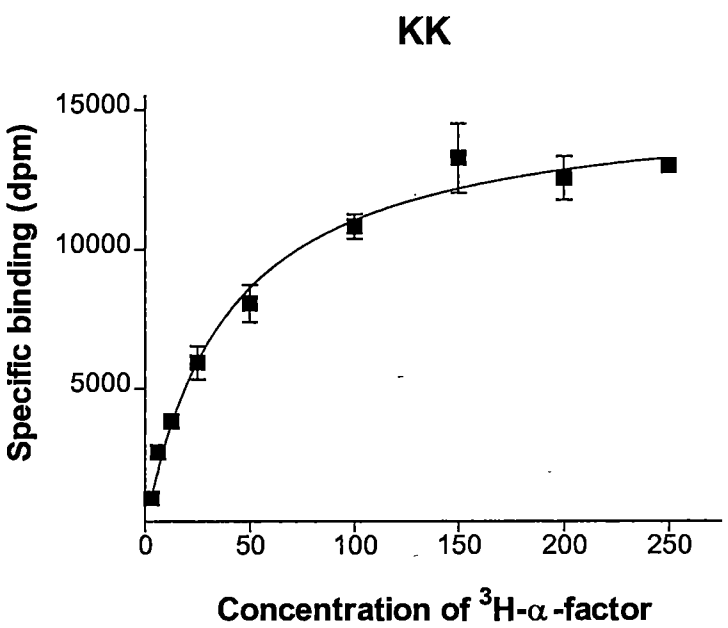
KK
Specific binding (dpm)
15000
10000
5000
0
50
100
150
200
250
Concentration of ^{3}H-α-factor

S47K

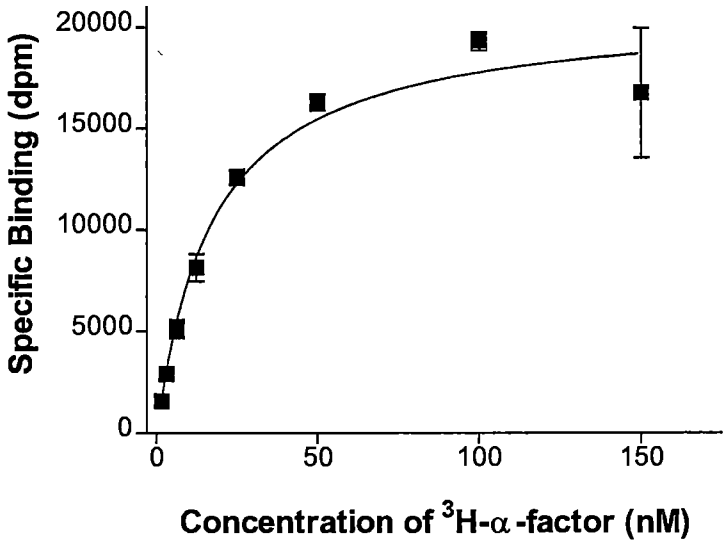
Specific Binding (dpm)
20000
15000
10000
5000
0
0
50
100
150
Concentration of ^{3}H-α-factor (nM)

T48K

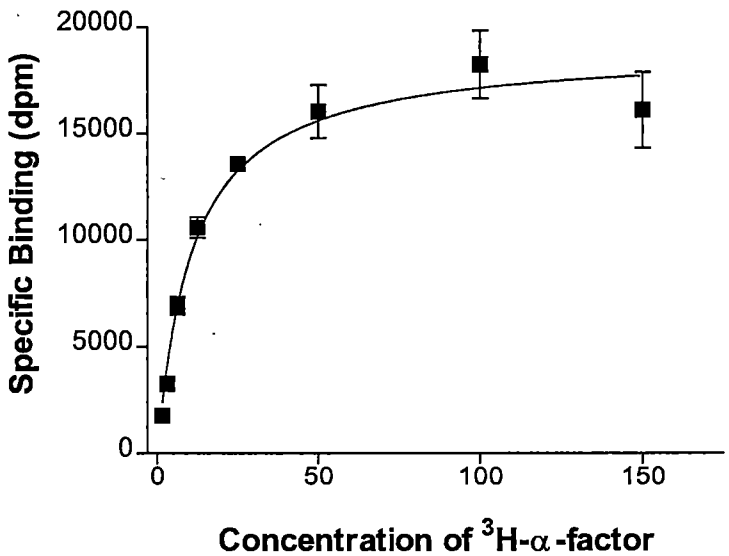
Specific Binding (dpm)
20000
15000
10000
5000
0
0
50
100
150
Concentration of ^{3}H-α-factor

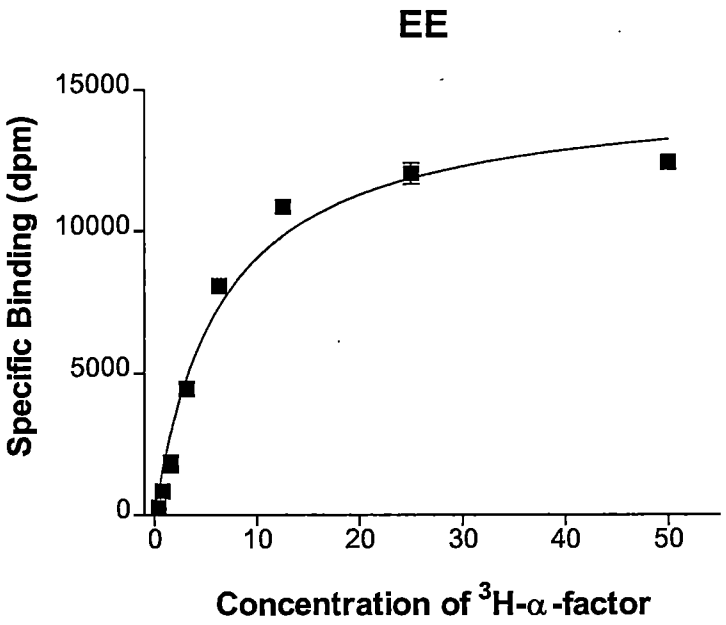
EE
15000
10000
5000
0
Specific Binding (dpm)
0
10
20
30
40
50
Concentration of ^{3}H-α-factor

(*Kd* = 6.8±1.5 nM) indicating EE substitution at 47 and 48 residues of the receptor does not alter α-factor binding. Affinity of [^{3}H]α-factor was decreased about 5-fold in KK mutant receptor and decreased about 3- and 2-fold in S47K and T48K mutants, respectively. While *Kd* values were changed up to 5-fold by mutations in this region of receptor, less change in the number of binding sites were observed (from 82% in EE mutant to 114 % in S47K mutant compared to wild type binding sites) indicating a comparable level of cell surface expression of the different mutant receptors. Ample amounts of receptor were detected in Western blots of the wild type and mutant receptors (Figure 3). The apparent doublet form of the receptor has been observed by others using various antibody preparations implying different levels of glycosylation (11). More variable expression levels among constructs compared to the results of binding studies were observed in the Western blots of membrane preparation. Part of the reason might be the change in epitope specificity of antibody by the mutations since the antibody used in the assay was generated against N-terminal 100 residues of the receptor (11).

The affinity of the *S. cerevisiae* α-factor analogs modified at the 10th residue and *S. kluyveri* α-factor (k-α-factor) was measured in competition binding assays by displacement of [^{3}H]α-factor (Table 3 and Figure 4). α-factor analogs showed variation from 28-fold (E^{10}-α-factor) to over 1700-fold (D^{10}-α-factor) decreased binding affinity for wild type receptor compared to that of α-factor implying the structural requirement at the 10th position of α-factor for high affinity

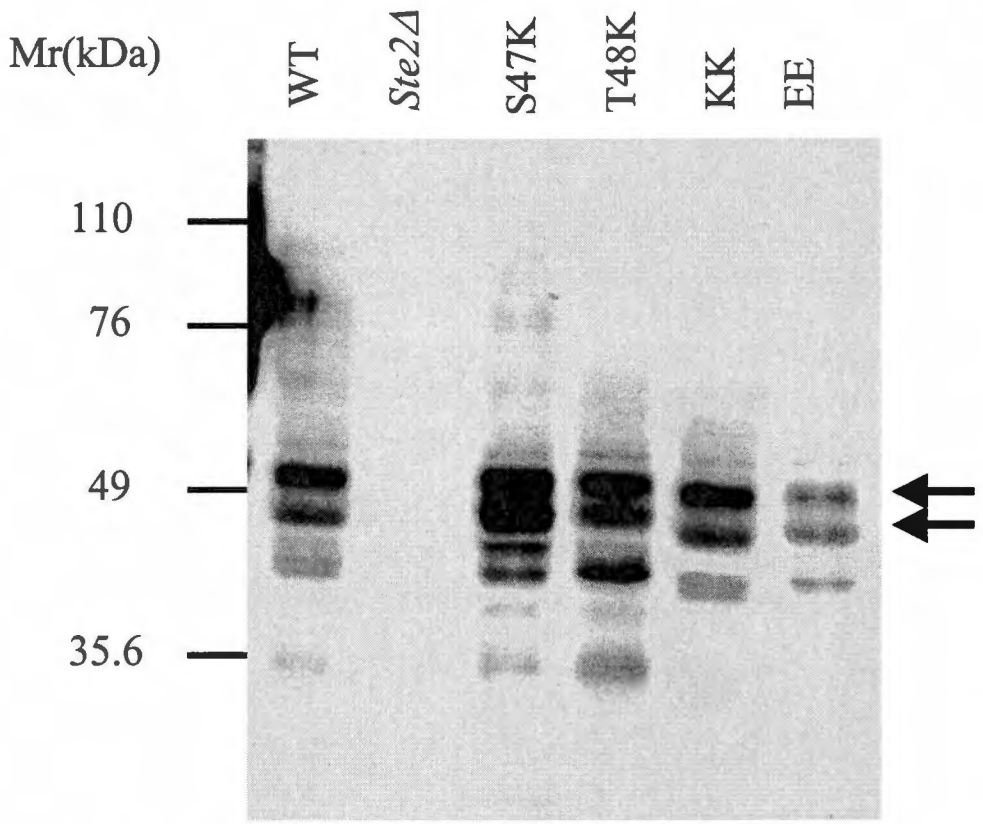

Figure 3. Western blots of cells expressing wild-type and mutant receptors. Mr., molecular weight marker; *Ste2Δ,* a strain that α-factor receptor coding gene was deleted. The positions, where α-factor receptor is predicted to migrate, are indicated by arrows.

Table 3. Binding parameters of wild type and mutant receptors for α-factor analogs. The *Ki* values (nM) of different analogs were determined in competition binding assays by displacement of [^{3}H]α-factor. All values are the means ± S.E. nd; not determined.

Analogs tested	WT	KK	S47K	T48K	EE
α-factor	5.6±0.8	90±17	41.7±5.7	26.9±3.2	7.4±1.1
N^{10}--α-factor	1610±135	1757±124	nd	nd	1204±99
S^{10}-α-factor	3769±365	6223±591	nd	nd	3183±254
K^{10}-α-factor	769±85	>10000	>10000	>10000	493±52
Orn^{10}-α-factor	232±27	3282±440	2824±233	1919±145	102±14
E^{10}-α-factor	160±21	273±35	673±56	583±43	476±36
D^{10}-α-factor	>10000	2083±261	nd	nd	>10000
k-α-factor	3464±350	162±19	1158±80	1225±78	>10000

Figure 4. Competition binding assays of α-factor and its analogs on wild type and mutant receptors. Yeast cells expressing wild type or each mutant construct were incubated 6 nM of [^{3}H]α-factor in the presence of increasing concentrations of α-factor or α-factor analogs. The results are average ± S.E. of three separate experiments with each point assayed in triplicate. Ki values are given in Table 3.

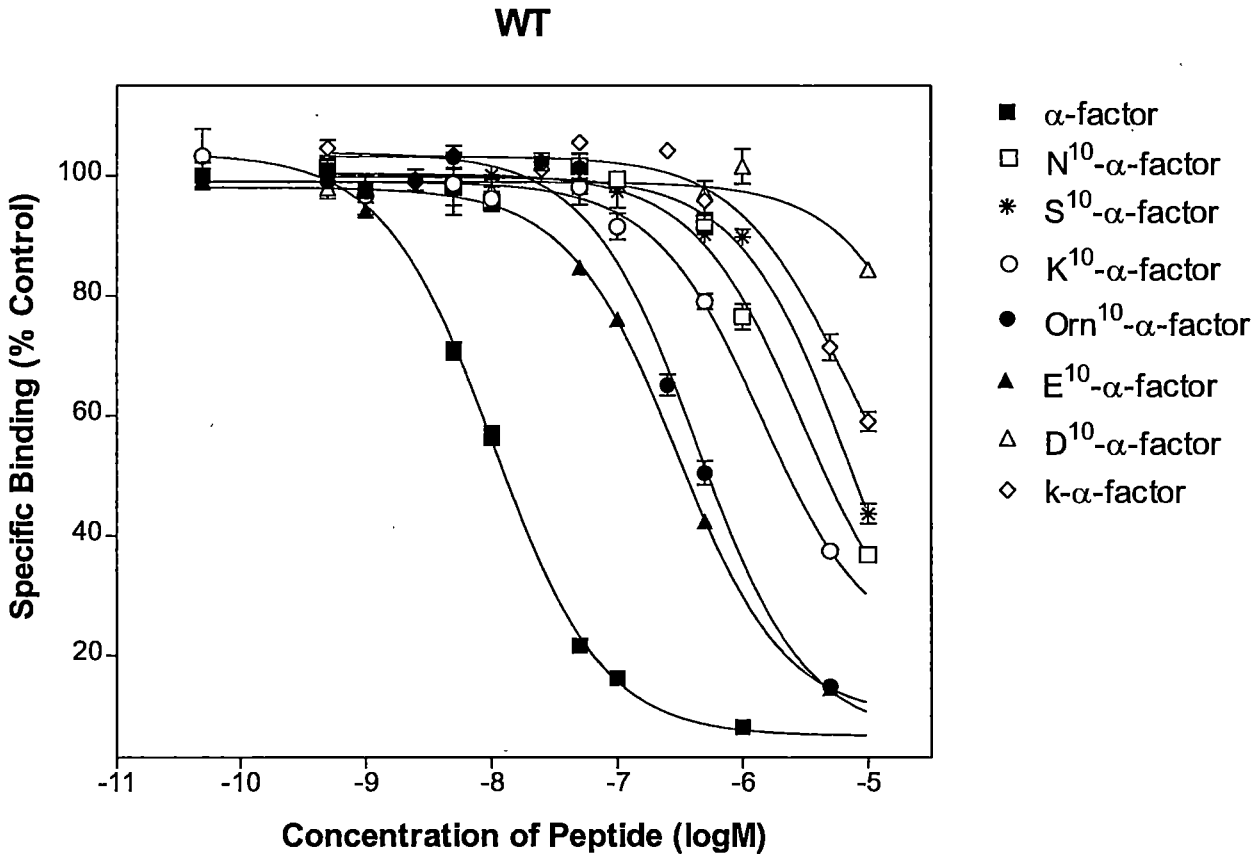
WT
Specific Binding (% Control)
100
80
60
40
20
-11
-10
-9
-8
-7
-6
-5
Concentration of Peptide (logM)
α-factor
N10-α-factor
S10-α-factor
K10-α-factor
Orn10-α-factor
E10-α-factor
D10-α-factor
k-α-factor

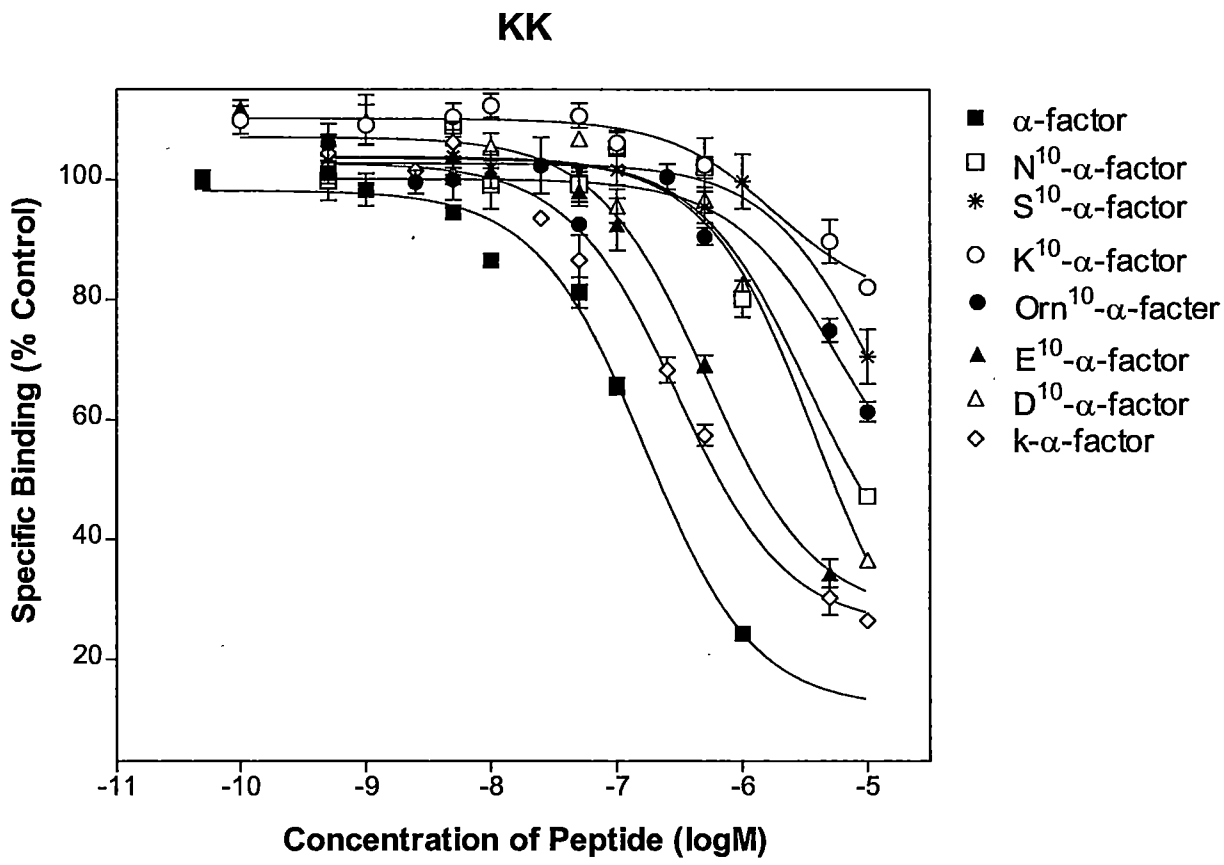
KK
Specific Binding (% Control)
100
80
60
40
20
-11
-10
-9
-8
-7
-6
-5
Concentration of Peptide (logM)
α-factor
N10-α-factor
S10-α-factor
K10-α-factor
Orn10-α-facter
E10-α-factor
D10-α-factor
k-α-factor

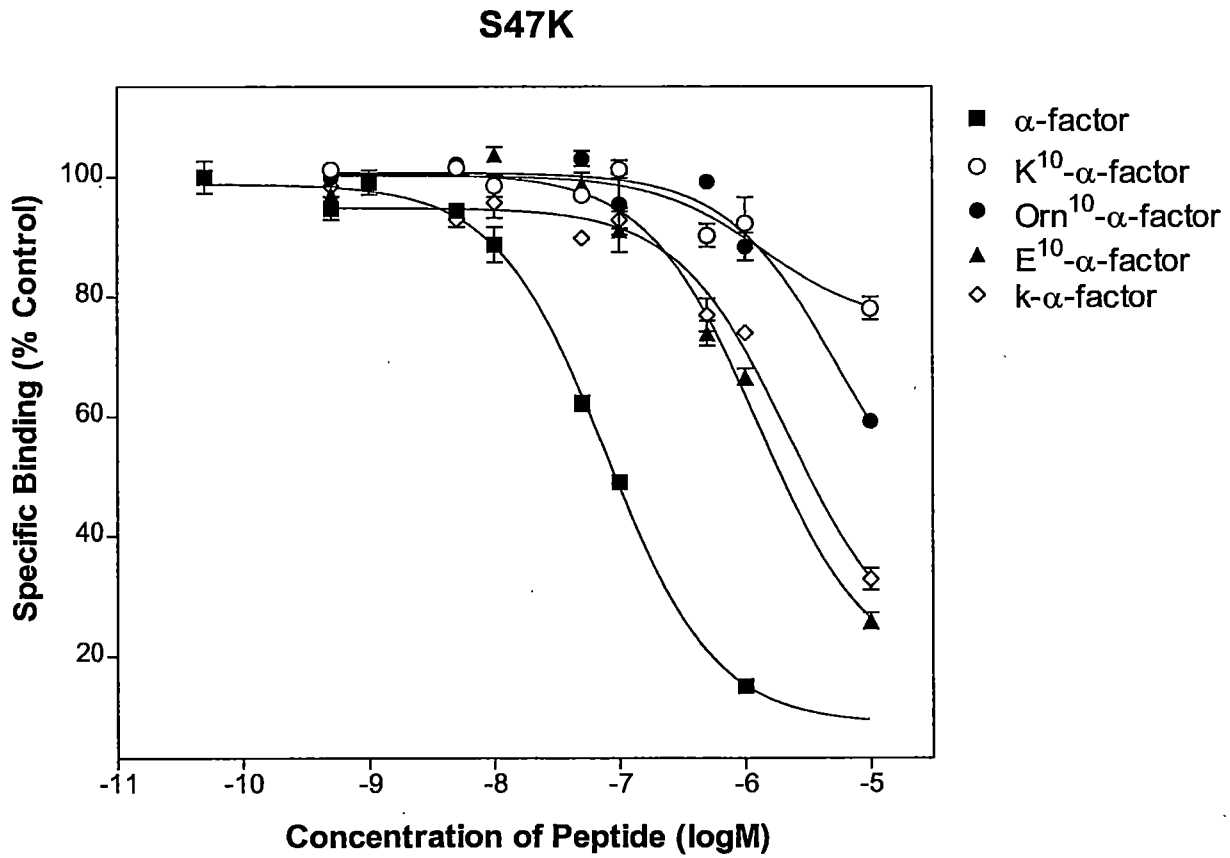
S47K
Specific Binding (% Control)
100
80
60
40
20
-11
-10
-9
-8
-7
-6
-5
Concentration of Peptide (logM)
α-factor
K10-α-factor
Orn10-α-factor
E10-α-factor
k-α-factor

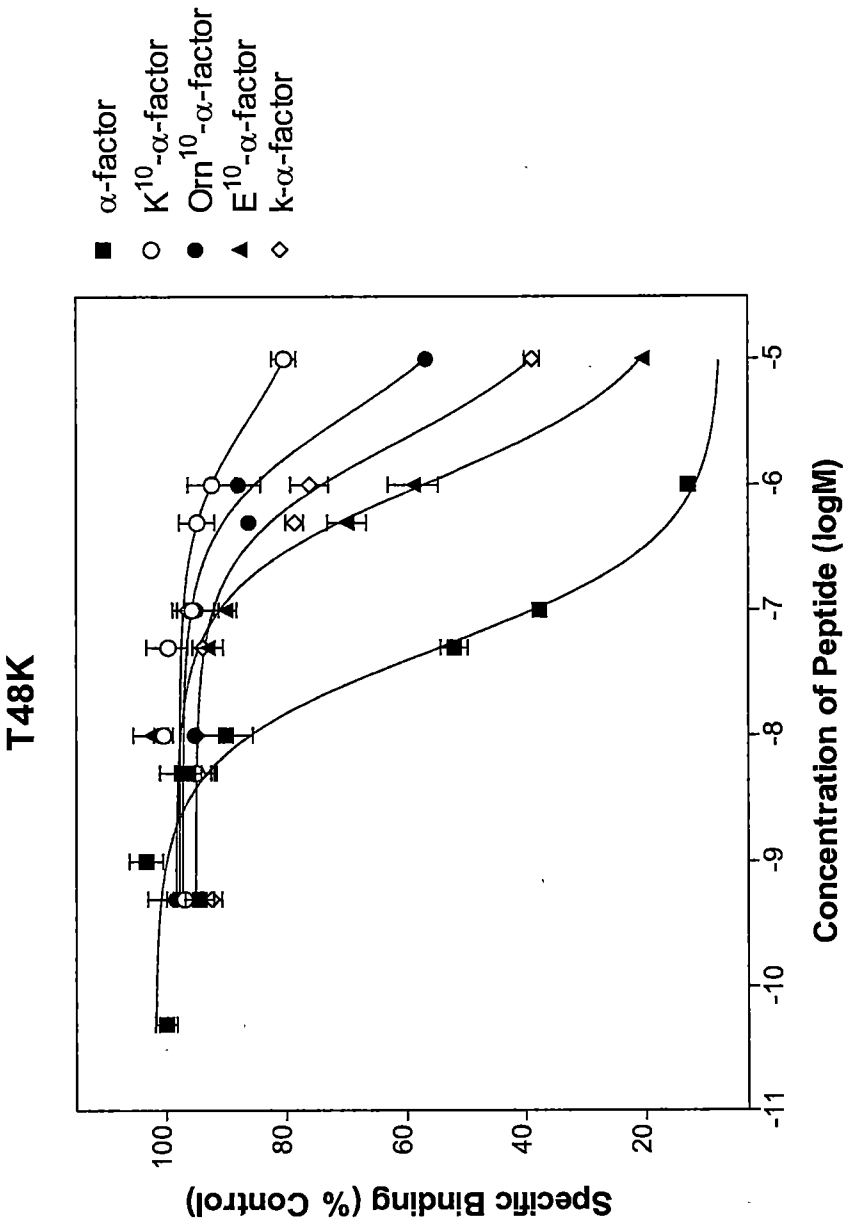
T48K
α-factor
K10-α-factor
Orn10-α-factor
E10-α-factor
k-α-factor
Specific Binding (% Control)
100
80
60
40
20
-11
-10
-9
-8
-7
-6
-5
Concentration of Peptide (logM)

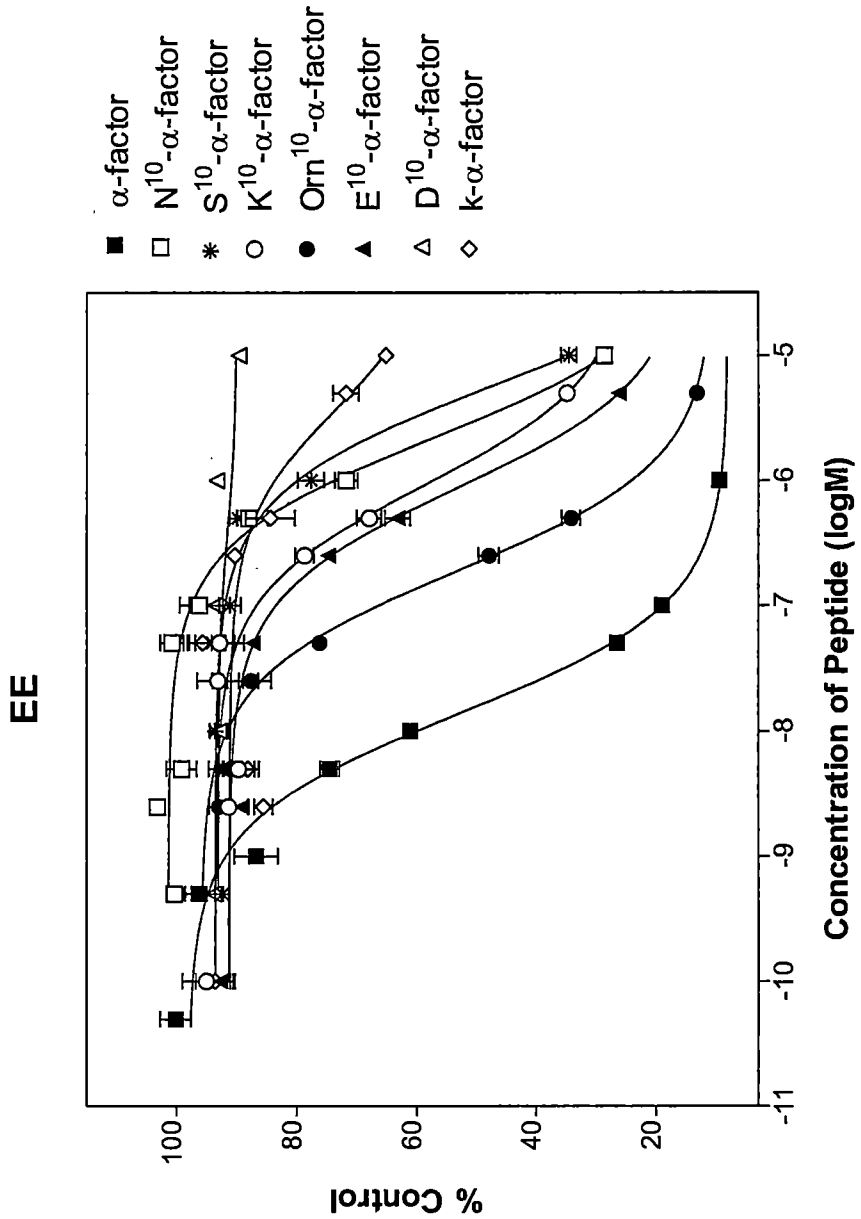
EE
α-factor
N10-α-factor
S10-α-factor
K10-α-factor
Orn10-α-factor
E10-α-factor
D10-α-factor
k-α-factor
% Control
100
80
60
40
20
-11
-10
-9
-8
-7
-6
-5
Concentration of Peptide (logM)

binding is extremely restrictive. Conservative substitutions (Gln to Asn, or Glu to Asp) with different side chain lengths dramatically altered the affinity profile. In general, substitutions with similar size to Gln side chain, a naturally occurring amino acid in α-factor, tended to be favorable for receptor binding. For example, Orn^{10}-α-factor had 3 times higher affinity than K^{10}-α-factor, and E^{10}-α-factor showed at least 60-fold better affinity than D^{10}-α-factor where the van der Waals volume (cu. Åa) of the various side chains are 114, 96, 117, 135, 109, and 91 for Gln, Asn, Orn, Lys, Glu, and Asp, respectively. Moreover, about a 280-fold decrease in affinity was observed when the Gln residue of α-factor was replaced by Asn. k-α-factor had 600-fold less affinity than α-factor to *S. cerevisiae* α-factor receptor confirming a previous study showing high selectivity of *S. cerevisiae* α-factor to its cognate receptor (20).

In KK mutant receptor, analogs with positively charged side chain at the 10^{th} residue of α-factor (K^{10}- and Orn^{10}-α-factor) showed a large drop in their affinity. In contrast, the affinity of D^{10}-α-factor and k-α-factor dramatically increased indicating close proximity of 10^{th} residue of both α-factor and k-α-factor to mutated residues of receptor. Interestingly, the affinity of E^{10}-α-factor decreased slightly in this mutant receptor and further decreased in S47K and T48K single mutant receptors. This contrasted to the affinity changes of k-α-factor for these receptors. Though the affinity of k-α-factor for S47K and T48K receptors were lower than the affinity for KK mutant, it was still better than the affinity of this analog for wild type receptor demonstrating KK residues at

corresponding regions of *S. kluyveri* α-factor receptor (Figure 1) are likely a direct binding sites of E^{10} of k-α-factor.

In EE mutant receptor, a dramatic increase in the affinity of K^{10}- and Orn^{10}-α-factor compared to that of these analogs for KK mutant receptor was observed while the affinity of D^{10}-α-factor and k-α-factor decreased so greatly that 50 % competition was not achieved even at the highest concentrations of peptide tested (Figure 4). These results indicated a close proximity of the 10^{th} residue of α-factor with mutated residues in the receptor. The affinity of E^{10}-α-factor was slightly decreased for this mutant compared to that for KK mutant receptor and was 3 times lower than wild type receptor. However, the *Ki* value of this analog for EE receptor was lower than S47K or T48K mutant receptors suggesting that, unlike k-α-factor, the interaction between 10^{th} residue of α-factor and the 47 and 48 residues of α-factor receptor is more complex.

Biological activities of α-factor and its analogs for wild type and mutant receptors – The growth arrest (halo) and *FUS1-lacZ* assays were used to determine the analogs' ability to activate wild type and mutant receptors. The comparison of activity of α-factor analogs in halo assay revealed some interesting features (Table 4). In general, KK mutation in the receptor led to very low activity to all analogs tested regardless of their binding for this receptor while EE mutation exhibited an opposite effect. These effects were more evident for analogs with a negatively charged side chain at the 10^{th} residue. For example, E^{10}-α-factor showed better activity to EE receptor than wild type receptor though

Table 4. Relative activity of α-factor and α-factor analogs for wild type and mutant receptors. The values presented here is the % ratio of the amount of peptide required for a 10 mm halo compared to the amount of α-factor required for a 10 mm halo in the wild type receptor. nd; not determined.

Analogs tested	Receptors				
	WT	KK	S47K	T48K	EE
α-factor	100±6[a]	43±3	92±7	97±5	130±14
N^{10}--α-factor	49±3	6±2	nd	nd	77±5
S^{10}-α-factor	27±3	3±0.7	nd	nd	47±4
K^{10}-α-factor	20±4	< 2	< 2	5±2	34±4
Orn^{10}-α-factor	59±5	2±0.9	7±2	6±2	83±9
E^{10}-α-factor	115±11	20±3	51±3	60±4	125±15
D^{10}-α-factor	14±3	4±1	nd	nd	21±4
k-α-factor	8±2	5±1	8±3	11±4	15±3

a; 0.22 μg of α-factor were required for a 10 mm halo in the wild type receptor

it had three times higher affinity for wild type receptor than EE receptor. D^{10}-α-factor, which basically lost its binding ability for EE receptor (Fig. 4), showed its highest activity for EE receptor in the halo assay and it was same for k-α-factor. In contrast to this, the lowest activity of D^{10}-α-factor and k-α-factor was observed in KK mutant receptor while these two analogs had their highest affinity for KK mutant receptor. A similar pattern was observed in the activity of N^{10}- and S^{10}-α-factor. These results could indicate that, in addition to the effect on the interaction with 10^{th} residue of α-factor, EE and KK mutations induces conformational changes in the microenvironment of receptor which facilitate or inhibit receptor activation process, respectively.

To further delineate the effect of mutation in the receptor or in α-factor analogs, *FUS1-lacZ* reporter gene induction level was examined with selected analogs (Table 5 and Figure 5). All mutant receptors were fully (93%-115%) activated by α-factor with different EC50 values. The similar expression of the mutated receptor and wild type receptor at the cell surface as well as the similar biological efficacy of α-factor for the mutant receptors indicated that the mutations did not introduce a gross conformational change in the receptor. Overall, the rank order of EC50 values for α-factor analogs in wild type and mutant receptors were close to that of *Ki* values. K^{10}-α-factor had maximum efficacy of 62% with 20-fold less potency for wild type receptor compared with α-factor. This result may indicate that if binding is allowed, analogs can activate wilde type and mutant receptors in a relatively early response in the signal

Table 5. *FUS1-lacZ* gene induction of α-factor and analogs for wild type and mutant receptor. EC50 and Emax values were calculated form dose response curves stimulated by the indicated analogs. Results are expressed as mean ± S.E. of at least three separate experiments, each of which were performed in duplicate. –; no detectable activity over basal level.

Receptors	α-factor		K^{10}-α-factor		E^{10}-α-factor	
	EC50 (nM)	Emax (%)	EC50 (nM)	Emax (%)	EC50 (nM)	Emax (%)
WT	41±8	100±9	800±56	62±4	170±20	115±6
KK	161±23	96±7	–	–	302±23	84±9
EE	47±7	115±11	453±37	75±7	272±18	114±8
S47K	89±12	93±6	–	–	340±16	110±6
T48K	98±11	105±7	–	–	370±15	97±8

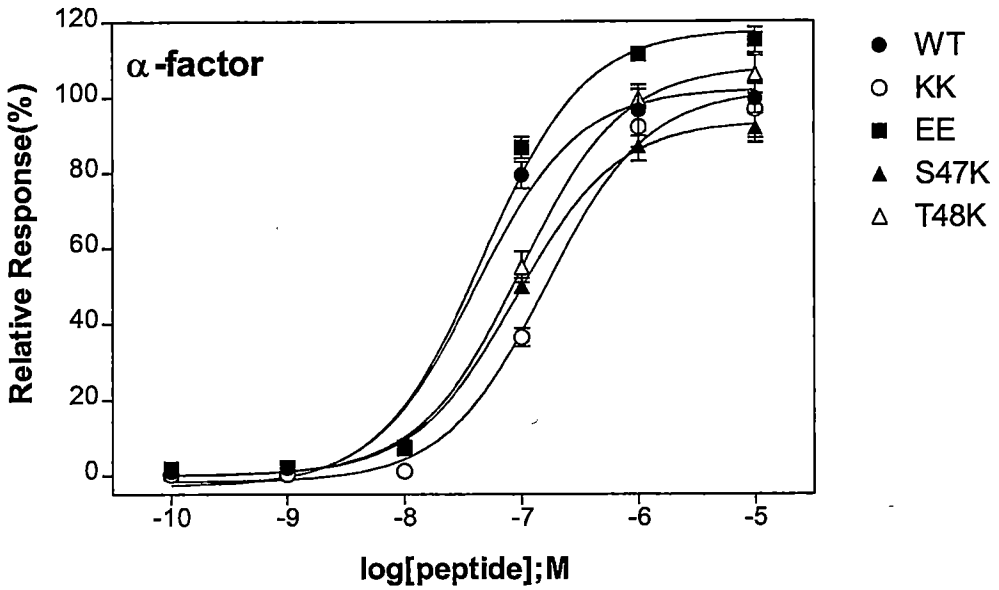

Figure 5. Dose-response analysis of *FUS1-lacZ* gene induction by α-factor and α-factor analogs for wild type and mutant receptors. The β-galactosidase levels were determined following incubation of strains with various concentration of α-factor analogs for 2hr. Points represents the mean of three separate experiments.

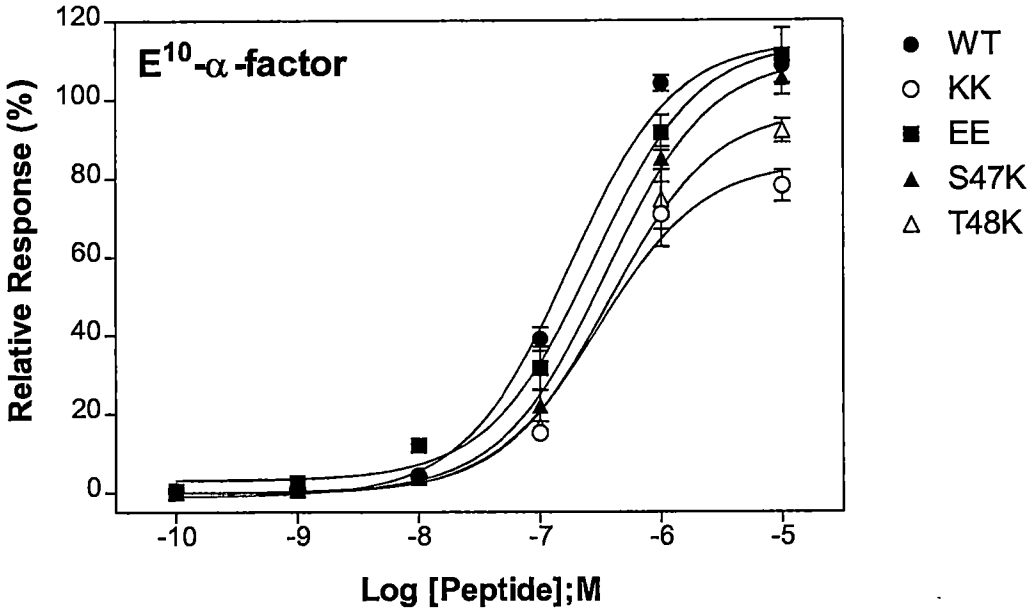
E10-α-factor
Relative Response (%)
120
100
80
60
40
20
0
-10
-9
-8
-7
-6
-5
Log [Peptide];M
WT
KK
EE
S47K
T48K

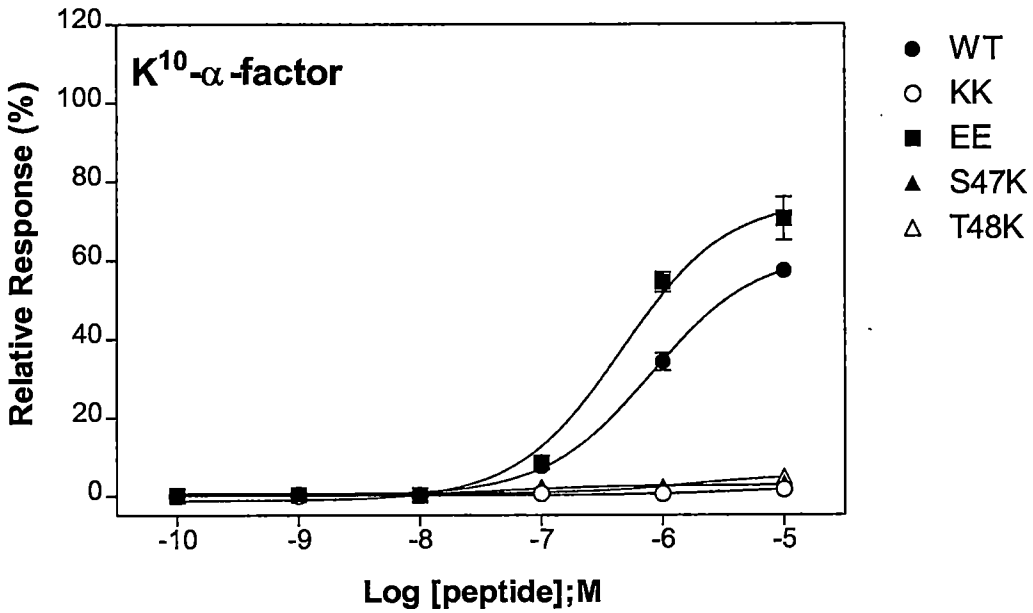
K10-α-factor
Relative Response (%)
120
100
80
60
40
20
0
-10
-9
-8
-7
-6
-5
Log [peptide];M
WT
KK
EE
S47K
T48K

transduction pathway. In contrast, the halo assay, which takes about 36 hr for analysis, represents activities encompassing many aspects of intracellular regulation including late responses after the initial singal transduction. K^{10}-α-factor failed to induce *FUS1-lacZ* reporter gene for KK, S47K, and T48K mutant receptor which is consistent with the poor binding affinity and growth arrest ability of this analog for these three mutant receptors. E^{10}-α-factor showed comparable activity for wild type and mutant receptors to that of α-factor despite the fact that higher EC50 values of E^{10}-α-factor were observed in this analog for all receptors. This result is similar to the result of the halo assay with E^{10}-α-factor and indicated that the presence of negative charge in either 47 and 48 residues of the receptor or the 10^{th} residue of α-factor may improve the initial receptor activation step.

Effects of high salt on ligand binding and activity to EE mutant receptor – If the increased binding affinity of Orn^{10}- and K^{10}-α-factor for EE mutant receptor is due to an ionic interaction between mutated region of receptor and the 10^{th} residue of α-factor, treatment of high salt may disrupt favorable interactions. To test this possibility, the competition binding and the halo assays of EE mutant receptor were performed in the presence of 1M NaCl. The Ki values of α-factor for either wild type or EE mutant receptors were not changed (Table 6 and Figure 6). The high salt did not affect the binding affinity of α-factor for either wild type or EE mutant receptor under same conditions suggesting that EE substitution at the 48 and 48 residues in the receptor are acceptable for α-factor binding. The

Table 6. High salt effect on binding of α-factor and α-factor analogs to wild type and EE mutant receptor. The affinity was measured in the presence or absence of 1M NaCl as described in Materials and Methods. *Ki* values (nM) presented were mean of two separate experiments.

Analogs	WT		EE	
tested	- Salt	+ 1M NaCl	- Salt	+ 1M NaCl
α-factor	5.6±0.7	5.9±0.6	7.7±0.8	7.0±0.5
K^{10}-α-factor	778±61	1390±103	483±35	1770±138
Orn^{10}-α-factor	231±21	390±33	105±16	696±58
E^{10}-α-factor	157±19	403±31	465±42	557±54

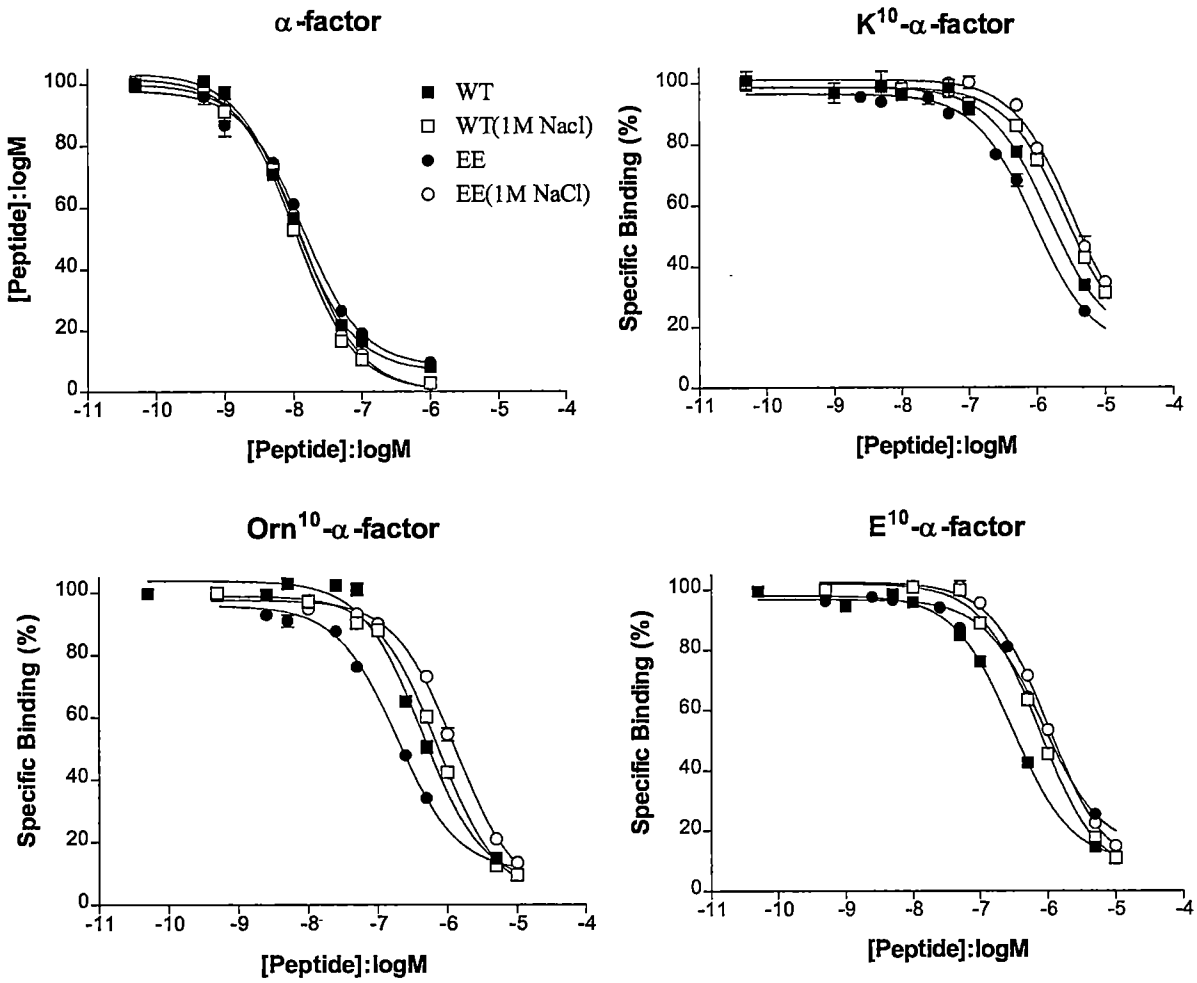

Figure 6. Competition binding assay in the presence of 1M NaCl. The effect of high salt on α-factor analog binding for wild type and EE mutant receptors was assayed as described under Material and Method. The results are average ± S.E. of two experiments with each point assayed in triplicate. *Ki* values are given in Table 6.

affinity of K^{10}- and Orn^{10}-α-factor for EE receptor was decreased about 4- and 6-fold, respectively, in the presence of 1M NaCl while the affinity of these analogs for wild type receptor was decreased only 1.8 fold under the same conditions demonstrating ionic interactions between EE residues in the receptor and K^{10} or Orn^{10} residue in α-factor. The affinity of E10-α-factor for wild type receptor decreased 2.6-fold in the presence of 1M NaCl and this decreased affinity (*Ki* of 403 nM) was similar to the affinity of this analog (*Ki* of 465 nM) for EE mutant receptor without high salt. In addition, high salt had minimal effect on the affinity of E^{10}-α-factor for EE receptor. These results might indicate that the existence of functional group(s) in the receptor which neutralize the negative charge of E^{10}-α-factor.

Since high salt transiently induces growth arrest (30), the size of halo in the presence of 1M NaCl was larger than the size of untreated sample. However, as the effect of 1M NaCl treatment for each peptide tested should be the same, the relative activity could be compared (Table 7). As expected, biological activity of E^{10}-α-factor for both wild type and EE mutant receptors decreased about 2.5-fold in the presence of high salt. Activity of EE mutant receptor for α-factor and analogs also dramatically decreased with high salt treatment. The better activity of K^{10}- and Orn^{10}-α-factor to EE receptor over wild type receptor in normal conditions was reversed in the presence of 1M NaCl consistent with the affinity changes with high salt (Table 6).

Table 7. High salt effects on growth arrest assay. The assay was done in the presence of 1M NaCl in the media and solutions as described in Materials and Methods. The % values presented are relative activity of α-factor analogs for the amount of α-factor to produce a 15 mm halo in the presence or absence of 1M NaCl.

Analogs tested	- 1M NaCl		+ 1M NaCl	
	WT	EE	WT	EE
α-factor	**100**±6	125±15	**100**±5	78±3
K^{10}-α-factor	22±4	37±3	2.8±0.3	1.9±0.2
Orn^{10}-α-factor	57±5	81±8	18±2	9.3±1.5
E^{10}-α-factor	110±8	118±11	43±4	40±4

CHAPTER 4

Discussion

The present study was conducted to explore the functional role(s) of two residues in the region at the first transmembrane domain (TM1) and the N-terminal domain of the yeast α-factor pheromone receptor. The potential importance of this region of the receptor was recognized previously in chimeric receptor studies between *S. cerevisiae* and *S. kluyveri* α-factor receptors (20,21). The results suggested that this particular region of the receptor was responsible for ligand binding specificity between two closely related α-factors, but not for the receptor activation step. Therefore it was tempting to speculate of a direct contact between this region and one or part of five variant residues *between S. cerevisiae* and *S. kluyveri* α-factors (Table 1) assuming that the interactions of receptor and ligand are shared between species. The conservation of functionally important α-factor domains (N-terminus for receptor activation, Gly^9 for forming a turn structure, and C-terminus for α-factor binding) further supported our assumption of sharing receptor interactions of these two α-factors.

Of the 5 candidate residues that may interact with the region between TM1 and N-terminal domain, we targeted the 10^{th} residue of α-factors based on the following reasoning: 1) The interaction between TM1 and C-terminal region of

α-factor was proposed (See PART 3 of dissertation), 2) The 10th residue of α-factor would be close to the junction between TM1 and N-terminal domain of the receptor if C-terminus of α-factor interact with TM 1, 3) A chimeric α-factor receptor which contains just three residues of *S. kluyveri* receptor sequence (K47K48I49) showed high binding affinity with the *S. kluyveri* α-factor (21). The E^{10} residue of the *S. kluyveri* α-factor is the only amino acid that might have an ionic interaction with the mutated residues.

To test this hypothesis, we synthesized and tested a number of α-factor analogs which were modified at the 10th residue. We believe that analysis of combinatorial mutations on both the receptor and ligand is a reasonable approach to evaluating the ligand binding regions thereby overcoming misinterpretations of binding data caused by indirect effects of receptor mutation.

In this study, we show that the two residues at the interface between TM1 and N-terminal extracellular domain and TM1 of α-factor receptor are adjacent to and responsible for discriminating between the 10th residue of *S. cerevisiae* (Gln) and *S. kluyveri* (Glu) α-factor pheromones when bound to the receptor. When this region of *S. cerevisiae* α-factor receptor was occupied by lysines (KK), which naturally occurs in the wild type *S. kluyveri* receptor, the Lys repelled α-factor analogs with positive charges at the 10th residue (Orn^{10}-α-factor and K^{10}-α-factor). On the other hand, the Lys attracted the negative charge at the 10th residue of α-factor (D^{10}-α-factor and k-α-factor). In contrast, EE substitution at this region of α-factor receptor attracted Orn^{10}-α-factor and K^{10}-α-factor while

repelled D^{10}-α-factor and k-α-factor. These results clearly demonstrated that E^{10} of k-α-factor directly interacts with KK residues in *S. kluyveri* receptor and this interaction is responsible for ligand specificity between *S. serevisiae* and *S. kluyveri* α-factors. In addition the results provide convincing evidence that Orn^{10} and K^{10} or D^{10} residues of *S. cerevisiae* α-factor analogs participate in ionic interaction with EE or KK residues in mutant receptors, respectively. This conclusion was further supported by the result that the effect of 1M NaCl, which would disrupt ionic interactions, was detrimental for the affinity and the activity of K^{10}-α-factor and Orn^{10}-α-factor in EE mutant receptor.

These data, however, do not allow us to conclude that there is a direct contact between Ser47 and Thr48 residues in *S. cerevisiae* α-factor and Gln^{10} residue of α-factor because mutation of Ser47 and Thr48 to Glu (EE) had no effect on the binding of α-factor and the affinity of E^{10}-α-factor for EE mutant receptor was only 1.7-fold less than the affinity for KK mutant receptor. Perhaps binding pocket of Gln^{10} of α-factor involves multiple residues at the surrounding region of Ser47 and Thr48 residues. Lys100 at the exterior part of TM2 would be one of candidates with close proximity to the interface between TM1 and N-terminal domain of receptor. Glu substitutions either in the 47 and 48 residues of receptor or in the 10^{th} residue of α-factor may attract Lys100 to the binding pocket favoring the formation of active receptor states leading to significant increases in agonist activity. Close location of Lys100 to this binding region also can minimize a charge repulsion when E^{10}-α-factor binds to EE mutant receptor.

This assumption is supported by the observation that in the presence of 1M NaCl, the activity of E^{10}-α-factor was dramatically decreased for EE mutant receptor while the affinity change was minimal. No change in binding affinity of α-factor for EE receptor may indicate that either the stabiliztion of active receptor conformation by the interaction between EE residues and Lys100 may compensate unfavorable binding of α-factor for this mutant or simply, the distance between S47 and T48 residues of the receptor and Gln^{10} of α-factor is enough for the introduction of Glu side chain. Testing a triple mutant receptor (S47E,T48E, K100E) with K^{10} and E^{10}-α-factor may answer some of questions.

The results of this study provide new and definitive information about the orientation of the α-factor when bound to the α-factor receptor. Indeed, this is one of only a few examples in a GPCR where the interaction of a ligand with specific residues in the receptor has been assessed by complementary mutations in the ligand and in the receptor. Evidence about the close location of Gln^{10} of α-factor to receptor interface between TM1 and N-terminal domain lead us to develop a hypothetical working model for α-factor binding as depicted in Figure 7. In our model, both N- and C-terminus of α-factor bind to the exterior part of TMs while the center region including a turn structure may interacts with the extracellular domains. In addition to the results of the present study, two experimental results allowed us to build this model: 1) A β-turn-like structure at Lys^7 through Gln^{10} in α-factor (6-9), 2) The high affinity and activity of α-factor

Figure 7. A proposed model for α-factor binding, Ste2p. This schematic shows counterclockwise orientation of TM domains (33). the structure of α-factor ligand except its turn structure was shown as extended form. For clarity only residue 4 (Leu) through 10 (Gln) is shown with single letter amino acid code. Boldfaced residues in α-factor represents five variant regions between *S. cerevisiae* and *S. kluyveri* α-factor. Two amino acid residues (Ser and Thr) that their proximity with Q^{10} of α-factor was tested in this study were italicized. EL; extracellular loop, I; intracellular loop.

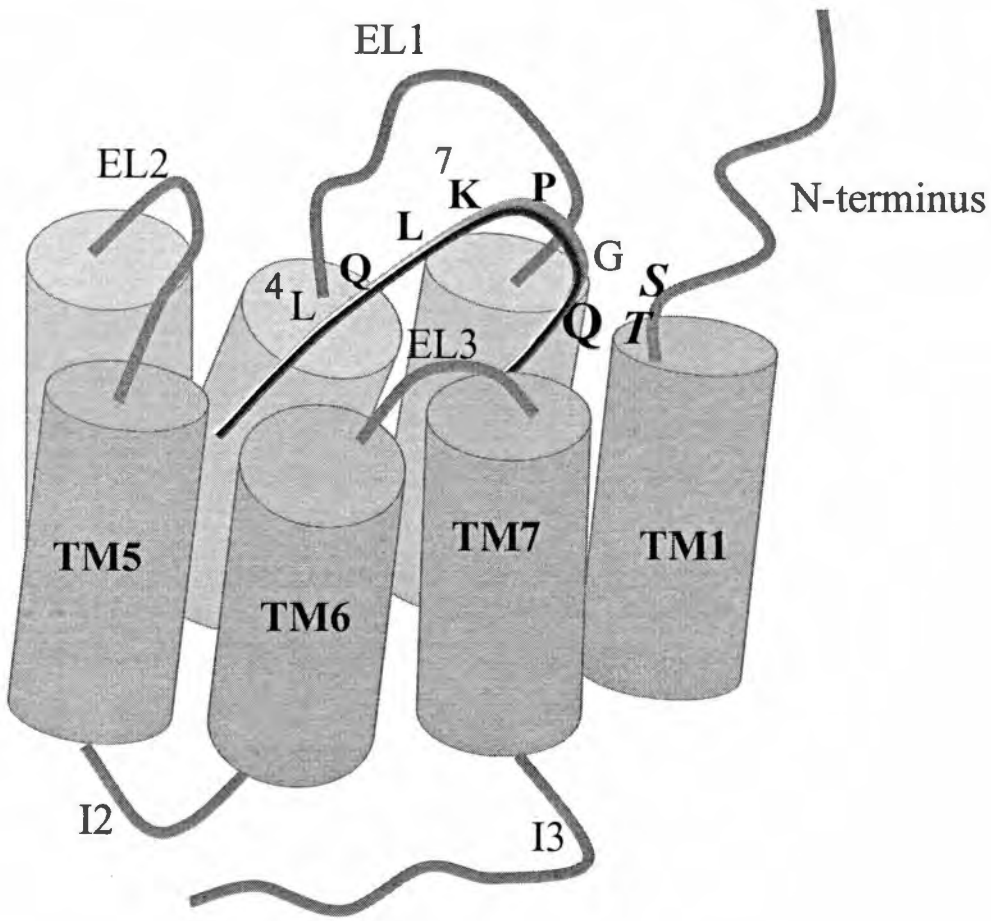

Figure 7. A Proposed model for α-factor binding to its receptor, Ste2p.

dimer which covalently linked at Lys^7 position of α-factor (Henry, L.K., Naider, F., and Becker, J.M. manuscript in preparation).

Our model implies that three small regions (residue 47-49, N-terminal half of EC1, and N-terminal end of EC3) of receptor which responsible for ligand specificity between *S. cerevisiae* and *S. kluyveri* α-factor are closely located with 5 variant residues of α-factors. Thus, EC1 and EC3 regions can be targeted for the identification of binding sites of residue 5 through 7 of α-factor. Another implication of the model is the interaction of N-terminus of α-factor with TM3,5, and 6. A key step in GPCR activation is movement of these three TMs upon binding of agonist (31). Since N-terminal residue of α-factor is important for receptor activation (10), the interaction between TM 3, 5, and 6 with N-terminal region of α-factor could be reasonable. F204 and Y 266,which previously suggested in α-factor binding, at the interface between TM5 and 6 and EC3 are likely candidates for the interaction with hydrophobic residues of N-terminus of α-factor (32,33).

Emerging evidence starts to indicate that agonist binding may involve an initial interaction between receptor and one structural group of the agonist (34-36). Following the initial binding of one structural group, binding of remaining groups occurs in a sequential manner as a result of random and spontaneous movement of TM domains to positions that permit interaction with functional groups. This in essence suggests a sequential binding of α-factor and is well presented in our model that the binding domain of α-factor (C-terminus) first

binds to receptor and a turn structure allows the binding of the signaling domain (N-terminus). The study of α-factor binding mode may open new concepts about receptor-ligand interactions.

Although this model is highly speculative and awaits much works for its verification, it will provide valuable information for understanding interactions between α-factor and its receptor and be a guide for future experiments.

List of References for Part 4

1. **Dohlman, H.G., Thorner, J., Caron, M.G., and Lefkowitz, R.J.** (1991) Model system for the study of seven transmembrane-segments receptors. *Annu. Rev. Biochem.* 60:653
2. **Ostrowski, J., Kjelsberg, M.A., Caron, M.G., and Lefkkowitz, R.J.** (1992) Mutagenesis of the β2-adrenergic receptor: how structure elucidates function. *Annu. Rev. Pharmacol. Toxicol.* 32:167
3. **Placzewski, K., Kumasaka, T., Hori, T., Behnke, C.A., Motoshima, H., Fox, B., Stenkamp, R.E., Yamamoto, M., and Miyano, M.** (2000) Crystal structure of rhodopsin: a G protein-coupled receptor. *Science* 289:739
4. **Strader, C.D., Fong, T.M., Graziano, M., and Tota, M.R.** (1995) The family of G protein-receptors. *FASEB J.* 9:745
5. **Leberer, E., Thomas, D.Y., and Whiteway, M.** (1997) Pheromone signaling and polarized morphogenesis in yeast. *Curr. Opin. Genet. Develop.* 7:59
6. **Jelicks, L.A., Naider, F., Shenbagamurthi, P., Becker, J.M., and Broidio, M.S.** (1988) *Biopolymers* 27:431
7. **Goundarides, J.S., Broido, M.S., Becker, J.M., and Naider, F.** (1993) *Biochemistry* 32:908
8. **Yand, W., McKinney, A., Becker, J.M., and Naider, F.** (1995) Systematic analysis of the *Saccharomyces cerevisiae* α-factor containing lactam constraints of different ring size. *Biochemistry* 34:1308

9. **Zhang, Y.L., Marepalli, H.R., Lu, H.-F., Becker, J.M., and Naider, F.** (1998) Synthesis, biological activity, and conformational analysis of peptidomimetic analogs of the *Saccharomyces cerevisiae* α-factor tridecapeptide. *Biochemistry* 37:12465

10. **Abel, M.G., Zhang, Y.L., Lu, H.-F., Naider, F., and Becker, J.M.** (1998) Structure-function analysis of the *Saccharomyces cerevisiae* tridecapeptide pheromone using alanine-scanned analogs. *J. Peptide Res.* 52:95

11. **Konopka, J.B., Margarit, M., and Dube, P.** (1996) Mutation in transmembrane domain 6 constitutively activates the G protein-coupled α-factor receptor. *Proc. Natl. Acad. Sci. USA* 93:6764

12. **Sommers, C.M., Martin, N.P., Akal-Strader, A., Becker, J.M., Naider, F., and Dumont, M.E.** (2000) A limited spectrum of mutations causes constitutive activation of the yeast α-factor receptor. *Biochemistry* 39:6898

13. **Clark, C.D., Palzkill, T., and Botstein, D.** (1994) Systematic mutagenesis of the yeast mating pheromone receptor third intracellular loop. *J. Biol. Chem.* 269:8831

14. **Schandel, K.A., and Jenness, D.D.** (1994) Direct evidence for ligand-induced internalization of the yeast α-factor pheromone receptor. *Mol. Cell. Biol.* 14:7245

15. **Chen, Q., and Konopka, J.B.** (1996) Regulation of the G protein-coupled α-factor pheromone receptor by phosphorylation. *Mol. Cell. Biol.* 16:247

16. **Dube, P., DeCostanzo, A., and Konopka, J.B.** (2000) Interactions between transmembrane domains five and six of the α-factor receptor. J. *Biol. Chem.* 275:26492

17. **Xie, H., Ding, F.-X., Schreiber, D., Eng, G., Liu, S.-F, Arshava, B., Arevalo, E, Becker, J.M., and Naider, F.** (in press) Synthesis and biophysical analysis of transmembrane domains of a *Saccharomyces cerevisiae* G protein-coupled receptor. *Biochemistry*

18. **Marsh, L., and Herskowitz, I.** (1988) STE2 protein of *Saccharomyces kluyveri* is a member of the rhodopsin/β-adrenergic receptor family and is responsible for recongnition of the peptide ligand α-factor. *Proc. Natl. Acad. Sci. USA* 85:3855

19. **Egel-Mitani, M., and Hansen, M.T.** (1987) Nucleotide sequence of the gene encoding the *Saccharomyces kluyveri* α mating pheromone. *Nucleic Acids Res.* 15:6303

20. **Sen, M., and Marsh, L.** (1994) Noncontiguous domains of the α-factor receptor of yeasts confer ligand specificity. *J. Biol. Chem.* 269:968

21. **Sen, M., Shah, A., and Marsh, L.** (1997) Tow types of α-factor receptor determinants for pheromone specificity in the mating-incompatible yeasts *S. cerevisiae* and *S. kluyveri. Curr. Genet.* 31:235

22. **Vieira, J., and Messing, J.** (1987) In *Methods in enzymology*. Wu, R., and Grossman, L. ed., Vol. 153, p. 3

23. **Kunkel, T.A.** (1987) Rapid and efficient site-specific mutagenesis without phenotypic selection. *Methods Enzymol.* 154:488

24. **Gietz, D., St. Jean, A., Woods, R.A., and Schiestl, R.H.** (1992) Improved method for high efficiency transformation of intact yeast cells. *Nucleic Acids Res.* 20:1425

25. **Rath, S.K., Naider, F., and Becker, J.M.** (1988) Peptide analogues compete with the binding of α-factor to its receptor *in Saccharomyces cerevisiae. J. Biol. Chem.* 263:17333

26. **Kippert, F.** (1995) A rapid permeabilization procedure for accurate quantitative determination of beta-galactosidase activity in yeast cells. *FEMS Microbiol. Lett.* **128**, 201-206.

27. **Guarente, L.** (1983) Yeast promoters and lacZ fusions designed to study expression of cloned genes in yeast. *Meth. Enzymol.* **101**, 167-180.

28. **Miller, J.H.** (1972) Experiments in Molecular Genetics, Cold Spring Harbor Laboratory, Cold Spring Harbor, New York.

29. **Cheng, Y. and Prusoff, W.H.** (1973) Relationship between the inhibition constant (K1) and the concentration of inhibitor which causes 50 percent inhibition (I50) of an enzymatic reaction. *Biochem. Pharmacol.* **22**, 3099-3108.

30. **Blomberg, A.** (2000) Metabolic surprises in *Saccharomyces cerevisiae* during adaptation to saline condition: questions, some answers and a model. *FEMS Microbiol. Lett.* 182:1

31. **Flower, D.R.** (1999) Modeling G protein-coupled receptors for drug design. *Biochim. Biophys. Acta* 142:207

32. **Dube, P., and Konopka, J.B.** (1998) Identifcation of a polar region in transmembrane domain 6 that regulates the function of the G protein-coupled α-factor receptor. *Mol. Cell. Biol.* 18:7205

33. **Dosil, M., Giot, L., Davis, C., and Konopka, J.B.** (1998) Dominant-negative mutations in the G protein-coupled α-factor receptor map to the extracellular ends of the transmembrane segments. *Mol. Cell. Biol.* 18:5981

34. **Jarnagin, K., Bhakta, S., Zuppan, P., Yee, C., Pease, H.B., Miller, A., and Freedman, R.** (1996) Mutations in the B2 bradykinin receptor reveal a different pattern of contacts for peptidic agonists and peptidic antagonists. *J. Biol. Chem.* 271:28227

35. **Turner, P.R., Mefford, S., Bambino, T., and Nissenson, R.A.** (1998) Transmembrane residues together with the amino terminus limit the response of the parathyroid hormone (PTH) 2 receptor to PTH-related peptide. *J. Biol. Chem.* 273:3830

36. **Bourne, H.R.** (1997) How receptors talk to trimeric G proteins. *Curr. Opin. Cell Biol.* 9:134

Vita

Byung-Kwon Lee was born in Kwangju, Korea on May 15, 1961. He graduated from Jin-Heng High School in February 1980. After few years of wandering and Army services, he entered Chosun University, Kwangju, Korea during March of 1987 where he received a Bachelor of Sciences in Biology in February 1991 and a Master of Sciences in Microbiology in February 1993. He worked for two years in the Center for Biotechnology, Kwangju, Korea as a research associate. He entered the Ph. D. program in Microbiology at the University of Tennessee, Knoxville in August of 1995 in the laboratory of Dr. Jeffrey M. Becker. During the course of his time in this program, he served as a Graduate Teaching Assistant (1997-1998) and as a Graduate Research Assistant (1999-2000). He officially received a Doctor of Philosophy degree in Microbiology in December 2000.

He continues to work in Dr. Becker's Lab for a time being while searching for a place where his interests fit in.